POLITECNICO DI TORINO

Master's Degrees in Civil Engineering

Master's Thesis

Assessment of aleatory and model uncertainties for non-linear analysis of slender reinforced concrete members

Supervisors
Dr. Eng. Gabriele Bertagnoli
Dr. Eng. Paolo Castaldo
Eng. Diego Gino

Candidate
Michele Virdis

July 2018

Ai miei genitori

Ringraziamenti

A conclusione di questo lavoro di tesi, vorrei ringraziare il Dott. Ing. Gabriele Bertagnoli, che mi ha permesso di intraprendere questo percorso. Ho avuto modo di conoscerlo e stimarlo durante il corso di studi magistrale e di conseguenza ho scelto di averlo come supervisore in questo ultimo importante step. Durante questo percorso di tesi è stato fonte di idee e soluzioni efficaci.
Infine, tutto ciò non sarebbe stato possibile senza l'aiuto di Dott. Ing. Paolo Castaldo e di Ing. Diego Gino. Li ringrazio per aver infuso in me l'interesse per gli argomenti trattati, attraverso la loro conoscenza in materia, la loro simpatia e il loro fondamentale supporto.

Abstract

This Master's Thesis proposes and evaluates the partial safety factors related to the aleatoric and the model uncertainties, regarding the overall structural resistance for non-linear analysis of slender reinforced concrete members.
Several experimental tests are found in literature, considering different types of columns subjected to an axial load or an eccentric load. Forty experimental tests have been selected in order to take into account of a slenderness range between five to eighty.

For each experimental test, one structural model is defined, in order to evaluate the aleatoric uncertainty on the non-linear analysis of reinforced concrete slender members. The Latin Hypercube Sample is performed for each column in order to sample a set of values which can be representative of the material aleatory characteristic. Subsequently, the partial safety factor related to the aleatoric uncertainty is evaluated.

Several structural models are defined, for each experimental test, in order to investigate the model uncertainty influence on the non-linear analysis of reinforced concrete slender structures, considering different possible approach available to describe the mechanical behaviour of reinforced concrete members. Consequently, the numerical results are compared to the experimental results. Then, a statistical treatment of the resisting model uncertainties is performed, following a Bayesian approach. Subsequently, the mean value and the coefficient of variation, which characterized the resisting model uncertainty, are identified. Finally, the partial safety factor related to the resisting model uncertainty is evaluated.

Contents

Chapter 1

Structural reliability

1.1 Basis requirement

Eurocode 0 (EC0) [1] established principles and requirements both for the safety and the durability of the structures. It describes the basis of their design and verification and gives guidelines related to structural reliability aspects.
Durability is defined, for both materials and structures, as the capability to preserve physical and mechanical characteristics. This essential property defines an adequate safety level, which shall be maintained over the design working life of the structures. The following basis requirements should be met:

- suitable materials shall be chosen;
- an appropriate design and detail level shall be considered;
- control procedures shall be specified for the design, production and execution.

Therefore, a structure shall be executed in such a way that, during its intended life, considering an appropriate level of reliability and taking into account economical aspects, it will:

- sustain all actions and influences likely to occur during its execution and use;
- remain fit for the use for which it is required.

1.1.1 Design working life

The structure design working life is defined as the period of time during which a desired level of functionality and structural stability need to be maintained (see [1]). Design working life depends on the structural typologies (see Tab. 1.1).

Design working life category	Indicative design working life (years)	Examples
1	10	Temporary structures
2	10 to 25	Replaceable structural parts
3	15 to 30	Agricultural and other similar structures
4	50	Building structures and other common structures
5	100	Monumental building structures, bridges and other civil engineering structures

Table 1.1: Indicative design working life (EC0 [1])

1.1.2 Design situations and limit states

According to EC0, the structural safety and performance may be assessed in relation to the limit states that may be occur during the design working life (see [1]). The limit state is the condition in which not all design requirements are satisfied by the structure. Structural requirements are distinguished in the different design situations. The relevant design situations shall be selected taking into account the circumstances at which the structure is required to fulfil its function.
Those situations shall be classifies as follows:

- persistent design situations, which refer to the conditions of normal use;
- transient design situations which refer to temporary conditions applicable to the structure, e.g. during execution or repair;
- accidental design situations, which refer to exceptional conditions applicable to the structure or to its exposure, e.g. to fire, explosion, impact or the consequences of localised failure;
- seismic design situations, which refer to conditions applicable to the structure when subjected to seismic events.

The selected design situations shall be sufficiently severe and varied, in order to encompass all conditions that can reasonably be foreseen to occur during the execution and use of the structure.

Ultimate limit states

The Ultimate Limit States (ULS) are the design conditions that concern: the safety of people, the safety of structure, the safety of environment and, in some circumstances, the protection of the contents (see [1]).
In the ULS, states prior to structural collapse is considered instead of the collapse itself.
The following ULS should be verified:

- loss of the equilibrium ot the structure or any part of it, considered as a rigid body;
- failure by excessive deformation, transformation of the structure or any part of it into a mechanism, rupture, loss of stability of the structure or any part of it, including supports and foundations;
- failure caused by fatigue ot other time-dependent effects.

Serviceability limit states

The Serviceability Limit States (SLS) are the design conditions that concern the functions of the structure or structural members under normal use, the comfort of people and the appearance of the construction works (see [1]).
The verification of SLS should be based on the following criteria:

- deformations that affect:
  - the appearance;
  - the comfort of the users;
  - the functioning of structure, which includes the function of machines or services.
- vibrations:
  - that causes discomfort to people;
  - that limits the effective functionality of the structure.

- damages that is likely to adversely affect:
  - the appearance;
  - the durability;
  - the functioning of the structure.

Structural robustness

The term robustness is used to indicate the ability of a structural system to resist to a damage under extreme loads (see [1]). This requirement is aimed to prevent an initial local failure from spreading progressively and resulting in the collapse of a disproportionately large part of the structure.
A limit state can leads to reversible or irreversible consequences. ULS are irreversible when: the structure or a part of it loss equilibrium; the maximum resistance capacity of a section or a junction is reached; an element or a junction is broken by fatigue or other time-dependent effects.
Differently, the SLS can be reversible or irreversible and it includes: localized damage that can reduce durability or affects the efficiency or appearance of structural and non-structural elements; unacceptable deformations that affect functionality or appearance; excessive vibrations that affect people or non-structural elements. When a limit state is reached, the structure may need to be recovered, or consolidated, or, in the most extreme cases, demolished.

1.2 Assessment of structural reliability

The previous sections define the purpose of the design: the structural safety. A structure can be evaluated as safe if it will fulfil all its functions and requirements during its design working life. This processes implies the evaluation of the structure resistance (R) and the corresponding action (S). The evaluation of R and S need a structural model and a structural analysis method. Using a deterministic method, this request can be express as follows:

$$S \leq R \tag{1.1}$$

In this way, it is also important, to define how a limit state is reached, then, when a structure is no more able to fulfil its functions. A limit state can be defined as follows:

$$S = R \tag{1.2}$$

However, S and R are not deterministic values, but they are affected by uncertainties, which are related to the used of : mathematical models, geometrical models, material behaviour and loads (which are random in nature). The consequently randomness of S and R can be characterized by their mean values (μ_S and μ_R), their standard deviations (σ_S and σ_R), and probability density functions ($f_S(s)$ and $f_R(r)$). In presence of uncertainties, the basic requirements are not simple to satisfy. For this reason, the probabilist approach and the definition of structural reliability need to be introduced (see [2]).
The structural reliability, also known as structural probability of success, can be defined as the probability that the structure will fulfil all its functions during a period of time.

$$P_{success} = P\left[S \leq R\right] \tag{1.3}$$

Therefore, the probability of failure is the converse of the reliability, and this can be expressed as follows:

$$P_{faillure} = 1 - P_{success} = P\left[S > R\right] \tag{1.4}$$

In this way, a structure can be evaluated as reliable if the probability, that the structure will fulfil all its functions during its design working life ($P_{success}$), is higher then a acceptable fixed value (P^*).

$$P^* \geq P_{success} = P\left[S \leq R\right] \tag{1.5}$$

Those relations define a probabilistic space of random variables. The probability of a point (X), which represents the structure and all the input parameters, to be found in the failure domain (U) or in the safety domain (S) can be expressed as follows:

$$\begin{aligned} P_{faillure} &= P\left[X \in U\right] \\ P_{safety} &= P\left[X \in S\right] \end{aligned} \tag{1.6}$$

Structural safety is assured when $P_{failure}$ is a small value, which is different than zero. EC0 gives those values, and for ULS, it can be between 10^{-5} and 10^{-6} (see [1]).

1.2.1 Semi-probabilistic method

In this method, the failure probability (Eq. (1.4)) is replaced by the verification of the Eq. (1.1), where, instead of the aleatory values of R and S, the characteristic values R_k and S_k, and the corresponding partial safety factors γ_R and γ_S are used. Hence, for the verification of a generic limit state, the following expression is used:

$$\gamma_S S_k \leq \frac{R_k}{\gamma_R} \tag{1.7}$$

where R_k and S_k are defined as the lower and the upper fractiles respectively:

$$\begin{aligned} P\left[R < R_k\right] = p \qquad &\longleftarrow \qquad lower\ fractile \\ P\left[S > S_k\right] = p \qquad &\longleftarrow \qquad upper\ fractile \end{aligned} \tag{1.8}$$

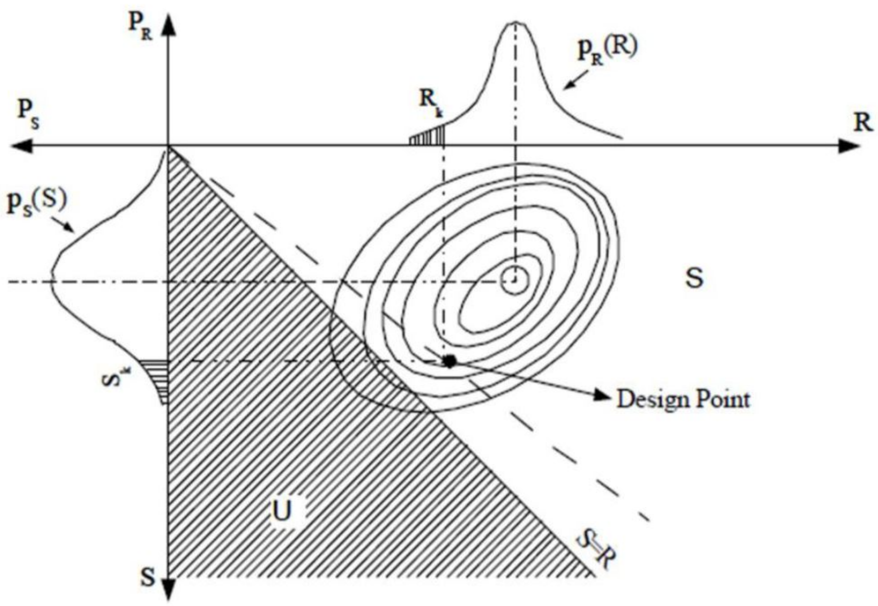

Figure 1.1: Characteristic values in full-probabilistic method

Fig. 1.1 shows those values in the safety and failure domain.

EC0 [1] suggests the values of p to be adopted. The lower fractile, related to the resistance (R_k), should be $p = 5\%$, which means that the resistance value has a 5% of probability to be lower. The upper fractile, related to the action (S_k), should be $p = 5\%$, which means that the action value has a 5% of probability to be higher.

1.2.2 Fist-Order Reliability Method (FORM)

In the precedent paragraph, the failure domain (U) was introduced and it was defined as the subspace of the variable X in which $S \leq R$ is not verified. The safety and the failure domains are showed in Fig. 1.2.

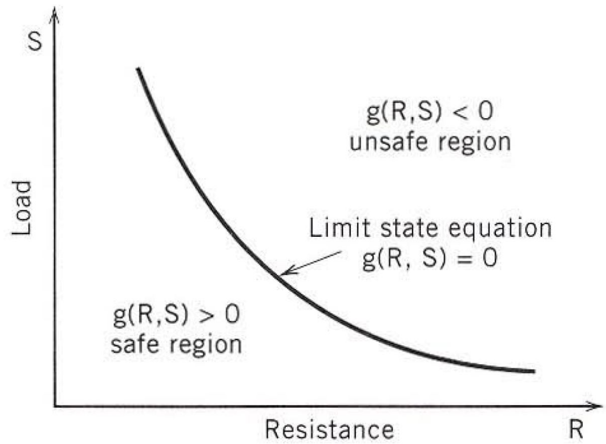

Figure 1.2: Limit State Concept [2]

Therefore, the probability of failure was expressed by the first of Eq. (1.6). Using the Joint Probability Density Function (JPDF) $f_x(x)$ of the vector X, which represents all the aleatory parameters that are involved, the failure probability can be rewritten as follows:

$$P_f = \int_U f_x\left(x\right)\, dx \tag{1.9}$$

The solution of this integral is not evident and it is necessary a numerical integration which is time-consuming. For this reason, many authors proposed the assessment of the reliability by means of a reliability index (β). This index, which has the standard deviation dimension, measures the minimum distance between the vector X mean value and the failure domain contour ($G(R, S) = 0$). Hence, the problem implies the evaluation of β, that can be found evaluating the minimum distance point on the limit state surface. This point is called design point.

The linear limit state equation in two variables is considered (Fig. 1.3):

$$G(X) = R - S = 0 \tag{1.10}$$

where R and S are supposed to be normal distributed ($N(\mu, \sigma^2)$). A set of reduced variables is introduced as:

$$\begin{aligned} R' &= \frac{R - \mu_R}{\sigma_R} \\ S' &= \frac{S - \mu_S}{\sigma_S} \end{aligned} \tag{1.11}$$

where μ and σ are mean and standard deviation values respectively, which are associated to the corresponding variable. The new variables R' and S' are normal distributed ($N(0, 1)$). If Eqs. (1.11) are substituted into Eq. (1.10), the limit state equation in the reduced coordinate system becomes:

$$\sigma_R R' - \sigma_S S' + \mu_R - \mu_S = 0 \tag{1.12}$$

The last expression represents the equation of a line. The distance from the origin point to this line is β (Fig. 1.3(b)).

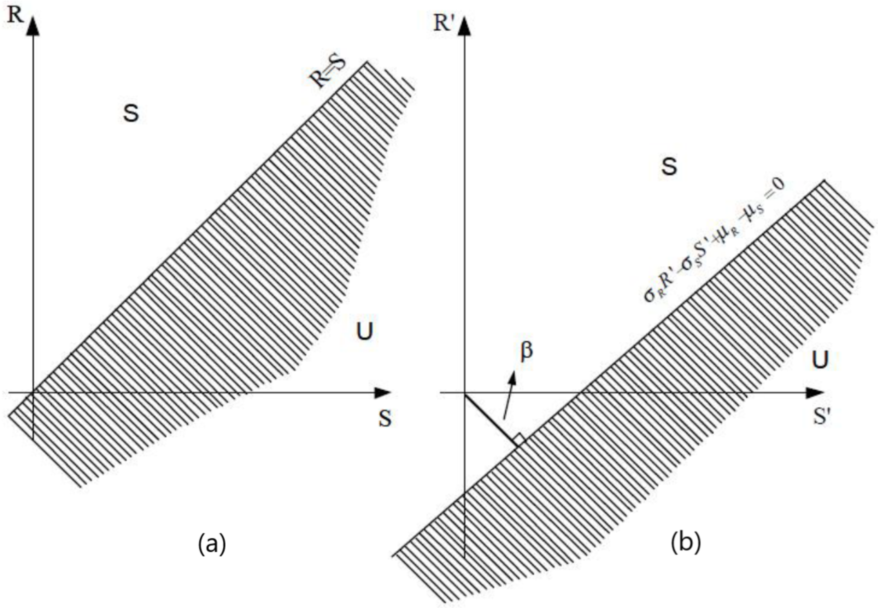

Figure 1.3: Linear limit state: (a) original coordinates, (b) reduced coordinates

Using simple trigonometry, it is possible to calculate the distance of the limit state line (Eq. (1.12)) from the origin as:

$$\beta = \frac{\mu_R - \mu_S}{\sqrt{\sigma_R^2 - \sigma_S^2}} \tag{1.13}$$

Reliability values prescribed by EC0

Tab. 1.2 shows the value of β and the corresponding values of failure probability.

P_f	10^{-1}	10^{-2}	10^{-3}	10^{-4}	10^{-5}	10^{-6}	10^{-7}
β	1.28	2.32	3.09	3.72	4.27	4.75	5.20

Table 1.2: β values and corresponding P_f values [1]

In order to define the reliability of the structure itself, EC0 establishes Consequence Classes (CC), by considering the consequences of failure or malfunction of the structure. Those classes are showed in Fig. 1.4.

Moreover, EC0 defines three Reliability Classes (RC), which are associated with

Consequences Class	**Description**	**Examples of buildings and civil engineering works**
CC3	**High** consequence for loss of human life, *or* economic, social or environmental consequences **very great**	Grandstands, public buildings where consequences of failure are high (e.g. a concert hall)
CC2	**Medium** consequence for loss of human life, economic, social or environmental consequences **considerable**	Residential and office buildings, public buildings where consequences of failure are medium (e.g. an office building)
CC1	**Low** consequence for loss of human life, *and* economic, social or environmental consequences **small or negligible**	Agricultural buildings where people do not normally enter (e.g. storage buildings), greenhouses

Figure 1.4: Definition of consequences classes (CC) [1]

the three consequences classes CC1, CC2, and CC3. The values of β are suggested considering a design working life either of 1 year or 50 years (Fig. 1.5).

1.2.3 Full-probabilistic method

This approach considers the material resistance and the permanent and variable loads as aleatory variables, with their Probability Density Functions (PDF).

The performance function ($G(X)$) describes the failure and the safe domains as follows:

Reliability Class	Minimum values for β	
	1 year reference period	50 years reference period
RC3	5,2	4,3
RC2	4,7	3,8
RC1	4,2	3,3

Figure 1.5: Reccomended minimum values of reliablity index β (ULS) [1]

$$\begin{cases} G(X) > 0, & \rightarrow \text{success} \\ G(X) < 0, & \rightarrow \text{failure} \end{cases} \tag{1.14}$$

Hence, the failure probability can be written as:

$$P_f = \int_{G(X) \leq 0} f(x)\, dx \tag{1.15}$$

The reliability problem can be solved by the last integral, however the evaluation of Eq. (1.15) rarely lead to a closed form solution. A resistance-action bi-dimensional space is considered, such as the linear limit state in two variables in Fig. 1.3(a), where R and S are independent variables, and the corresponding PDFs ($f_R(r)$ and $f_S(s)$) are known. Eq. (1.15) can be rewritten as:

$$P_f = \int_{G(X) \leq 0} f(x)\, dx = \iint_{[R-S \leq 0]} f_{R,S}(r,s)\, dr\, ds \tag{1.16}$$

As R and S are independent variables, it results:

$$f_{R,S}(r,s) = f_R(r) \cdot f_S(s) \tag{1.17}$$

Therefore, Eq. (1.16) can be considered as follows:

$$P_f = \iint_{[R-S \leq 0]} f_{R,S}(r,s)\, dr\, ds = \int_0^{\infty} f_S(s) \cdot F_R(s)\, ds \tag{1.18}$$

Hence, P_f can be evaluated by a convolution integral of two functions, where $f_S(s)$ is JPDF related to the variable S, and $F_R(s) = P\,[R < S]$ is the Cumulative Distribution Function (CDF) related to the variable R. Fig. 1.6 illustrates the geometrical meaning of this integration.

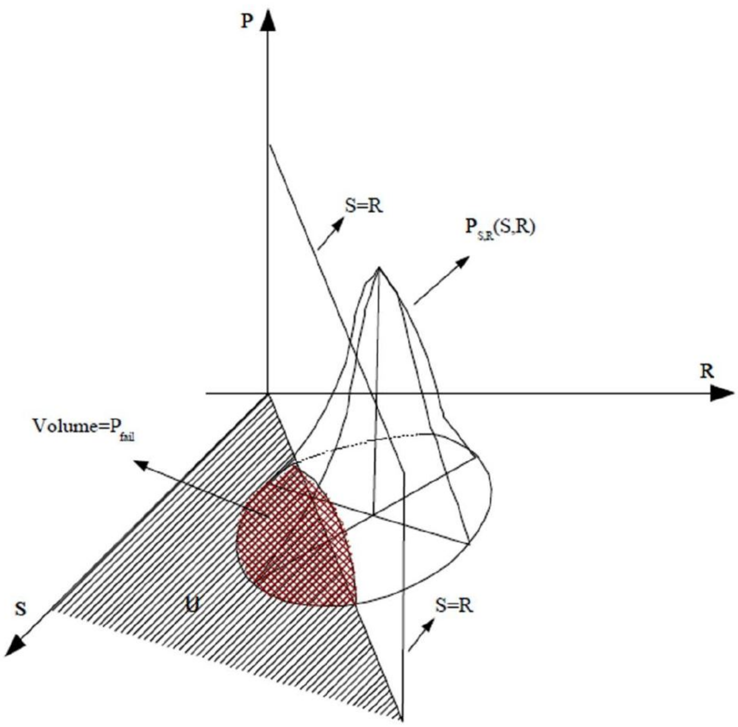

Figure 1.6: Geometrical meaning of the integration Eq. (1.18)

1.3 Simulation techniques

The treatment of aleatory and model uncertainties, which will be discus in Chapter 3, requires a strong background in probability and statistics.
In the simplest form of the basic simulation, each random variable in a problem is sampled several times, in order to represent its real distribution according to its probabilistic characteristics. The method commonly used for this purpose is called the Monte Carlo (MC) simulation technique [2].

1.3.1 Monte Carlo simulation technique

In a probabilistic approach, the uncertainty linked to the input parameter, such as material properties, applied loads and geometric properties, are modelled with various probability distributions. In this way, the first step of MC method is the

definition of the problem in terms of all random variables [2].
Hence, the limit state function of this problem can be written as:

$$G(X) = G(X_1, X_2, X_3, ..., X_n) \tag{1.19}$$

where X_i are the problem variables. Consequently, it is necessary quantifying the probabilistic characteristics of all the random variables in terms of their PDFs, which depends on the parameter nature. The next paragraphs describe the Monte Carlo methodology.

Creating the sample: random number generation

For the creation of a sample of interest, a domain of definition of possible inputs is established and the inputs are randomly generated from a well-defined probability distribution. The random variables to be generated could be continuous or discrete.

Running the Numerical Model

All the generated values X can be substituted in G function to verify if the corresponding G value is positive (success) or negative (failure). This process needs a huge number of values, which means that for a failure probability of 10^{-6}, $N = 10^{8.9}$ samples are required in order to achieve a good accuracy of results.

Analysing the data

The probability of failure is obtained as follows:

$$P_f = P\left[G(X) \leq 0\right] = \lim_{N \to \infty} \frac{n}{N} \tag{1.20}$$

where n is the number of failure cases ($G(X) \leq 0$) and N is the total number of MC simulations. The value of this ratio is generally small, and the estimated probability is subjected to uncertainty. Moreover, the variance value of this ratio decreases when N increases; hence, the related uncertainty decreases when N increases.

Advantages and limitations of using Monte Carlo

The main advantage of Monte Carlo is its easy numerical implementation, especially for complex cases where the analytical expressions are too complicated. The results are reliable and accurate. However, it may take a lot of time, depending on the complexity of the problem and the number of samples drawn.

1.3.2 Latin Hypercube Sampling

Latin Hypercube Sampling (LHS) is a form of stratified sampling that can be applied to multiple variables. The method is commonly used to reduce the number of samples necessary in a Monte Carlo simulation, to achieve a reasonably accurate random distribution [2]. MC simulation provide statical answers to problems by performing many calculation with randomized variables, and analysing the trends in the output data. The concept behind LHS is based on the same approach: the variables are sampled using a sampling method, and then randomly combined sets of those variables are used for one calculation of the target function. The sampling algorithm ensures that the distribution function is sampled evenly, but still with the same probability trend. Fig. 1.7 reports the difference between a pure random sampling (red line) and a stratified sampling of a log-normal distribution (blue line).

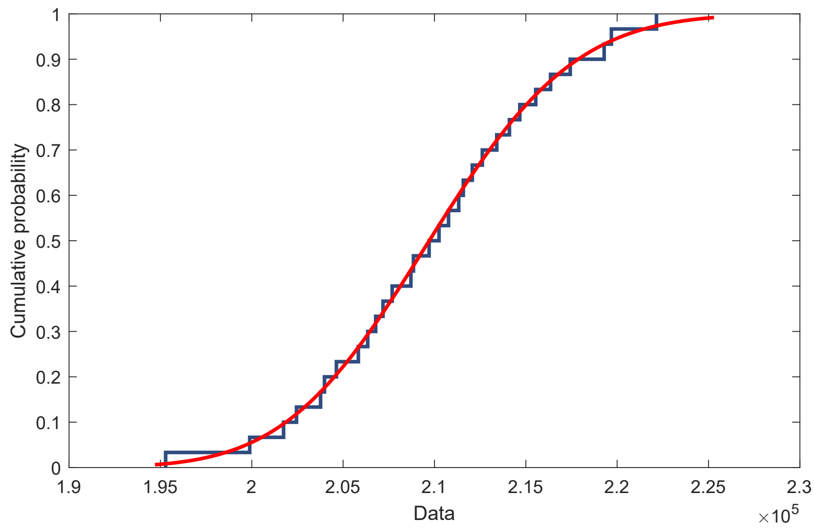

Figure 1.7: Cumulative frequency plot

The process is described in the following paragraphs.

Sampling

In this method, n different values, from each k random variables X_1,...,X_k, are sampled. The range of each variable is divided into n non-overlapping intervals on the basis of equal probability of occurrence, which means that the area of each interval under the density function should be equal to the probability value of:

$$P(X) = \frac{1}{n} \tag{1.21}$$

In case of a normal distribution and for a sample size n=10, the probability density function should be divided into five portions of equal probability:

$$P(X) = 0.10 \tag{1.22}$$

Consequently, the interval limits can be easily be determined from the cumulative distribution function in Fig. 1.8.

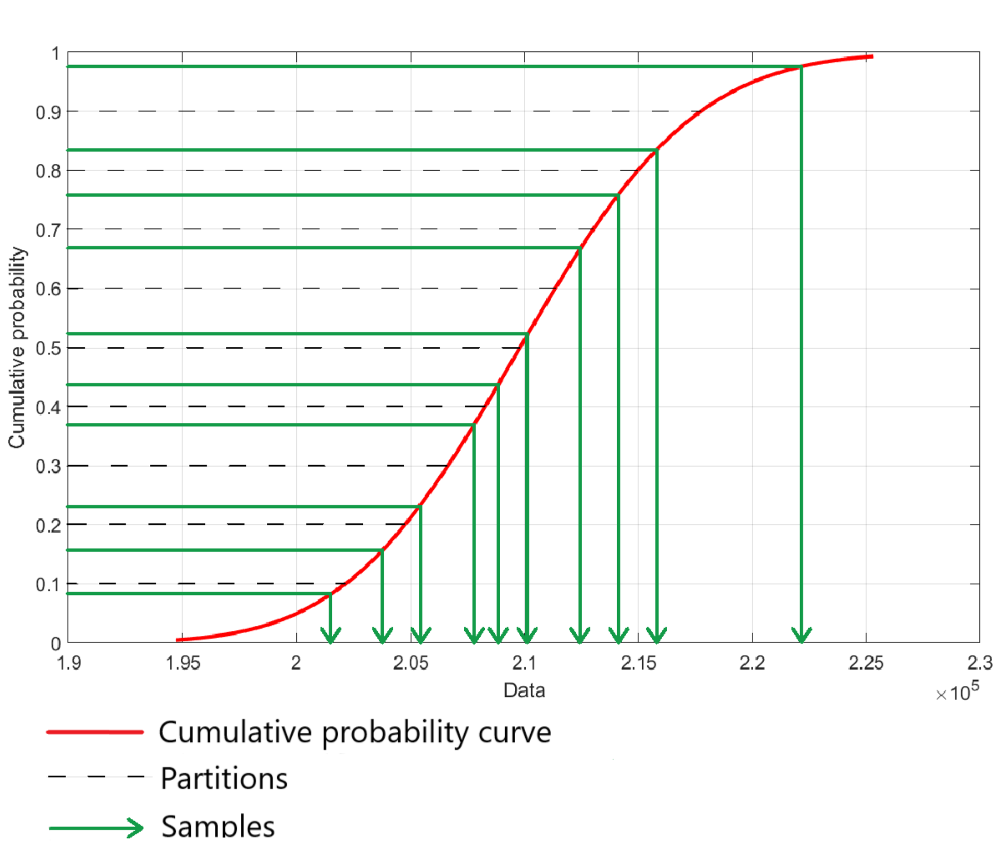

Figure 1.8: Sampling in LHS

Then, n different values (between 0 and 1) in n non-overlapping intervals are randomly selected for each random variable, consequently one value per interval is generated. Next step is to convert these random variables into cumulative probabilities for each of the n intervals by the following linear transformation:

$$P_m = \left(\frac{1}{n}\right) U_m + \left(\frac{m-1}{n}\right) \tag{1.23}$$

where m is the integer counter between 1 and n corresponding to the interval number, U_m is the random number generated between 0 and 1, and P_m is the cumulative probability value for the m^{th} interval obtained from the randomly generated number. Only one generated value falls into each of the n intervals since:

$$\frac{m-1}{n} < P_m < \frac{m}{n} \tag{1.24}$$

where $(m-1)/n$ and m/n are the lower and the upper bound for the m^{th} interval. Then, P_m values are inserted in the inverse distribution function (F_X^{-1}) to obtain the specific values of the sample:

$$X_{k,m} = F_X^{-1}(P_m) \tag{1.25}$$

Grouping

The generated values for each random variable are paired together. To achieve this, random permutation of n numbers corresponding to n generated values is used for each variable. Finally, grouping is accomplished by associating those different random permutation. Each value must be used once.

1.4 Statistical tests

In this work, statistical tests have been used in hypothesis testing as goodness of fit of a log-normal distribution, in other word, those tests establish if an observed distribution differs from a theoretical distribution [3].
The Pearson's chi-squared test and the Anderson-Darling test have been used, and they are explained in the following paragraphs.

Pearson's chi-squared test

This test uses the statistic variable χ^2, which is a normalized sum of squared deviations between observed and theoretical values (see [4]). It can be expressed as follows:

$$\chi^2 = \sum_{i=1}^{n} \frac{(O_i - E_i)^2}{E_i} \tag{1.26}$$

where:

- n is the classes number in which the sample is divided;
- O_i are the observed values;
- E_i are the expected values.

The test compare χ^2 to the critical value, from the chi-squared distribution, defined for a particular degree of freedom and a choose confidence level.
The Degree Of Freedom (DOF) is defined as:

$$DOF = n - s - 1 \tag{1.27}$$

where s is the number of distribution parameters. For example, a log-normal distribution has 2 parameters
The confidence level is defined by the p-value.

Anderson-Darling test

This test compares the data cumulative distribution function ($F(X)$), to the theoretical cumulative distribution ($P(X)$) (see [5]). The test statistic is defined as follows:

$$A^2 = n \int_{ALLX} \frac{(P(X) - F(X))^2}{P(X)(1 - P(X))} dP(X) \tag{1.28}$$

This is a parameter that represent the area between $F(X)$ and $P(X)$.
The test compare the value of A^2 to the critical value, for a specified significance level.

Those tests are implemented in MATLAB [6]. Using the function $[h, p] = adtest(x)$ and $[h, p] = chi2gof(x)$, where x is the vector of the observed values. When:

- $h = 1$, x is not from a population with a normal distribution;
- $h = 0$, x is from a population with a normal distribution;
- p (p-value) is the corresponding confidence level.

Chapter 2

Structural instability

2.1 Introduction

Failures of many structures are caused by either material failure or structural instability [7].

The first type of failure can usually be adequately predicted by analysing the structure on the basic of equilibrium conditions or in terms of equations of motion, that are written for the initial undeformed configuration of the structure itself.
On the other hand, a large number of structures can suffer a change in their deformation during loading. This change is usually accompanied by a major or minor reduction of stiffness and, consequently, the prediction of failures needs equations of equilibrium formulated on the basis of the deformed configuration of the structure itself. Since the deformed configuration is not known in advance, but depends on the deflections to be solved, the problem is non-linear. This change of shape may affect the distribution and the magnitude of the internal forces and the loading capacity of the structural element.

Structural failures caused by failure of the material (typical for shorten columns) are governed by the value of the material strength (the crushing of the concrete) or yield limit (the excessive yielding of the tensile reinforcement), and it is independent of the structural geometry and size.
At the same time, the load at which a structure becomes unstable can be, in simple way, treated as independent of the material characteristics; but it depends on structural geometry and size, in particular by slenderness, and it is governed firstly by the stiffness of the material. In fact, when failure instability occurs, the material

does not reach its strength limit.

In general, the columns behaviour is affected by the following parameters: the slenderness, the loading system, the shape of the column, the bearings, the material properties, and the amount of reinforcement.

In the following paragraphs it is treated a description of instability problems. The second order effects are considered relevant just in one direction. Moreover, the effect of torsion are neglected.

A distinction between columns and beam-columns is needed [8]. A column is defined as a structural element loaded by a concentric axial load only. A beam-column is defined as a beam loaded with axial load and an applied moment, either owing to an eccentrically applied axial load or a transverse load.

2.2 Buckling with stable brunching

This form of instability, also known as Euler instability, occurs in axially loaded elastic element such as columns. In this case, the unbuckled and the buckled states are very close to each other. At the same time, the buckled structure is still able to sustain loads larger than the critical (see [9]).
The buckling structural deformation is completely different from the structural deformation in the pre-buckling states. For example, a rectilinear column axially loaded, remain rectilinear in the pre-buckling loaded state, while it bends at buckling.
It is theoretically possible that the column could remain rectilinear under load larger than the critical. However, these equilibrium states are unstable and cannot be maintained if any disturbance, however small, is applied to the structure.
The existence of various equilibrium branches, that depart from the critical state, implies that a symmetric and stable equilibrium bifurcation occurs at buckling.

Fig. 2.1 shows a hinged supported beam subjected to a compressive force (N) applied at the centre of gravity. Starting from an unload condition, the load can be increase. In the $N - w$ plane, where w is the axial shortening, the loading path will firstly be represented by the rectilinear segment OB, in which N increasing from zero up to the critical value N_c. This segment describes the linearly elastic shortening of the column. The equilibrium configuration is given in a deformed shape which is similar to the initial straight shape configuration. In the $N - v$ plane, where v is the transversal displacement, the loading path will be represented by the linear segment $O'B'$, along the N axis. This means that, if $N < N_c$, the equilibrium configuration does not show any inflection, and the deformed shape is similar to the undeformed configuration.

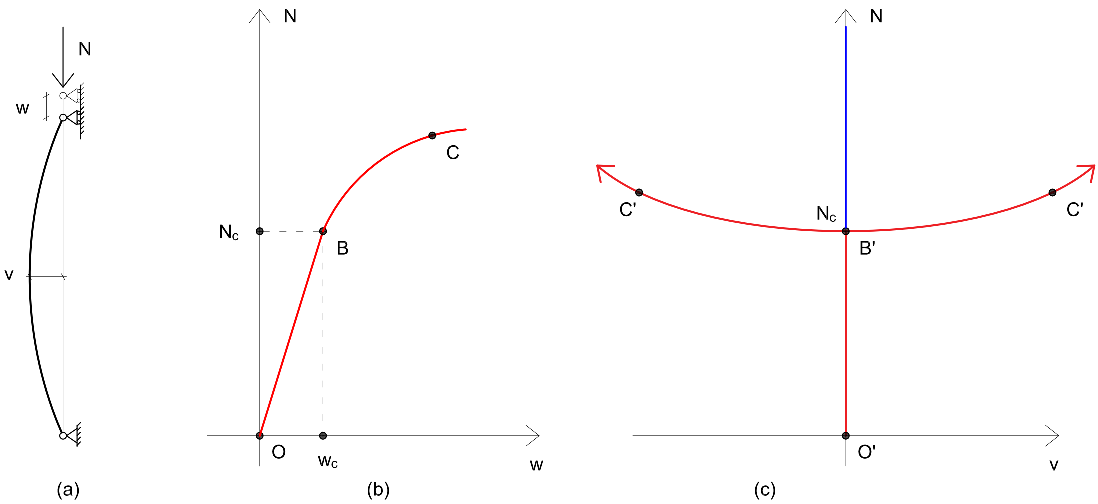

Figure 2.1: Buckling with stable brunching: (a) the deflection of the axially loaded column, (b) $N - w$ plane, (c) $N - v$ plane

Furthermore, when the axial load reaches the critical load ($N = N_c$), the $N - w$ curve suddenly bends, but N continues to be an increasing function of the shortening w. This curve shows also the deformability increase, when $N > N_c$.
Other informations can be obtained in the $N - v$ plane, where $N = N_c$, in point B'. There are two symmetrical branches $B'C'$ corresponding to the buckled column, which represent the stable buckled states.
The unstable rectilinear equilibrium states are then represented by points along the vertical axis (blue line), in which suppose a pure compression.

2.3 Columns

2.3.1 Instability of linear elastic columns

As first example, it is considered a column of length l on two simple supports and concentrically loaded [8]. If secondary order effects are token into account, the axial force N causes a bending moments which can not be found until the deflections are determined. The column is therefore statically indeterminate, and it is necessary to solve the differential equation for the deflection curve of the column.
In fig. 2.2 is showed a simply supported column.

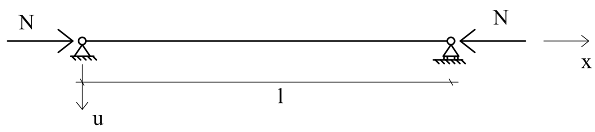

Figure 2.2: Simply supported column concentrically loaded

The section rigidity EI is constant along the column.
As the secondary effects are taken into account, the moment equilibrium gives as follow:

$$M - Nu = 0 \tag{2.1}$$

where u is the displacement along the transversal direction of the column axis. The bending moment (M) is determined by the well-know formula:

$$M = -EI\frac{d^2u}{dx^2} \tag{2.2}$$

which inserted in the Eq. (2.1) gives the following differential equation:

$$EI\frac{d^2u}{dx^2} + Nu = 0 \tag{2.3}$$

This is an ordinary homogeneous second order differential equation, which must be solved using the following boundary conditions:

$$u(x = 0) = 0 \qquad u(x = l) = 0 \tag{2.4}$$

It can be introduced the factor α as follows:

$$\alpha^2 = \frac{N}{EI} \tag{2.5}$$

The Eq. (1.3) can be rewritten as:

$$\frac{d^2u}{dx^2} + \alpha^2 u = 0 \tag{2.6}$$

The complete solution of Eq. (2.6) is:

$$u = Acos(\alpha x) + Bsin(\alpha x) \tag{2.7}$$

The two constants A and B are determinate from the boundary conditions (discarding the trivial solution A=B=0) and as a result, the solution of Eq. (2.7) is given by:

$$sin(\alpha l) = 0 \qquad \rightarrow \qquad \alpha l = \pi + n\pi \qquad (n = 0, 1, 2, ...) \tag{2.8}$$

The axial loads (N) obtained through this solution are the eigenvalues and the corresponding solutions $u(x)$ are eigenfunctions. The eigenfunctions give the information about the column deformed shape, but the deformed magnitude can not be determinate. When $n = 0$, $\alpha l = \pi$, which gives the first and lowest value of N, which corresponds to the Euler's equation:

$$N_{CR} = \frac{\pi^2 EI}{l^2} \tag{2.9}$$

The corresponding eigenfunction is shows in Fig. 2.3.
The Euler's equation (2.9) can be use to define the critical buckiling stress:

$$\sigma_b = \frac{N}{A} = \frac{\pi^2 EI}{Al^2} = \frac{\pi^2 E\rho^2}{l^2} \tag{2.10}$$

Introducing the slenderness factor λ, defined as the ratio of the length of the column over the radius of gyration of the transversal section, the Eq. (2.10) can be rewrite as:

$$\sigma_b = \frac{\pi^2 E}{\lambda^2} \tag{2.11}$$

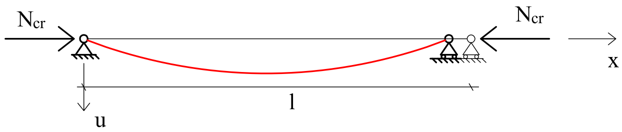

Figure 2.3: First eigenfunction for a simply supported column

Firstly this equation means that when the material characteristics are fixed, the strength critical value (σ_c) depends only by λ. Secondly, it shows that the critical buckling stress (that can be seen as the load-carrying capacity) goes to infinity when $l \to 0$.

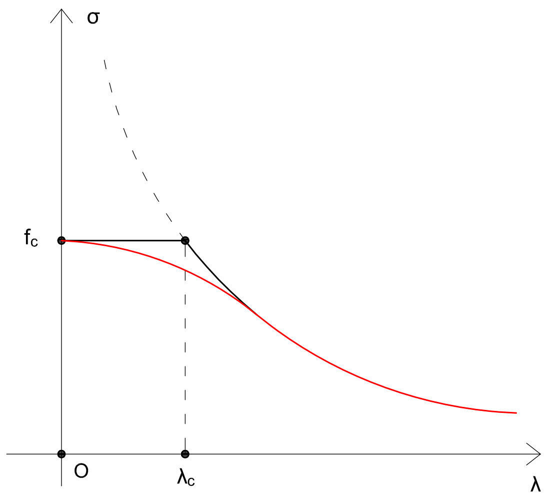

Figure 2.4: The Euler hyperbola with a cut off at the limited strength f_c

Since this condition can not be physically possible and the materials have limited strength, the Euler's equation has to be cut off at the corresponding material strength (see Fig. 2.4).
Therefore, for slender columns, critical stress is usually lower than the compressive strength. As contrary, a stocky column has a critical buckling stress higher than the compressive strength, which means that the element reaches the material capacity. The red curve in Fig. 2.4 identifies an interaction between the two types of failures. If there was no interaction, a critic slenderness λ_c could be identified as:

$$\lambda_c = \pi\sqrt{\frac{E}{f_c}} \tag{2.12}$$

2.3.2 Instability of inelastic columns

Structural problems related to instability can occur when applied loads generate stress beyond the elastic limits. In this case the structure behaviour depends on two non-linearities: the rigidity decrease due to the compression force and the deformability increase of the material due to stress beyond the linear limits.

Engesser's method

Engesser's method is based on the Euler's equation, with a modification of the modulus of elasticity (see [8]). He introduces the tangent modulus of the stress-strain relationship at the current stress level. Therefore,the corresping inclination is used as elastic modulus (E_σ) of the material (see Fig. 2.5).

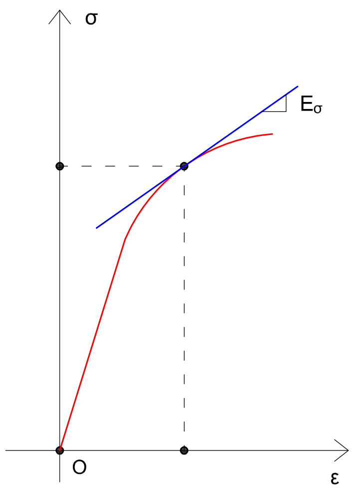

Figure 2.5: Stress-strain curve for a soft material

Hence, the critical stress can be calculated as:

$$\sigma_{cr} = \frac{N_{cr}}{A_c} = \frac{\pi^2 E_\sigma}{\left(\frac{l}{i}\right)^2} \tag{2.13}$$

For a reinforced concrete column, it possible to consider a parabolic stress-strain behaviour of the concrete. The tangent modulus is determined as:

$$E_\sigma = E_0\sqrt{1-\frac{\sigma}{f_c}} \tag{2.14}$$

which can be inserted into Eq. (2.13) to derive the critical stress (σ_{cr}).
As this column is reinforced, the influence of the steel can be token into account as a contribution calculated on the basis of the critical stress assumed for the concrete. Thus, the critical load (N_{cr}) for the column can be calculated as:

$$N_{cr} = \sigma_{cr}bh + \sigma_s A_s \tag{2.15}$$

However, this simplification returns a σ_{cr} value that is underestimated since the stiffness of the reinforced column is higher than the stiffness of the unreinforced column.

Ritter's method

Ritter took the Engesser's method introducing a simplification. His theory determined the stiffness-stress relation of concrete as follows:

$$E_\sigma = E_0\left(1-\frac{\sigma}{f_c}\right) \tag{2.16}$$

which leads a difference between the stiffness corresponding to a parabolic law (calculated with Engesser's method) and the Ritter stiffness (see Eq. (2.16)).
Substituting the Eq. (2.16) into Eq. (2.13) leads to:

$$\sigma_{cr,Ritter} = \frac{f_c}{1+\frac{f_c}{\pi^2 E_{c0}}\left(\frac{l}{i}\right)^2} \tag{2.17}$$

2.4 Beam-Columns

2.4.1 Instability of linear elastic beam-columns

In this section, the solution of the linear elastic problem for beam-columns is briefly introduced (see [8] and [9]) . The load carrying capacity for beam-columns loaded with either an eccentric axial load or a concentrically axial load along with lateral loading will be derived.

Beam-columns loaded with an eccentric axial load

Figure 2.6: Statical system of an eccentrically loaded beam-column

The equilibrium equation for the deflected beam-column loaded with an eccentric axial load is:

$$M - M_0 - Nu = 0 \tag{2.18}$$

where M_0 is the first order moment. With Eq. (2.2), Eq. (2.18) becomes:

$$EI\frac{d^2u}{dx^2} + N(u + e) = 0 \tag{2.19}$$

This is an inhomogeneous second order differential equation, which must be solved with the following boundary conditions:

$$u(x = 0) = 0 \qquad u(x = l) = 0 \tag{2.20}$$

The complete solution is the sum of the homogeneous and an inhomogeneous solution.
Eq. (2.19) may be rewritten as:

$$\frac{d^2u}{dx^2} + \alpha^2(u + e) = 0 \tag{2.21}$$

The solution of this equation is:

$$u = Asin(\alpha x) + Bcos(\alpha x) + e \tag{2.22}$$

The two costants A and B can be determined by means of the boundary conditions, Eqs. (2.20):

$$B = 0 \; and \; A = \frac{e}{sin\alpha l} \tag{2.23}$$

The values of those two costants can be inserted into Eq. (2.22), that gives:

$$u = e\left(1 + \frac{sin(\alpha x)}{sin\frac{\alpha l}{2}}\right) \tag{2.24}$$

This solution can be inserted into the equilibrium equation for the deflected beam-column, Eq. (2.18) and consequently the combination of N and M can be determined.

Beam-columns loaded with concentrated lateral load

Fig. 2.7 shows a simply supported beam-column under a concentrated lateral load (V) applied in the mid spam of the element.

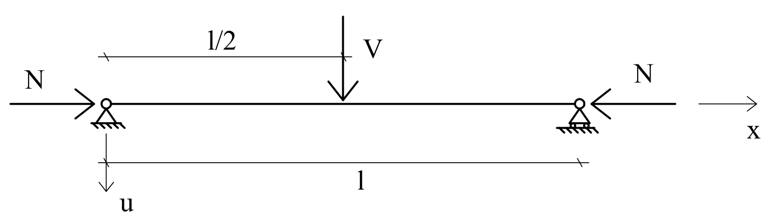

Figure 2.7: Beam-column with concentrated lateral load

The equilibrium of the bending moments, in the left and right-hand portions, gives respectively:

$$\begin{aligned} M - Nu - \frac{V}{2}x = 0 \\ M - Nu - \frac{V}{2}(l - x) = 0 \end{aligned} \tag{2.25}$$

Sobstituting Eq. (2.2) in Eqs. (2.25):

$$\begin{aligned} EI\frac{d^2u}{dx^2} + Nu + \frac{V}{2}x = 0 \\ EI\frac{d^2u}{dx^2} + Nu + \frac{V}{2}(l-x) = 0 \end{aligned} \tag{2.26}$$

Eq. (2.26) may be rewritten as:

$$\begin{aligned} \frac{d^2u}{dx^2} + \alpha^2 u + \frac{V}{2EI}x = 0 \\ \frac{d^2u}{dx^2} + \alpha^2 u + \frac{V}{2EI}(l-x) = 0 \end{aligned} \tag{2.27}$$

The general solutions of those equations are:

$$\begin{aligned} u = A\cos\alpha x + B\sin\alpha x - \frac{V}{2N}x \\ u = C\cos\alpha x + D\sin\alpha x - \frac{V}{2N}(l-x) \end{aligned} \tag{2.28}$$

The constants of integration A, B, C and D are determined from the boundary conditions, at the end of the beam and at the point of load V application. Since the deflections at the ends of the beam column are zero:

$$\begin{aligned} A = 0 \\ C = -D\tan\alpha x \end{aligned} \tag{2.29}$$

At the point of application of the load, the deflections given by Eq. (2.23) have to be the same. Moreover, a common tangent is the second condition of this problem. These conditions give:

$$\begin{aligned} B = \frac{V\sin\alpha\frac{l}{2}}{N\alpha\sin\alpha l} \\ D = -\frac{V\sin\alpha\frac{l}{2}}{N\alpha\tan\alpha l} \end{aligned} \tag{2.30}$$

Substituting A, B, C and D into Eqs. (2.28):

$$\begin{aligned} u = \frac{V\sin\alpha\frac{l}{2}}{N\alpha\sin\alpha l}\sin\alpha x - \frac{V}{2N}x \qquad 0 \le x \le \frac{l}{2} \\ u = \frac{V\sin\alpha\frac{l}{2}}{N\alpha\sin\alpha l}\sin\alpha\frac{l}{2} - \frac{V(l-x)}{2N} \qquad \frac{l}{2} \le x \le l \end{aligned} \tag{2.31}$$

This solution can be inserted into the equilibrium equation for the deflected beam-column Eq. (2.25), hence, the combination of V, N and M can be determined.

2.5 Procedures for columns

The analysis methods for reinforced concrete structures subjected to second order effects are formulated by Euro Code 2 (EC2) [10].
In general, the verification for instability is made by showing that, under the most unfavourable conditions of design actions, it is possible to achieve a stable state of equilibrium between the external and internal force, by taking account of second order deformations.
All structures are subjected to geometrical imperfections, which leads to accidental eccentricity in columns and beam-columns. Considering this problem, an additional eccentricity (e_a) needs to be introduced in the most unfavourable direction:

$$e_a = \frac{l_0}{300} \tag{2.32}$$

In this way, in a column of constant cross-section, subjected to an equal eccentricity, with the same sign at both ends, the total eccentricity to be token into account in the analysis is (see Fig. 2.8):

$$e_{tot} = e_1 + e_2 = e_0 + e_a + e_2 \tag{2.33}$$

where:

- $e_0 = M_{Sd1}/N_{Sd}$ is the first order eccentricity;
- M_{Sd1} is the first order applied moment;
- N_{Sd} is the applied axial load;
- e_2 is the second order eccentricity.

EC2 shows three methods to be used for the analysis and the design of columns and beam-columns, in which the second order effects ar consider, but with different

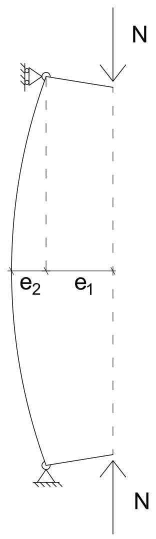

Figure 2.8: Eccentricities in a column

degree of accuracy.
The most accurate method is:

- General method;

and the other two are simplified methods:

- Method based on nominal stiffness;
- Method based on nominal curvature.

EC2 shows that if the λ of the column is higher than a critical value λ_{lim}, second order effects can not be neglected, otherwise they could be ignored. The recommended value of λ_{lim} is:

$$\lambda_{lim} = 20AB\frac{C}{\sqrt{n}} \tag{2.34}$$

where:

- A=$\frac{1}{1+0.2\varphi_{ef}}$ where φ_{ef} is the effective creep ratio;

- B=$\sqrt{1+2\omega}$ where ω is the percentage of reinforcement;

- C=1.7-r_m where r_m is the ratio between the first order end moments at the column extremities;

- n=$\frac{N_{Ed}}{A_c f_{cd}}$ is the relative normal force;

- $r_m = \frac{M_{01}}{M_{02}}$ is the moment ratio, with $|M_{02}|>|M_{01}|$

Column slenderness is evaluated as the ratio of the effective length over the gyration radius of the un-cracked concrete section:

$$\lambda = \frac{l_0}{i} \tag{2.35}$$

The effective length (l_0), so called effective buckling length, is evaluated for isolated columns and it depends on the end conditions. Fig. 2.9 shows three columns characterized by different l_0, owing to different end conditions.

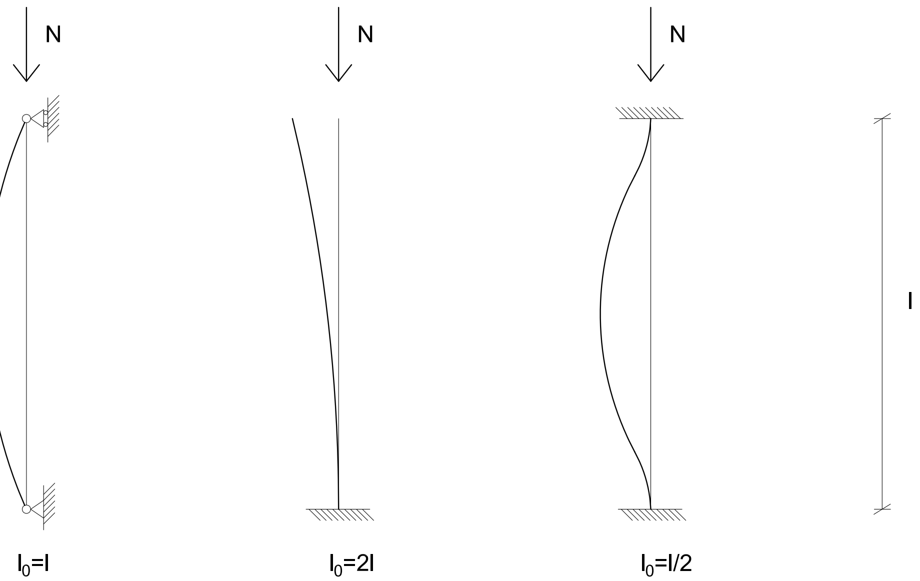

Figure 2.9: Effective lenght for columns on different end conditions

2.5.1 General method

This method represents the best approximation of the real column behaviour. It is based on non-linear analysis, which is carried out ensuring that equilibrium and

compatibility are satisfied. As this method is used as a verification, the column have to be pre-dimensioned in advance.
Firstly, a model column have to be defined from a generally restrained column. A model column is a cantilever column, clamped at the base, that is characterized by a length equal to l_0 which is the determinant length of the real column, however constrained. In the most general case a variable section is considered.
The finite element method is used for this analysis, hence the first step is the subdivision of the column in segments having height equal to the biggest depth of the section. Each segment is subjected to an horizontal force (V), a bending moment (M_n) and a vertical force (N_n). The vertical force is given by the applied top force combined with the self-weight of the column it self.
Fig. 2.10 shows the column displacement (y_n), and the bending moment:

- y_n column displacement;
- bending moments:
  - M_{1n} first order contribution, which is trapezoidal, starts from M_0 and increases due to the horizontal force;
  - M_{2n} second order contribution given by force N_n due to the eccentricity.
- $1/\tau_n$ curvature diagram.

The displacement of the point n can be approximated given by the Taylor series:

$$y_n = y_{n-1} + xy'_{n-1} + \frac{x^2}{2}y''_{n-1} \tag{2.36}$$

From Eq. (2.36) it is possible to derive the mean slope as follows:

$$y'_{n-1} = \frac{1}{2x}\left(y_n - y_{n-2}\right) \tag{2.37}$$

and the curvature:

$$y''_{n-1} = \frac{1}{\tau_{n-1}} \tag{2.38}$$

Substituting Eq.(2.37) and (2.38) in Eq. (2.36):

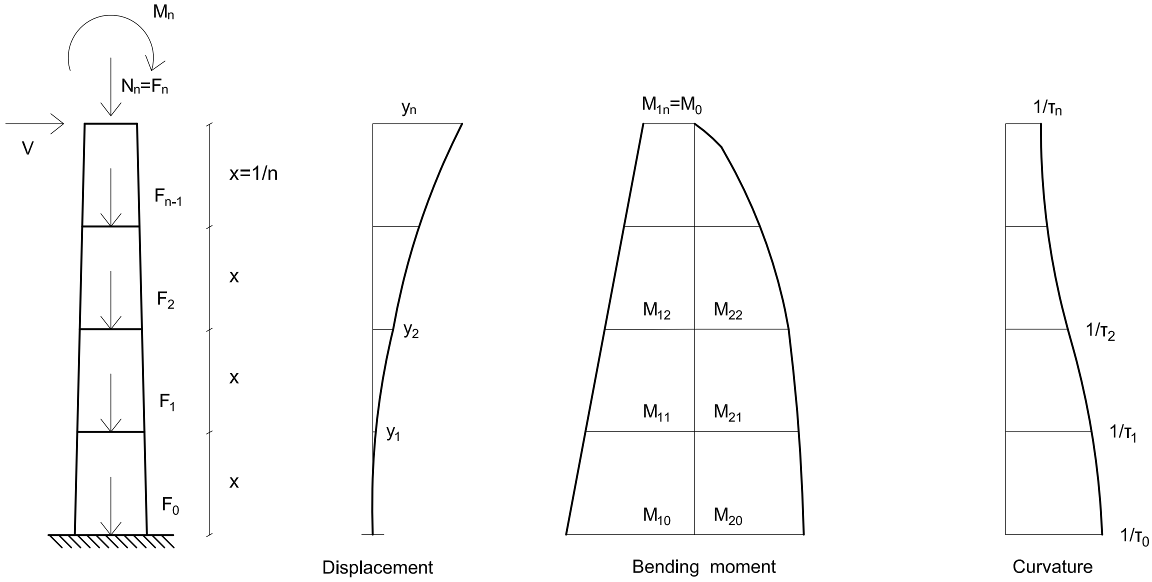

Figure 2.10: Cantilever column with variable cross-section

$$y_n = y_{n-1} + x\frac{1}{2x}\left(y_n - y_{n-2}\right) + \frac{x^2}{2}\frac{1}{\tau_{n-1}} = 2y_{n-1} - y_{n-2} + \frac{x^2}{\tau_{n-1}} \tag{2.39}$$

The same expression can be written for the point $(n-1)$:

$$y_{n-1} = 2y_{n-2} - y_{n-3} + \frac{x^2}{\tau_{n-2}} \tag{2.40}$$

Writing the Eq. (2.40) for the point n=3:

$$y_2 = 2y_1 + \frac{x^2}{\tau_1} \tag{2.41}$$

As $y_0 = 0$, Eq. (2.40) can be written also for the point $n = 2$ and if a symmetrical deformation for $x < 0$ is supposed, the obtained results is:

$$y_1 = -y_1 + \frac{x^2}{\tau_0} \qquad \rightarrow \qquad y_1 = \frac{x^2}{2\tau_0} \tag{2.42}$$

The displacement for each point can be expressed as a function of the curvatures:

$$\begin{cases} y_1 = \frac{x^2}{2\tau_0} \\ y_2 = \frac{x^2}{2\tau_0} + \frac{x^2}{\tau_1} = x^2\left(\frac{1}{2\tau_0} + \frac{1}{\tau_1}\right) \\ y_3 = x^2\left(\frac{4}{2\tau_0} + \frac{1}{\tau_1}\right) - x^2\left(\frac{1}{2\tau_0}\right) = x^2\left(\frac{3}{2\tau_0} + \frac{2}{\tau_1} + \frac{1}{\tau_2}\right) \\ ... \\ y_n = x^2\left(\frac{n}{2\tau_0} + \frac{n-1}{\tau_1} + \frac{n-2}{\tau_2} + ... + \frac{2}{\tau_{n-2}} + \frac{1}{\tau_{n-1}}\right) \end{cases} \tag{2.43}$$

Considering $1/\tau_i = 1/\tau_0$, it is assumed that all sections have the same curvature of the first element, resulting in:

$$\begin{cases} y_1 = 0.5x^2\frac{1}{\tau_0} \\ y_2 = 0.5\left(2x^2\right)\frac{1}{\tau_0} \\ y_3 = 0.5\left(3x^2\right)\frac{1}{\tau_0} \\ ... \\ y_3 = 0.5\left(nx^2\right)\frac{1}{\tau_0} \end{cases} \tag{2.44}$$

As the first order bending moments are known, the total bending moment can be expressed as follows:

$$\begin{cases} M_0 = M_{10} + V_n y_n + V_{n-1}y_{n-1} + ... + V_1 y_1 \\ M_1 = M_{11} + V_n\left(y_n - y_1\right) + V_{n-1}\left(y_{n-1} - y_1\right) + ... + V_2\left(y_2 - y_1\right) \\ ... \end{cases} \tag{2.45}$$

Moreover, the axial loads and concrete capacity are:

$$\begin{cases} N_0 = F_0 + F_1 + F_2 + ... + F_n & N_{c0} = A_{c0}f_c \\ N_1 = F_1 + F_2 + F_3 + ... + F_n & N_{c1} = A_{c1}f_c \\ ... \end{cases} \tag{2.46}$$

where F_n are the axial loads at each sections. Knowing the value of M_i and N_i, it is possible to calculate the curvature in each point as a function of those values:

$$\frac{1}{\tau_i} = f\left(M_i, N_i\right) \tag{2.47}$$

The procedure has to be iterated till the results do not change significantly from one

step to the next. If the results do not converge, it means that there is no equilibrium and the failure occurs.
Finally, the load capacity of a column can be reported in a interaction diagram between the external first order moment M_1 and the axial load N.

2.5.2 Method based on nominal stiffness

This method takes into account a geometric non linearity and a material linear behaviour (see [10]). The material non linearity is considered evaluating the distribution of flexural stiffness on the elements. The rigidity can be estimate as follows:

$$EI = K_c E_{cd} I_c + K_s E_s I_s \tag{2.48}$$

where:

- K_c is a factor that takes into account of cracking and creep effects;
- K_s is a factor that takes into account of the reinforcement contribution;
- E_{cd} is the design value of the concrete Young modulus;
- I_c is the moment of inertia of the concrete area;
- I_s is the moment of inertia of the reinforcement area;
- E_s is the design value of the reinforcement Young modulus.

The value of K_c depends on the reinforcement ratio ρ. If:

- $\rho \geq 2$ ‰:
  - $K_s=1$;
  - $K_c=\frac{K_1 K_2}{1+\varphi_{ef}}$;
  - $K_1 = \sqrt{\frac{f_{ck}}{20}}$;
  - $K_2 = n\frac{\lambda}{170} \leq 0.2$;
  - $n = \frac{N_{Ed}}{A_c f_{cd}}$;
  - φ_{ef} is the effective creep ratio.
- 1‰ $\leq \rho \leq 2$ ‰:

- K_s=0;
- $K_c=\frac{0.3}{1+0.5\varphi_{ef}}$;
- φ_{ef} is the effective creep ratio.

Hence it is possible to evaluate the second order moment (M_2) as follows. The first order moment (M_{0Ed}) is evaluated taking into account the design value of the axial load (N_{Ed}) and the eccentricity (e_1). The total design moment, that includes the second order moment, can be expressed as an amplification of the first order moment:

$$M_{Ed} = M_{0Ed}\left[1 + \frac{\beta}{\left(\frac{N_B}{N_{Ed}}\right)} - 1\right] \tag{2.49}$$

where:

- M_{0Ed} is the first order moment evaluated by means of a linear analysis;
- $\beta = \frac{\pi^2}{c_0}$, where c_0 is a factor that depends on the 1^{st} order distribution;
- N_{Ed} is the design value of the axial load;
- $N_B = \pi^2 \frac{EI}{l_0^2}$ is the buckling load based on nominal stiffness, Eq. (2.48).

Finally, the second order moment is:

$$M_2 = M_{Ed} - M_{0Ed} \tag{2.50}$$

2.5.3 Method based on nominal curvature

This method is mainly used for isolated columns loaded by a constant normal force and a defined effective length, (see Fig. 2.9) (see [10]).
The method evaluates the total bending moment (M_{Ed}) based on a deflection, that is calculated considering l_0 and an estimated maximum curvature.
The total design bending moment is:

$$M_{Ed} = M_{0Ed} - M_2 \tag{2.51}$$

It is recalled that M_{0Ed} is the first order moment due to e_1, that includes also geometry imperfections. While the nominal second order moment M_2 is:

$$M_2 = N_{Ed} e_2 \tag{2.52}$$

where N_{Ed} is the design value of the axial force. The others parameters are evaluated as follows:

$$e_2 = \frac{1}{r}\frac{l_0^2}{c} \tag{2.53}$$

where c is a factor which is approximately equal to π^2. The estimated curvature is defined as follows:

$$\frac{1}{r} = K_r K_\varphi \frac{1}{r_0} \tag{2.54}$$

where:

- K_r is a correction factor which depends on axial load,

  $$K_r = \frac{n_u - n}{n_u - n_{bal}} \leq 1$$

  where:

  – n is the relative axial force;

  – $n_u = 1 + \omega$;

  – $n_{bal} = 0.4$, which is the value of n at maximum moment resistence.

- K_φ is a factor that takes into account the creep,

  $$K_\varphi = 1 + \beta\varphi_{ef}$$

  where:

  – φ_{ef} is the effective creep ratio;

  – $\beta = 0.35 + \frac{f_{ck}}{200} - \frac{\lambda}{150}$;

  – λ is the slenderness ratio.

- $\frac{1}{r_0} = \frac{\epsilon_{yd}}{0.45d} = \frac{f_{yd}}{E_s}\frac{1}{0.45d}$
  where d is the effective depth of a cross-section.

Chapter 3

Safety format for non-linear FEM analysis

3.1 Introduction

Nowadays, for realistic modelling, the use of non-linear models is widespread and inevitable, in order to solve the problem of load capacity of reinforced concrete structures. Those models have to be appropriate to represent the material behaviour, the geometry and all the other structural parameters. Sometimes, the classic design approach does not fulfil the purpose of this type of analysis. From this point of view, for a actual structural analysis, the mean values of the material parameters are used. Consequently, the objective of a non-linear analysis is to formulate the most probable resistance of a structure, thus the resistance mean value. It means that the goal is to determine the actual structural behaviour.
However, the numerical simulation of structure and material are subjected to uncertainties to deal with. Those uncertainties are non-negligible because the aim of this type of analysis is to represent the actual structure. Attentions on those problems have to be spent in order to ensure that all results and conclusions made by the analysis are realistic. (see [11] and [12]).

The uncertainties affect the analysis of structure reliability. The role plays by those uncertainties depends on their nature, which is influenced by both the context and the application. They can be distinguished as aleatory and epistemic uncertainties. As defined by [12] "The word aleatory derives from the Latin *alea*, which means the rolling of dice. Thus an aleatoric uncertainty is one that is presumed to be the intrinsic randomness of a phenomenon." . This kind of uncertainty concerns the

intrinsic randomness of the variables that are related to the structure. For instance, those type of uncertainties are representative of the uncertainty of a repeated measure (concrete strength), because it leads to random and systematic errors in the measurement of this physical quantity.
As defined by [12] "The word epistemic derives from the Greek $\epsilon\pi\iota\sigma\tau\eta\mu\eta$ (episteme), which means knowledge. Thus, an epistemic uncertainty is one that is presumed as being caused by lack of knowledge (or data)." . Therefore, this kind of uncertainty is related to the definition of the structural model. The theoretical model made during the design phase may be incomplete or inexact due to lack of knowledge or due to accepted simplifications. For example, the connection model between two structural elements can be supposed to be a hinge. During the construction phase, it is not sure that this connection will act as a hinge. This case is a clear example of epistemic uncertainty.

3.2 Model uncertainties

Empirical relations between relevant variables (X_i) are the basis of a calculation model, which can be express as follows:

$$R = f\left(X_1, X_2, X_3, ..., X_n\right) \tag{3.1}$$

In case of a complete and exact model ($f\left(...\right)$), and if X_i are supposed exacts, the outcome R can be evaluated without any error. However, this is not an ordinary situation, because in most cases the model is incomplete and inexact, and X_i are never exacts. This is a result of a lack of knowledge, or a deliberate model simplification. The difference between the real outcome and the model prediction can be expressed as follows:

$$R = f'\left(X_1, X_2, X_3, ..., X_n; \theta_1, \theta_2, \theta_3, ..., \theta_n\right) \tag{3.2}$$

where θ_i are variables which contain the model uncertainties and are treated as random variables. Their statistical properties can be evaluated from experiments and observations.(see [13])

It is important to define model uncertainties, and a methodology for their qualification and their treatment in practical applications.
Generally, model uncertainty can be obtained by a comparison of physical tests and model results. Fig. 3.1 shows a general concept for the assessment of model uncertainties.
All the parameters that affect test and model results and real structure behaviour

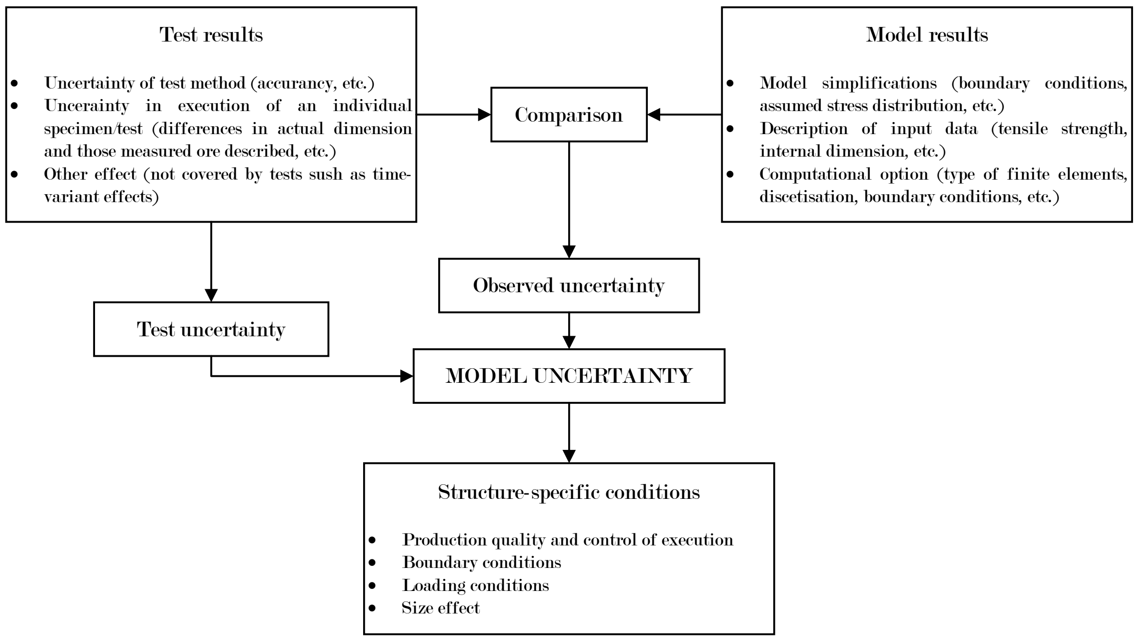

Figure 3.1: General concept of the assessment of model uncertainties [14]

depend on both structural members and failure mode.

- Test results: test methods based on general experience and calibration accuracy.
- Model results: the chose of a particular FEM model, all the uncertainties related to input data and all the possible simplifications.
- Structural conditions: it leads to investigate the differences between real structures and tests under ideal conditions.

This approach has led to the definition of appropriate safety formats, which are still under discussion.

3.3 Safety Formants for non-linear analysis *fib* in MC2010

3.3.1 Introduction

In 1995, König at al. [15] proposed a generalized safety format for non-linear analysis. It is based on the assumption that in structures only the sensitivity of the overall structural behaviour has to be investigated. It is also assumed that the material property scattering and action scattering are known and evaluable by means of their aleatoric distribution functions. In this way, the global safety factor γ_G, which is a coefficient related to the overall structural resistance, was introduced.
The first approach, that allowed to evaluate γ_G, was defined by Holicky and Sykora [16]. It can be obtained as the ratio between the mean value R_m and the design value R_d of the structural resistance distribution:

$$\gamma_G = \frac{R_m}{R_d} \approx \exp\left(\alpha_R \beta V_R\right) \tag{3.3}$$

where R_m is the mean resistance evaluated by means of a non-linear analysis with material properties mean values. The design value R_d is defined by means of a probabilistic relationship (Euro Code 0 [1]):

$$R_d = R_m \exp\left(-\alpha_R \beta V_R\right) \tag{3.4}$$

where:

- β is the reliability index;
- α_R is the FORM (first order reliability method) resistance sensitivity factor;
- V_R is the coefficient of variation related to the resistance distribution.

The values $\beta = 3.8$ and $alpha = 0.8$ are used for an expected structural life of fifty years. The coefficient of variation V_R, related to the structural resistance, can be obtained by a Monte Carlo simulation.
It can be underlined that:

- the global resistance factor γ_R may not be unique;
- the hypothesis of log-normal distribution may not be verified.

Because log-normal hyphotesis and γ_R depend on the analysed structure and on the faillure mode.

The fib MC2010 [17] proposed the design conditions to be used in the safety format for non-linear analysis:

$$F_d \leq R_d \tag{3.5}$$

where:

- F_d is the design value of the actions;
- R_d is the design value of the resistance.

There are three different approaches to evaluate the design resistance R_d in Eq. (3.5), based on different typology of probabilistic theory implementation:

- the probabilistic method;
- the global resistance methods;
- the partial factor method.

3.3.2 Probabilistic method

The value of R_d can be evaluated by the general safety format, which follows the probabilistic analysis. The design value can be expresses as:

$$R_d = \frac{R(\alpha\beta)}{\gamma_{Rd}} \tag{3.6}$$

where:

- γ_{Rd} is the model uncertainty factor;

- β is the reliability index;
- α is a resistance sensitivity factor (which is $\alpha < 1$ and reduced β);
- R is the resistance predicted by non-linear structural model, which corresponds to β.

This safety format method can be complicated and time-consuming.

3.3.3 Global resistance methods

This method proposes to evaluate R_d by dividing the resistance $R\left(f_{rep}\right)$ with either the global resistance factor γ_R or the model uncertainty factor γ_{Rd}. R_{rep} is the structural resistance evaluated by a non-linear analysis in which a representative values for the material resistances f_{rep} are chosen.

$$R_d = \frac{R(f_{rep})}{\gamma_R \gamma_{Rd}} \tag{3.7}$$

In fib MC2010 are demonstrated two methods for the derivation of R_d: the global resistance factor method and the method of Estimation of a Coefficient of Variation of Resistance (ECOV method).

The global resistance factor method

The global resistance factor is evaluated as the ratio between the representative and the design values of the material properties. The mean value for the yield stress of the steel is considered:

$$f_{ym} = 1.1 f_{yk} \tag{3.8}$$

where f_{yk} is the characteristic yield stress.
While the concrete properties are evaluated as follows:

$$f_{cm} = 1.1 f_{ck} \frac{\gamma_s}{\gamma_c} \approx 0.85 f_{ck} \tag{3.9}$$

where f_{ck} is the characteristic compressive strength. The value of f_{cm} is reduced to take into account the great random variability of concrete.

The proposed partial factor of global resistance is $\gamma_R = 1.2$. While the proposed model uncertainty factor is $\gamma_{Rd} = 1.06$.

Method of estimation of the resistance coefficient of variation

This method is based on the hypothesis that the random distribution of resistance of RC structures R can be modelled by a two-parameter log-normal distribution. This distribution can be identified by two random parameters: mean resistance R_m and coefficient of variation of resistance V_R.
Firstly, it is needed to estimate the mean and the characteristic values of resistance using two non-linear analyses, which can be calculated using corresponding values of material parameters:

$$R_m = r(f_{ym}, f_{cm}, ...) \qquad R_k = r(f_{yk}, f_{ck}, ...) \tag{3.10}$$

where the function r represents the non-linear analysis and f_m and f_k are mean and characteristic values of material, respectively. The characteristic value R_k can be obtained as an acceptable approximation :

$$R_k = R_m \exp(-1.65 V_R) \tag{3.11}$$

Thus, the coefficient of variation V_R can be estimated by the following expression:

$$V_R = \frac{1}{1.65} \ln\left(\frac{R_m}{R_k}\right) \tag{3.12}$$

Finally, the global resistance factor can be estimated as:

$$\gamma_R = \frac{R_m}{R_d} = \exp(\alpha_R \beta V_R) \tag{3.13}$$

The parameter α and β are fixed: 0.8 and 3.8, respectively. As regards the model uncertainty factor, under the hypothesis of well validated numerical models, it is assumed as $\gamma_{Rd} = 1.06$. This value can be inserted in Eq. (3.7), which is used to evaluate the design resistance R_d.
This method depends on the reliability of mean and the characteristic value of the material parameters used in the analysis.

3.3.4 Partial Factor Method (PFM)

In this method, the structural analysis is based on extremely low value of material parameters, which are the design values. Thus, the design resistance R_d is calculated as follows:

$$R_d = r(f_d, ...) \tag{3.14}$$

where $r(f_d, ...)$ is a non-linear analysis function.
The partial factor method can cause deviations in structural response, for example the failure mode. Therefore, this method should be avoided. However, it can be used for safety resistance estimation in absence of a more refined solution.

3.4 Safety Formats for non-linear analysis after *fib* in MC2010

After the *fib* Model Code 2010, two contributions were formulated. The first method was proposed in 2011 by Schlune et al. [11]. The second method was published in 2013 by Allaix et al. [18].

3.4.1 Schlune method

The methods described in *fib* Model Code 2010 have been tested for non-linear analysis of both beams and columns, which are subjected respectively to bending moments and normal forces.

This new method obviates the need to use a safety format for all types of reinforced concrete structures that can also be subjected at shear failures. This safety format is based on the global resistance method. For what concern the material parameters, the mean yield strength of steel reinforcement (f_{ym}) and the mean in situ concrete compressive strength ($f_{cm,is}$) are used. The taken geometric parameters are the nominal values a_{nom}. The design resistance R_d is calculated as:

$$R_d = \frac{R\left(f_{ym}, f_{cm,is}, a_{nom}\right)}{\gamma_R} \tag{3.15}$$

In the same way of the previous methods, a log-normal resistance distribution is assumed, Thus, γ_R is evaluated as:

$$\gamma_R = \frac{\exp\left(\alpha_R \beta V_R\right)}{\theta_m} \tag{3.16}$$

The factor θ_m takes into account the model uncertainties, and it is defined as the mean ratio between the experimental and predicted resistances. It can vary between 0.7 and 1.2 and it depends on the failure mode. The Coefficient Of Variation (COV) in Eq. (3.16) is evaluated as follows:

$$V_R = \sqrt{V_g^2 + V_m^2 + V_f^2} \tag{3.17}$$

where V_g, V_m e V_f are the COV respectively of the geometrical, the model and the material uncertainties. Values of V_g and V_m are proposed. If the main material parameters are the concrete compressive strength and the steel yield stress, V_f can be evaluated as:

$$V_f \approx \frac{\sqrt{\left(\frac{R_m - R_{\Delta fc}}{\Delta f_c}\right)^2 \sigma_{f_c}^2 + \left(\frac{R_m - R_{\Delta fy}}{\Delta f_y}\right)^2 \sigma_{f_y}^2}}{R_m} \tag{3.18}$$

where:

- σ_{fc} is the standard deviation of concrete compressive strength and σ_{fy} is the standard deviation related on yield stress of the steel;
- Δf_c, Δf_y are the finite variations of the material resistances;
- $R_{\Delta fc}$, $R_{\Delta fy}$ are the resistances results of non-linear analyses performed using the values $(f_{cm} - \Delta f_c)$ for the concrete compressive strength and $(f_{ym} - \Delta f_y)$ for the yield stress.

Thus, the coefficient of variation V_R can be estimated by means of three non-linear analyses: the first one performed with the mean values of material parameters and the other two performed with the values $(f_{cm} - \Delta f_c)$ and $(f_{ym} - \Delta f_y)$, respectively.

3.4.2 Global safety format (GSF)

This method, as the Schlune method, is based on the global resistance methods and on the assumption that the random distribution of resistance fits a log-normal distribution. The non-linear analysis is performed using the mean values of the material resistance (f_m) and the nominal values of the geometrical dimensions (a_{nom}). Then, the design values R_d is evaluated dividing the result of the analysis by both the global resistance factor γ_R and the model uncertainty factor γ_{Rd}.

$$R_d = \frac{R\left(f_m, a_{nom}\right)}{\gamma_R \gamma_{Rd}} \tag{3.19}$$

The global resistance factor is derived, as already explained, from:

$$\gamma_R = \exp\left(\alpha_R \beta V_R\right) \tag{3.20}$$

where the coefficient of variation of the structural resistance V_R is estimated from a probabilistic simulation using the Monte Carlo method. This method is performed by a non-linear analysis up to failure, using a finite element model, for each sample of random variables. It leads to obtain a distribution of the structural resistance R from which is possible to estimate V_R.

The value of the model uncertainty factor γ_{Rd} takes into account the differences between the real behaviour of the structure and the numerical model behaviour of the structure. In this way, γ_{Rd} can be evaluated by a comparison between experimental tests and numerical calculations, but also through probabilist considerations. If the distribution of resistance model uncertainty θ_R is given, γ_{Rd} can be evaluated as follows:

$$\gamma_{Rd} = \frac{1}{\exp\left(-\tilde{\alpha}_R \beta V_{\theta R}\right)} = \exp\left(\tilde{\alpha}_R \beta V_{\theta R}\right) \tag{3.21}$$

where $\tilde{\alpha}_R = 0.4\alpha_R$ is the sensitivity factor for the resistance model uncertainty and $V_{\theta R}$ is the COV of the resistance model uncertainty θ_R.

Chapter 4

Database of RC slender columns

4.1 Investigators and experiments

In this section is presented a database of experimental tests performed on slender columns, which data have been taken from literature. The experimental columns are characterized by a rectangular (or square) section.

1. Kim, J.K. and Yang, J. K. 1993 [19]

In this investigation, 30 tests on simply supported columns were reported. Two of the columns failed at the ends and are therefore disregarded from the list. The investigation contained three different levels of compressive strength (low, medium and high). For the purposes of the analysis, just 8 columns, with a low compressive strength, were considered. Furthermore, two different reinforced ratios were tested, 1.98% and 3.95%. Columns characterized by a reinforced ratio of 3.95% present reinforcement placed at the centre of the cross-section. The data are reported in the appendix, section $A.1$.

2. Mehmel, A., Schwarz, H.,Kasparek, K. H. and Makovi, J. 1969 [20]

This investigation contained 16 tests. Fourteen of these present the same eccentricity in both ends and two have different eccentricities at the ends. For this reason, those two columns, were disregarded. Three different types of reinforcement were used and the cross-section had three different sizes. The data are reported in the appendix, section $A.2$.

3. Drysdale, R. G. and Huggins, M. W. 1971 [21]

This investigation contained 58 tests, but just 4 columns were considered because those tests are characterized by short term loading to failure and eccentricity along principal axes of inertia. Those columns were characterized by a square cross-section and a reinforcement ratio of 3.14%. The data are reported in the appendix, section $A.3$.

4. Khalil, N., Cusens, A. R. and Parker M. D. 2001 [22]

In this investigation 20 columns were tests. Just 11 columns are considered because they are characterized by a short-term load. The considered columns have a constant width of 152mm. The slenderness and the reinforcement ratio were varied. The data are reported in the appendix, section $A.4$.

5. Saenz, L. P. and Martin, I. 1963 [23]

This test campaign were performed at the University of Havana with 52 rectangular section concrete columns. Reinforcement ratio and slenderness were varied. Columns were restrained at the ends, but the authors declared that there were no certainty that absolute fixedness was developed. The data are reported in the appendix, section $A.5$.

6. Foster, S. J. and Attard, M. M. 1997 [24]

In this investigation, the data related to 68 eccentrically loaded conventional and high-strength concrete columns were reported. Just 26 conventional concrete columns were considered. The columns were 150 x 150 mm at the mid-section and two different percentage of steel reinforcement ratio were used. The data are reported in the appendix, section $A.6$.

7. Pancholi, V. R. 1977 [25]

The tests were performed on 38 columns and those included creep investigations. Hence, just 29 columns were considered. Those elements were characterized by a high slenderness ratio, two different dimensions of square cross-section and two different reinforcement ratios. The load were applied at the centre of gravity of the section, then no eccentricity were considered. The data are reported in the appendix, section $A.7$.

8. Dracos, A. 1982 [26]

This paper included short and long term studies, hence, just 36 columns were considered. Slenderness, cross-section, reinforcement ratio and eccentricity were varied. All columns were simply supported. The data are presented in the appendix, section $A.8$.

9. Iwai, S., Minami, K. and Wakabayashi, M. 1986 [27]

A total of 396 column with rectangular cross sections, including square sections, were testes. The ratio of column length to minimum depth ranged from 6 to 26. Loads were applied monotonically at each column end with equal eccentricities at various angles from an axis of symmetry. For this reason just 11 columns were considered. The data are reported in the appendix, section $A.9$.

10. Chuang, P. H. and Kong, F. K. 1997 [28]

In this investigation, 26 eccentrically loaded simply supported columns were tested. Normal strength concrete as well as high strength concrete was used, then, just 20 columns were considered. The concrete cross-section had two different sizes and three types of reinforcement and reinforcement ratio were used. The data are reported in the appendix, section $A.10$.

11. Barrera, A. C., Bonet, J. L., Romero, M. L. and Miguel, P. F. 2011 [29]

In this experimental program, 44 rectangular columns with different sections were executed. The length of the columns are 3 m for all the specimens and these were subjected first to a constant axial load and later to a monotonic lateral force up to failure. These specimens symbolize two semi-columns connected by a central element, which represents the stiffener effect of an intermediate floor or the connection between a column and the foundation, represented by a stub element. Normal strength concrete as well as high strength concrete was used, then, just 23 columns were considered. The data are reported in the appendix, section $A.11$.

12. Baumann, O. 1935 [30]

The experimental investigation made by Baumann was subdivided into two sections, a pilot series and a main series. Both series consider both axially and eccentrically loaded columns. The pilot series consists of 12 tests and the main series of 31 tests. The columns in the pilot series and in the first 15 tests of the main series were simply supported. In the remaining data of the main series, the end conditions were changed, and, consequently all these columns were disregarded. The cross-section was varied in many of the tests.The data are presented in the appendix, section $A.12$.

Fig. 4.1 shows column types, with end supports and applied loads.

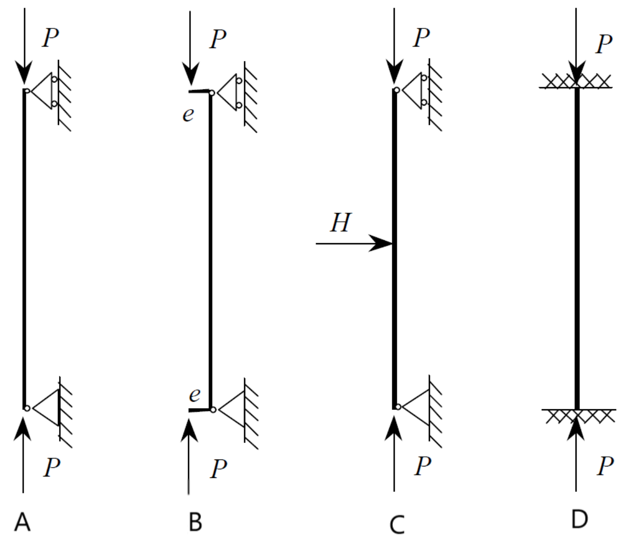

Figure 4.1: Column types

In Tab. 4.1 the number and the type of tests made by each investigator is presented.

4.2 Verification of EC2 requirements for columns

All columns were verified for the EC2 [10] requirements. These requirements ensure safety, serviceability and durability, and they are satisfied by following the rules given in the following paragraph.

4.2.1 Column requirements

This requirements deal with columns for which tha larger dimension b is not greater than 4 times the smaller dimension h.

References	Investigators	Year	Number and type of tests
[19]	Kim, J.K. and Yang, J. K.	1993	8 B
[20]	Mehmel, A., Schwarz, H.,Kasparek, K. H. and Makovi, J.	1969	14 B
[20]	Drysdale, R. G. and Huggins, M. W.	1971	4 B
[22]	Khalil, N., Cusens, A. R. and Parker M. D.	2001	11 B
[23]	Saenz, L. P. and Martin, I.	1963	52 D
[24]	Foster, S. J. and Attard, M. M.	1997	23 B
[25]	Pancholi, V. R.	1977	29 A
[26]	Dracos, A.	1982	36 A
[27]	Iwai, S., Minami, K. and Wakabayashi, M.	1986	4 A and 7 B
[28]	Chuang, P. H. and Kong, F. K.	1997	20 B
[29]	Barrera, A. C., Bonet, J. L., Romero, M. L. and Miguel, P. F.	2011	23 C
[30]	Baumann, O.	1935	14 A and 13 B

Table 4.1: Investigated columns

Longitudinal reinforcement

- Longitudinal bars shall have a diameter of not less than ϕ_{min}. The recommended value is 8 mm.
- The total amount of longitudinal reinforcement shall not be less than $A_{s,min}$. The recommended value is $0.002A_c$.
- The area of longitudinal reinforcement shall not exceed As, max. The recommended value is $0.04A_c$.

A minimum areas of reinforcement are given in order to prevent a brittle failure, wide cracks and also to resist forces arising from restrained actions.

Transverse reinforcement

- The diameter of the transverse reinforcement shall not be less than 6 mm or one quarter of the maximum diameter of the longitudinal bars, whichever is the greater.

- The transverse reinforcement shall be anchored adequately.
- The spacing of the transverse reinforcement along the column shall at maximum of $s_{cl,tmax}$. The recommended value is the least of the following three distances:
  - 20 times the minimum diameter of the longitudinal bars;
  - the lesser dimension of the column;
  - 400 mm.
- Every longitudinal bar placed in a corner shall be held by transverse reinforcement. No bar within a compression zone shall be greater than 150 mm from a restrained bar.

Chapter 5

Structural models for RC slender columns

5.1 Material behaviour

In order to analyse the behaviour of RC column, some basic assumptions regarding the material behaviour for concrete and steel reinforcement have to be introduced. All material parameters were used as input for the column modellings.

5.1.1 Concrete

Compression behaviour

The Razvi-Saatcioglu model [31] is assumed for the stress-strain relationship of concrete in compression. This model makes a distinction between confined and unconfined concrete behaviour. The unconfined concrete strength (f_{cm}) should be determined from a standard cylinder test results. Differently, the confined concrete strength (f_{ccm}) takes into account of the contribution of transversal reinforcement. This phenomena is take into account because a triaxial state of stress is considered. A column subjected to longitudinal compression develops longitudinal strains. Consequently, transversal tensile strains are generated by these loading. Transverse strains, caused by later pressure, counteract the tendency of material to expand in lateral direction, and this results an increasing of strength (Eq. (5.1)).

$$f'_{cc} = f'_c + k_1 f_1 \tag{5.1}$$

where k_1 is a function of the Poisson's ratio and f_1 is the lateral pressure, which depends on the diameter of the stirrups and their spacing. Fig. 5.1 shows those different behaviours for confined and unconfined concrete. From the literature, pre-

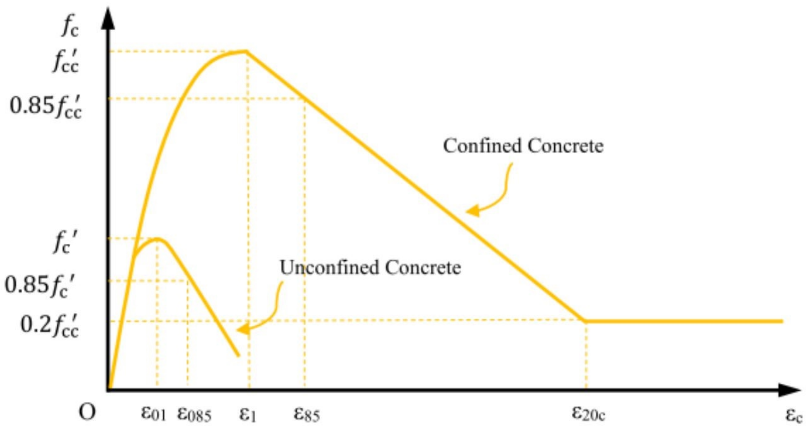

Figure 5.1: Razvi-Saatcioglu model [31]

vious reported in Chapter 4, only the information related to f_{cm} is available. The f_{ccm} values are calculate by the Razvi-Saatcioglu formula. All the other parameters, necessary to describe the compressive behaviour of concrete, were evaluated by EC2 [10] prescriptions as following reported:

Young's Modulus	$E_{cm} = 22\left[\frac{f_{cm}}{10}\right]^{0.3}$
Compressive strain at the peak stress f_{cm}	$\varepsilon_{c1}(‰) = 0.7f_{cm}^{0.31} < 2.8$
Compressive strain at 0.85% of f_{cm}	$\begin{cases} \varepsilon_{c0.85} = 3.5 & f_{cm} \leq 58\ [MPa] \\ \varepsilon_{c0.85} = 2.8 + 27\left[\frac{98-f_{cm}}{100}\right]^4 & f_{cm} > 58\ [MPa] \end{cases}$

Table 5.1: Concrete parameters by EC2 [10]

The values of ultimate compressive strain in the confined concrete (ε_{cu}) and in the unconfined concrete (ε_{ccu}) are evaluated by Razvi-Saatcioglu model [31].

Tension behaviour

Stress-strain curve of concrete in tension is considered with a bilinear law (Fig. 5.2).

A linear behaviour is assumed until the tensile strength (f_{ctm}) is reached.

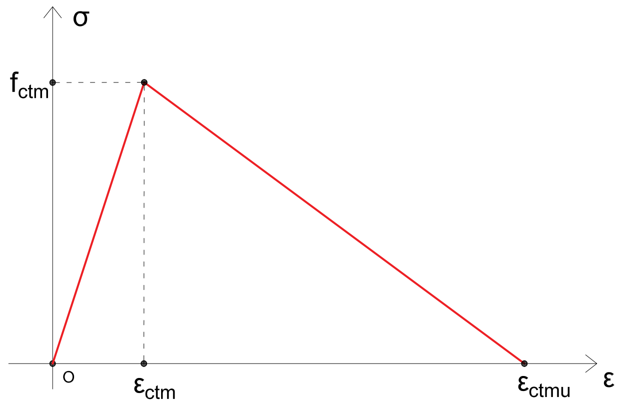

Figure 5.2: Concrete tensile behaviour

The value of this strength is derived from f_{cm} by EC2 [10] prescription:

$$\begin{cases} f_{ctm} = 0.30\,(f_{cm} - 8\,[MPa])^{\frac{2}{3}} & f_{cm} \leq 58\,[MPa] \\ f_{ctm} = 2.12\ln\left(1 + \left(\frac{f_{cm}}{10}\right)\right) & f_{cm} > 58\,[MPa] \end{cases} \tag{5.2}$$

After the peak value, a linear tension softening branch is followed. On first attempt, the softening has been considered dependant on f_{cm}, as reported by many authors (see [32]) This slope is graphically defined as:

$$SLOPE = \frac{f_{ctm}}{\varepsilon_{ctmu} - \varepsilon_{ctm}} = \frac{f_{ctm}}{\varepsilon_{ctm}\left(\frac{\varepsilon_{ctmu}}{\varepsilon_{ctm}} - 1\right)} \tag{5.3}$$

In Fig. 5.3 is defined the ratio $\varepsilon_{ctmu}/\varepsilon_{ctm}$ which values depends on f_{cm}.

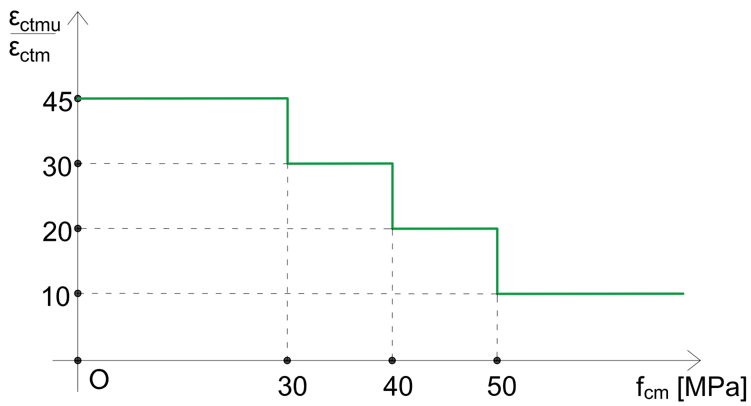

Figure 5.3: Softening slope

However, the concrete tensile behaviour has been calibrated in each software, starting form the first attempt, with the aim to best fit the experimental results.

5.1.2 Steel reinforcement

Steel reinforcement behaviour is considered equal in both compressive and tensile field. It is characterized by a bilinear law.
A elastic behaviour is assumed until the yield tension value (f_{ym}) is reached. The elastic slope is the Young's modulus (E_s), which is always considered equal to 210000 [MPa]. The value of f_{ym} is given in the database.
When the ultimate tension strength (f_{su}) is not declared by the authors, it is supposed to be as follows:

$$f_{su} = 1.03 f_{ym} \tag{5.4}$$

The value of f_{su} is supposed to correspond at a strain value of 0.070. Fig. 5.4 shows the steel reinforcement stress-strain law.

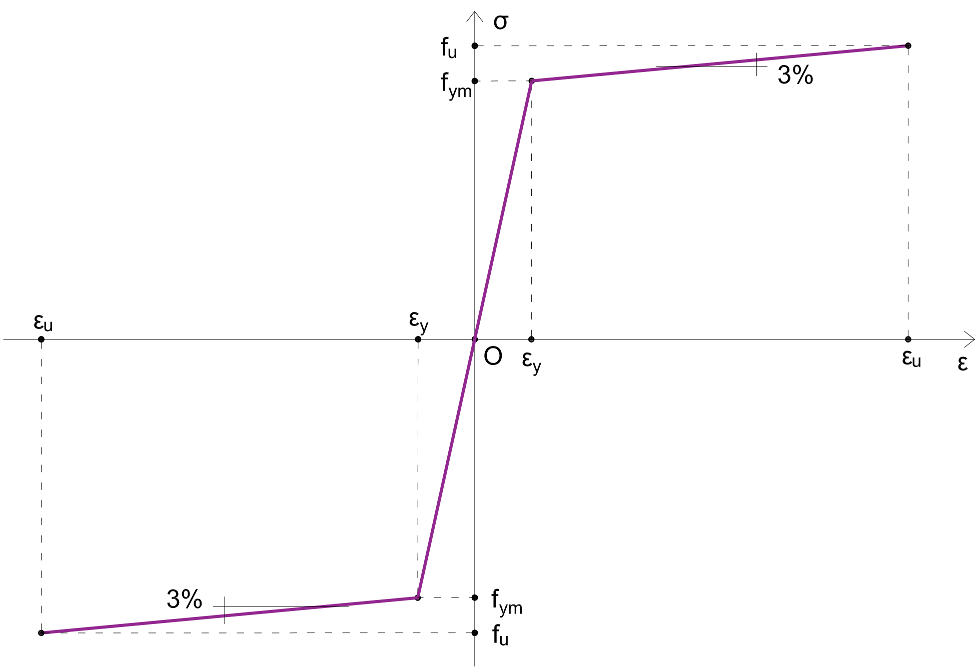

Figure 5.4: Steel reinforcement stress-strain law

5.2 Softwares

In this work, three different software have been used: DIANA FEA, ADINA, and OpenSees.

Each software is characterized by different hypotheses and mechanical parameters, which are related to equilibrium, compatibility and constitutive laws. Moreover, the meshes are defined after a calibration procedure.The standard Newton-Raphson iterative procedure, which is based on the linear approximation hypothesis, is used to solve the non-linear system of equation. Perfect bond between the reinforcement and the surrounding concrete is assumed.

Tab. 7.6 shows a summary of the main hypotheses assumed in the definition of 2D non-linear numerical models.

<table>
<tr><th></th><th>ADINA</th><th>DIANA</th><th>OpenSees</th></tr>
<tr><td>Equilibrium</td><td colspan="3">Standard Newton-Raphson</td></tr>
<tr><td rowspan="2">Compatibility</td><td colspan="2">Finite Elements
-Isoparametric 2 nodes (1X1 Gauss points integration scheme with linear interpolation)</td><td>Fiber Elements
-Force-based approach
5 integration points</td></tr>
<tr><td>-Macro element</td><td colspan="2">-Discrete reinforcements</td></tr>
<tr><td rowspan="2">Costitutive laws</td><td>Moment-curvature law</td><td colspan="2">Stress-strain law</td></tr>
<tr><td colspan="3">CONCRETE
Compression: Razvi-Saatcioglu model
Tension: (3 different solutions):
1. Elastic - brittle
2. Elastic - linear tension softening
3. Elastic - perfectly plastic
REINFORCEMENTS STEEL
Tri-linear elastic with hardening</td></tr>
</table>

Table 5.2: Summary of the basis hyphoteses assumed in the definition of non-linear numerical method

5.2.1 DIANA

DIsplacement ANAlyser (DIANA) is a Finite Element Analysis (FEA) solver developed and distributed by DIANA FEA BV [33]. The used element is a beam element, which can have axial deformation, shear deformation and curvature. DIANA offers three classes of beam elements, Class-III is used in this analysis. Class-III are fully numerically integrated Mindlin beam elements. For those type of elements, the normal strain (ϵ_{xx}) varies linearly over the cross-section area and the transverse shear

strains are forced to be constant. Since the actual transverse shear stress and strain vary quadratically over the cross-section area, the shear strain is an equivalent constant strain on a corresponding area.
The L12BEA element (Fig. 5.5) has been used.

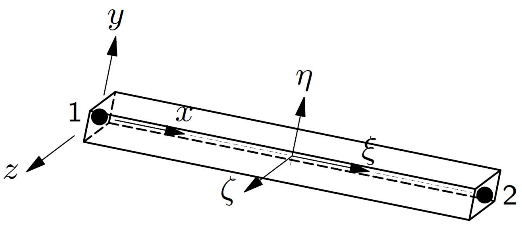

Figure 5.5: L12BEA

The L12BEA is a two-node, three-dimensional class-III beam element. Basic variables are the translations u_x, u_y, and u_z and the rotations ϕ_x, ϕ_y, and ϕ_z in the nodes. The interpolation polynomials for the displacement can be expressed as follows:

$$\begin{cases} u_i(\xi) = a_{i0} + a_{i1}\xi \\ \phi_i(\xi) = b_{i0} + b_{i1}\xi \end{cases} \rightarrow i = x, y, z \tag{5.5}$$

Due to these polynomials the strains are constant along the center line of the beam. The solution domain is divided into a finite number of elements, which are connected by nodal points at the inter-element boundaries. In this way the solution domain is discretized and represented as a patch of elements. The unknown displacements in each element are approximated by continuous functions expressed in terms of nodal variables. The functions over each finite element are called interpolation functions.

5.2.2 ADINA

Automatic Dynamic Incremental Nonlinear Analysis (ADINA) is a commercial engineering simulation software program that is developed and distributed worldwide by ADINA R & D, Inc. [34]. This program is used to solve non-linear structural problems.
Adina uses the Finite Element Method (FEM)in order to solve engineering problems.
The elements used in the analysis for the modelling of the columns was the beam elements, which is a two-nodes Hermitian beam with a constant cross-section and initially straight. This element can be employed for large displacement analysis

(which take into account of geometry non-linearities), for which case the displacements and rotations can be large. Moreover, material non-linearities are taken into account.
The material and the section behaviour of the beam were described using a moment-curvature input.
The beam element cross-section, and the local coordinate system, is showed in Fig. 5.6. The cross-section coordinate system has its origin on the line connecting the beam end-nodes.

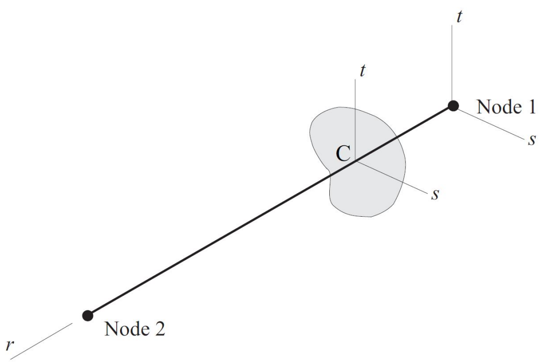

Figure 5.6: Beam element

The formulation of the beam is a generalization of the Euler-Bernoulli beam formulation. Moreover, the cross-section of the beam is assumed to be rigid in its own plane, hence, no distortion of the cross-section is considered. The two nodes and the origin of the local coordinate system (s,t) are located at the centroid of the beam cross-section.
The displacements and rotations are interpolated from the nodal displacements and rotations using the following expressions:

$$\begin{aligned} u &= L_1 u^1 + L_2 u^2 \\ v &= H_1 v^1 + H_2 \theta_t^1 + H_3 v^2 + H_4 \theta_t^3 \\ \theta_t &= H_{1,r} v^1 + H_{2,r} \theta_t^1 + H_{3,r} v^2 + H_{4,r} \theta_t^2 \end{aligned} \tag{5.6}$$

where the nodal displacements and rotations are u^1, v^1, θ_t^1 for node 1 and u^2, v^2, θ_t^2 for node 2, and in which L_1, L_2 are the linear interpolation functions and H_1, H_2, H_3, and H_4 are the cubic interpolation functions (Hermitian displacement functions).

5.2.3 OpenSees

Open System for Earthquake Engineering Simulation (OpenSees) is an object-oriented, software framework created at the Pacific Earthquake Engineering Center [35]. This software is used for the development of applications to simulate the performance of structural systems. The element used in the analysis for the modelling of the columns were fiber beam elements, which takes into account of a distributed plasticity. Moreover, the force-based approach has been used, which means:

- Equilibrium between element and section forces is exact;
- Section forces are determined from the basis forces by interpolation within the basic system. Interpolation comes from static equilibrium and provides constant axial force and linear distribution of bending moment, in the absence of distributed element loads;
- A low number of nodes can be used.

5.3 Models for non-linear simulations

5.3.1 Geometry models

This analysis requires accurate geometrical models, which depend on the characteristics of the specimens. It will follows a description of the models:

- *Type A.* The load is applied through the center of gravity of its cross-section (which is an axial load), hence, the specimens are not subjected to a first order eccentricity e_0. However a RC column is never a perfectly straight element, and it presents some imperfections, which generate an unwanted eccentricity. This eccentricity have to be considered in the models. A model calibration process owed to consider a eccentricity of $0.5mm$.
  All specimen present massive elements at both ends, those parts were modelled considering a linear behaviour.
- *Type B.* Those columns presents an eccentric load along an axis of symmetry of the cross-section. Hence, the first order eccentricity (e_1) were considered into the models. Also those columns presented massive elements at both ends, hence, those parts were modelled considering a linear behaviour.
  In Fig. 5.7 is presented a model example of this type of column.

- *Type C*. A constant axial load is applied, and in this case no additional imperfection were considered into the model. A lateral force is applied in the column mid spam.

  Those columns present a stub element in the point of application of the transversal load, which is modelled as a linear behaviour element. At both ends two steel elements, which allow the free rotation of the specimen, were models considering a linear behaviour.

  In Fig. 5.8 is presented a model example of this type of column.

5.3.2 Load models

For *Type A*, and *Type B* columns, the axial load or the eccentric load is applied up to the failure of the columns. A load path with displacement control were considered. For *Type C* columns, the axial load is applied and maintained constant during the tests. Later a transversal load is applied up to the failure of the column. A load path with displacement control were considered.

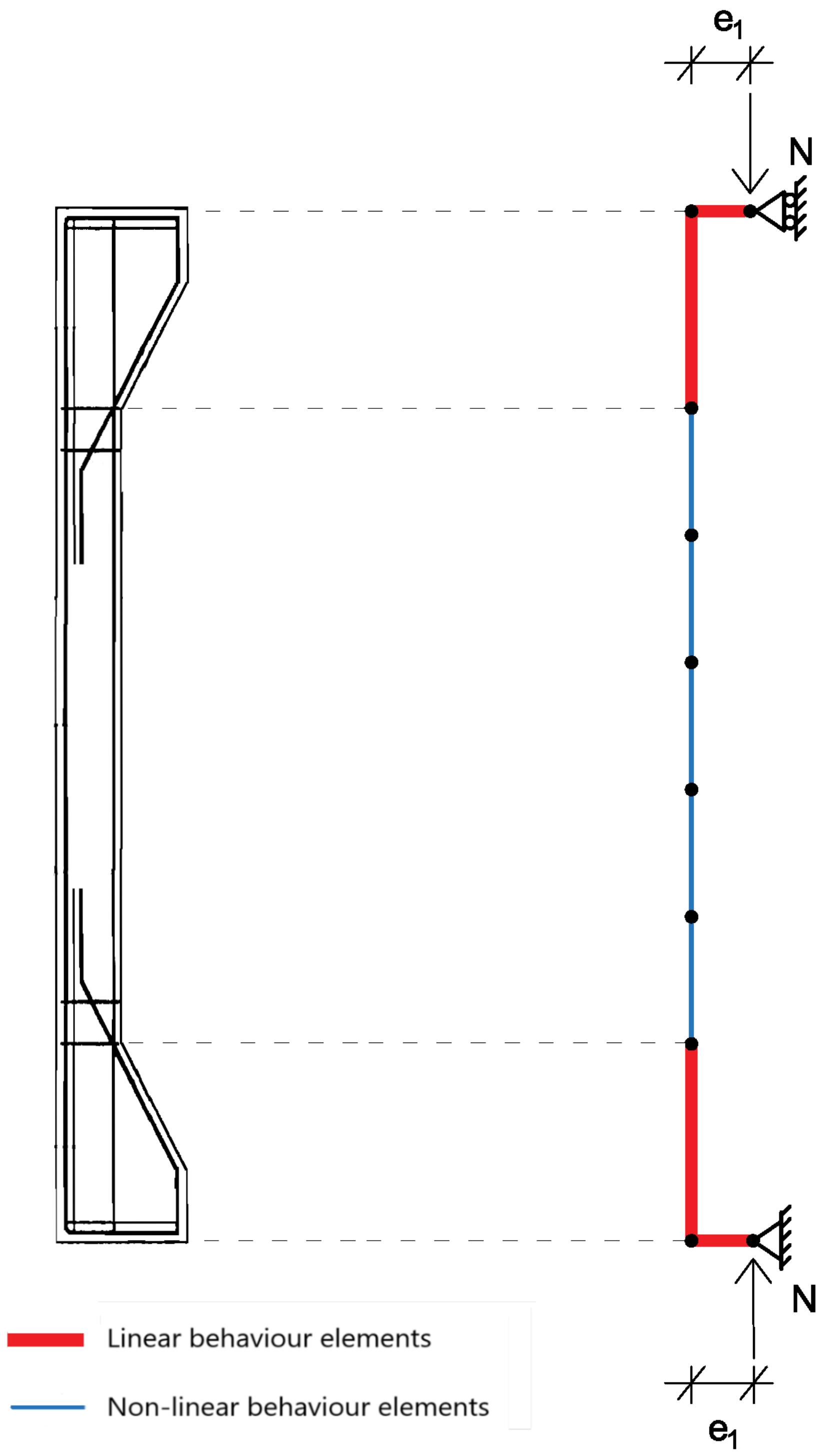

Figure 5.7: Geometrical model for type B column

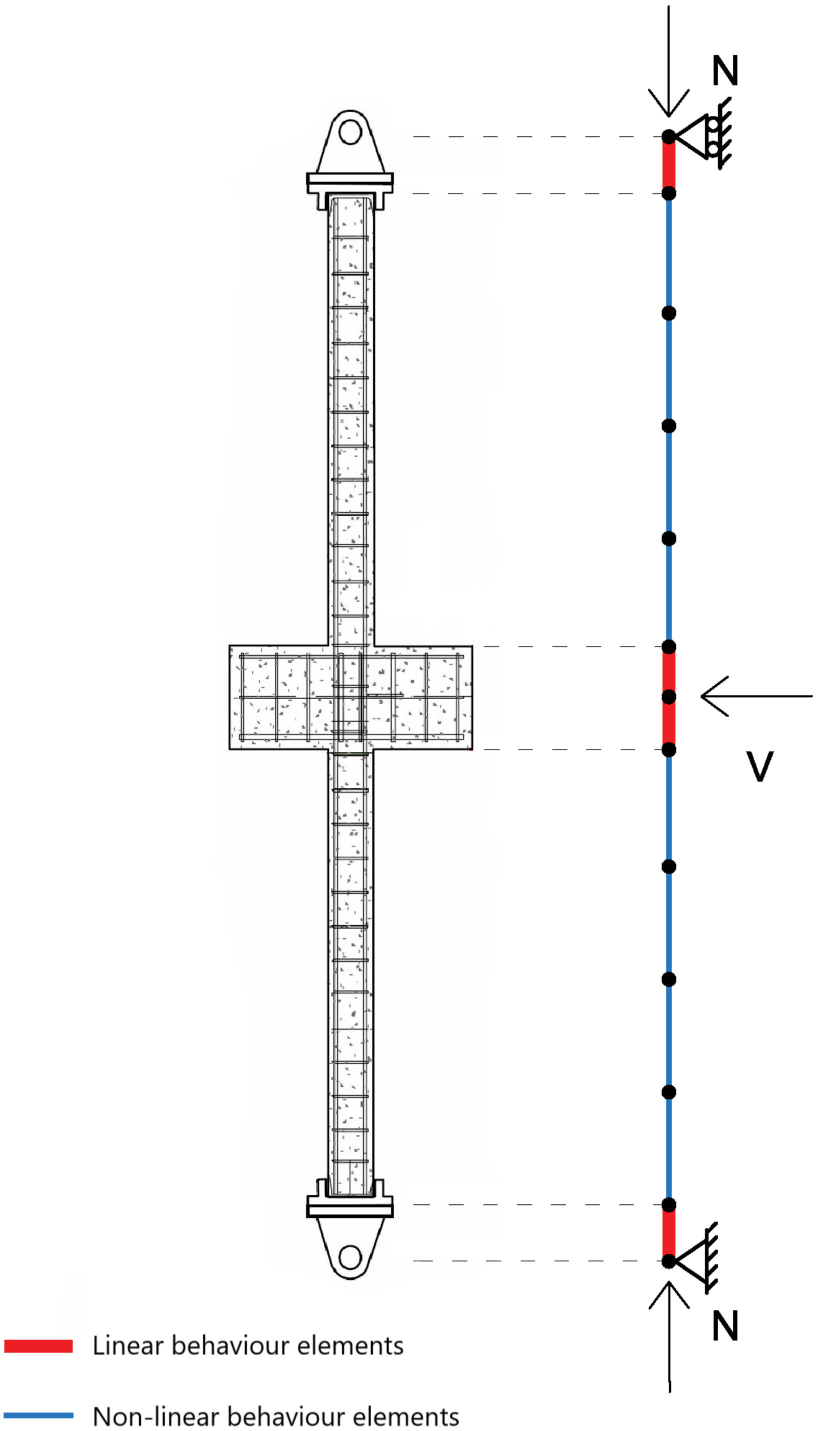

Figure 5.8: Geometrical model for type C column

Chapter 6

Assessment of the Global Resistance Factor for slender RC members

6.1 Introduction

As described by JCSS Probabilistic Model Code [13], the description of each material property consists of a mathematical model (for example, the $\sigma - \epsilon$ function), and parameters, which are random variables (for example, the concrete strength). Moreover, all the relationships between the parameters, described in Paragraph 5.1.1, are a part of the material model.
Generally, material properties are defined as the properties of material specimens of defined size and conditioning, sampled according to given rules. Then, the variability of the mean and standard deviation is a typical form of global parameters variation, considered by the coefficient of variation. In Tab. 6.7 are reported the COV values given by [13].

6.1.1 Procedure for the assessment of γ_R

The Global Safety Format (GSF) can be used for the evaluation of the resistance design value (R_d) of a structure. This value can be calculated performing a non-linear analysis, using the mean values of the material resistance(f_m) and the nominal values of the geometrical dimensions (a_{nom}). Then, R_d can be evaluated dividing R_m by both the global resistance factor (γ_R) and the model uncertainty factor (γ_{Rd}); this expression is reported in Eq. 3.19.

The aim of this chapter is the assessment of the global resistance factor for slender RC members. This value can be derived by means of the following relation:

$$\gamma_R = \exp\left(\alpha_R \beta V_R\right) \tag{6.1}$$

where:

- β is the reliability index. Considering a design working life of 50 years, and consequences class 2 (CC2, see Tab. 1.2), the proposed β is 3.8. CC2 means that, in case of failure, medium consequences for loss of human life, economic, social or environmental occurs.

- α_R is the resistance sensitivity factor (which is $\alpha < 1$ and it reduces β), and is taken equal to 0.8.

Considering the given values of those two parameters, the corresponding failure probability is $p_f = 10^{-3}$.

- V_R is the COV, related to the structural resistance, which can be obtained by means of LHS method (see Paragraph 1.3).

V_R can be evaluated for each column; as a result, it is possible to calculate a γ_R for each column. A a consequence, appropriate evaluations lead to propose a unique γ_R.

6.2 Investigated columns

The database, described in Chapter 4, contains all the essential informations about 258 columns. This database is dividend into 5 groups of slenderness. These groups are reported in Tab. 6.1.

For each groups, 8 columns are selected considering the following criteria:

- All the EC2 requirements, previously reported in paragraph 4.2, shall be satisfied. However, in some cases, the limitations imposed by the experimental testing on the columns with a high value of slenderness implies that the requirements are not completely satisfied. Consequently, in this selection, the number of columns affected by this limitation were minimized.

- The column slection criteria are summarized in Fig. 6.1.

Slender intervals	Number of columns
3-10	29
10-25	66
25-40	93
40-55	42
55-80	28

Table 6.1: Slenderness groups

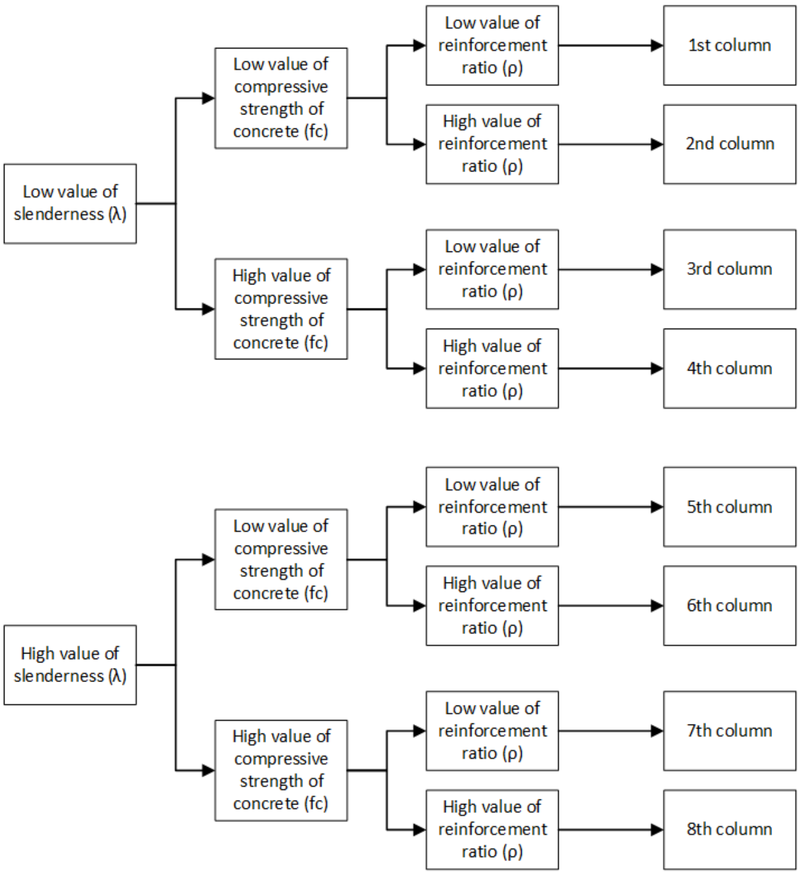

Figure 6.1: Column selection

In the following tables, the selected columns are reported, together with their main informations about: literature reference, test number identification (Test No.), slenderness (λ), reinforcement ratio (100ρ), and typology (see Fig. 4.1).

No.	Reference	Test No.	λ	100ρ	Type
1	[24]	2L20-30	9.7	2.04	B
2	[24]	2L20-60	9.7	2.04	B
3	[27]	C000	5.7	3.96	A
4	[24]	2L8-120R	9.7	2.04	B
5	[27]	C020	5.7	3.96	B
6	[24]	4L8-30	9.7	4.09	B
7	[24]	4L20-120	9.7	4.09	B
8	[24]	4L8-120R	9.7	4.09	B

Table 6.2: Investigated columns, λ [3-10]

No.	Reference	Test No.	λ	100ρ	Type
9	[30]	III	22.9	1.60	A
10	[27]	B020	15.7	3.96	B
11	[29]	N30-10.5-C0-3-30	23.6	3.23	D
12	[20]	3.3	21.4	1.10	B
13	[28]	A-17-0.25	17.0	3.27	B
14	[20]	5.1	21.5	3.10	B
15	[29]	H60-10.5-C0-1-30	23.6	1.44	D
16	[30]	Va	23.1	2.50	A

Table 6.3: Investigated columns, λ [10-25]

No.	Reference	Test No.	λ	100ρ	Type
17	[30]	I	32.1	1.60	A
18	[23]	24D-2	30.0	2.50	E
19	[28]	C-31.7-0.25	31.7	3.35	B
20	[27]	RL300	25.0	2.64	B
21	[30]	2	25.8	0.60	A
22	[20]	4.1	30.0	1.20	B
23	[30]	8	25.6	0.60	B
24	[30]	VI	32.8	1.60	A

Table 6.4: Investigated columns, λ [25-40]

No.	Reference	Test No.	λ	100ρ	Type
25	[23]	15E -2	40.0	2.50	A
26	[26]	S28	48.1	4.18	B
27	[30]	9	40.2	0.80	B
28	[26]	S30	48.1	4.18	B
29	[30]	12	40.2	0.80	B
30	[30]	6	40.7	0.80	B
31	[30]	15	40.4	0.80	A
32	[30]	3	40.7	0.80	A

Table 6.5: Investigated columns, λ [40-55]

No.	Reference	Test No.	λ	100ρ	Type
33	[26]	S25	57.7	4.18	B
34	[25]	17A	65.0	5.44	A
35	[25]	5	60.0	4.52	A
36	[25]	6	60.0	4.52	A
37	[25]	8	79.0	5.44	A
38	[25]	20	70.1	5.44	A
39	[25]	18	70.1	5.44	A
40	[25]	7	79.0	5.44	A

Table 6.6: Investigated columns, λ [55-80]

6.3 Evaluation of V_R

6.3.1 Application of LHS

The LHS method is performed for each selected column, considering the following variables:

- f_c, compressive strength of concrete;
- f_y, yield strength of steel reinforcement;
- E_s, Young's modulus of steel reinforcement.

The other material parameters depend on the material parameters listed above.
A log-normal distribution is assumed for each material variable [13], with the mean

and the COV values reported in Tab. 6.7.

	f_c	f_s	E_s
mean	f_c^*	f_y^*	E_s^*
COV	15%	5%	3%

Table 6.7: Distribution parameters

The mean values of f_c^* and f_y^* are given for each column. The mean values of E_s^* is taken equal to 210000[MPa] for each column.
The LHS process is explained in Paragraph 1.3.2. A sample size of 30 were used to model those variables. Tab. 6.9 shows the ranked values obtained using the variable mean values (Tab. 6.8) associated to Test No. 2L8-120R.

	f_c **[MPa]**	f_s **[MPa]**	E_s **[MPa]**
mean	56.00	480.00	210000
COV	15%	5%	3%

Table 6.8: Distribution parameters for column no 2L8-120R

Each row represents a set of input variables that are inserted into the 2L8-120R column model, and, consequently, 30 values of mean resistance R_m are obtained.
This process is accomplished for the 40 columns, obtaining 40 distribution of resistance (N).

6.3.2 Characterization of probability distributions

As the GSF is based on the assumption that a random distribution of resistance fits a log-normal distribution (see [13]), the 40 distributions, obtained in the previous phase, are tested considering Pearson's Chi-squared test and Anderson-Darling tests. In Fig. 6.2 are reported the frequency histogram, the probability plot, and the p-value, for a log-normal fit related to the distribution resistance related to 2L8-120R column.
In *Appendix B*, the frequency histogram, the probability plot and the p-values, for some resistance distribution, are reported.

	f_c **[MPa]**	f_y **[MPa]**	E_s **[MPa]**
1	54.89	504.36	217146
2	66.99	434.37	204039
3	41.25	485.23	215249
4	59.85	455.61	212603
5	53.26	458.46	209109
6	44.56	493.52	211032
7	48.23	514.65	202747
8	53.79	441.47	208206
9	73.05	521.49	218361
10	69.19	496.75	210603
11	43.46	471.90	209559
12	71.20	468.21	204650
13	57.69	461.94	208432
14	51.36	459.14	211622
15	56.65	473.92	213860
16	50.09	476.58	206049
17	50.88	501.67	207357
18	63.19	534.65	221167
19	61.04	487.90	197867
20	61.98	465.83	222031
21	55.88	494.95	212523
22	46.15	479.38	216445
23	57.03	448.13	201702
24	65.12	509.91	205294
25	54.61	484.29	206706
26	60.32	478.17	213448
27	58.30	490.53	199767
28	49.40	481.80	215129
29	52.23	452.65	203228
30	47.72	470.17	210316

Table 6.9: Input variables that characterize the material variability in column no 2L8-120R

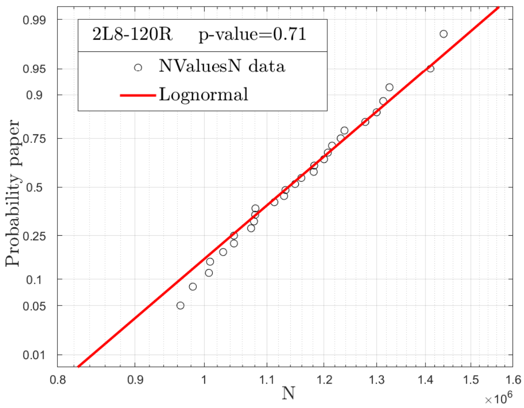

(a) Probability Plot

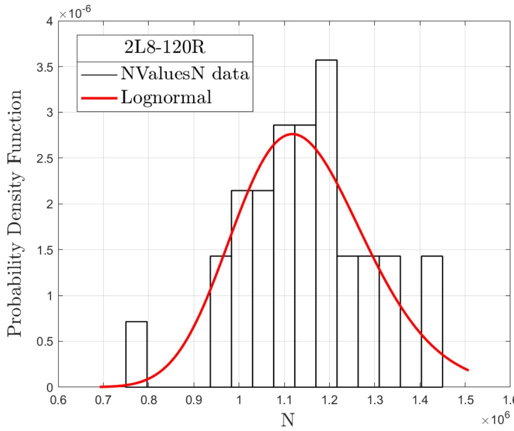

(b) Probability Density Function

Figure 6.2: Log-normal fit - 2L8-120R

The resistance distribution fits a log-normal distribution for all the 40 columns considered, which confirms the assumption made by [13].

6.3.3 Evaluation of V_R

The V_R can be evaluated, for each column, using the mean value and the standard deviation of the resistance distribution. This two distribution parameters can be obtained by means of the Maximum Likehood Estimator method (MLE). MLE attempts to find the parameter values that maximize the likehood function of the distribution.

Then, COV is obtained as follows:

$$V_R = \frac{\sigma_R}{\mu_R} \tag{6.2}$$

The obtained values are reported in Tab. 6.10.

no	V_R	γ_R	no	V_R	γ_R	no	V_R	γ_R	no	V_R	γ_R
1	0.11	1.40	11	0.12	1.46	21	0.11	1.41	31	0.10	1.37
2	0.11	1.41	12	0.12	1.42	22	0.09	1.30	32	0.10	1.37
3	0.10	1.35	13	0.08	1.26	23	0.06	1.19	33	0.07	1.24
4	0.12	1.45	14	0.09	1.33	24	0.09	1.33	34	0.08	1.27
5	0.09	1.31	15	0.12	1.43	25	0.09	1.31	35	0.09	1.32
6	0.10	1.37	16	0.10	1.35	26	0.08	1.28	36	0.09	1.31
7	0.10	1.34	17	0.09	1.31	27	0.09	1.32	37	0.08	1.27
8	0.10	1.37	18	0.09	1.32	28	0.07	1.24	38	0.09	1.30
9	0.10	1.36	19	0.07	1.24	29	0.09	1.30	39	0.09	1.31
10	0.09	1.31	20	0.10	1.35	30	0.09	1.32	40	0.08	1.27

Table 6.10: V_R and γ_R for each columns

6.4 Evaluation of γ_R

It is possible to evaluate γ_R, for each column, by means of Eq. 6.1. Values are reported in Tab. 6.10.

6.4.1 γ_R dependence on slenderness factor

In Fig. 6.3 γ_R is plotted in function of the slenderness λ.

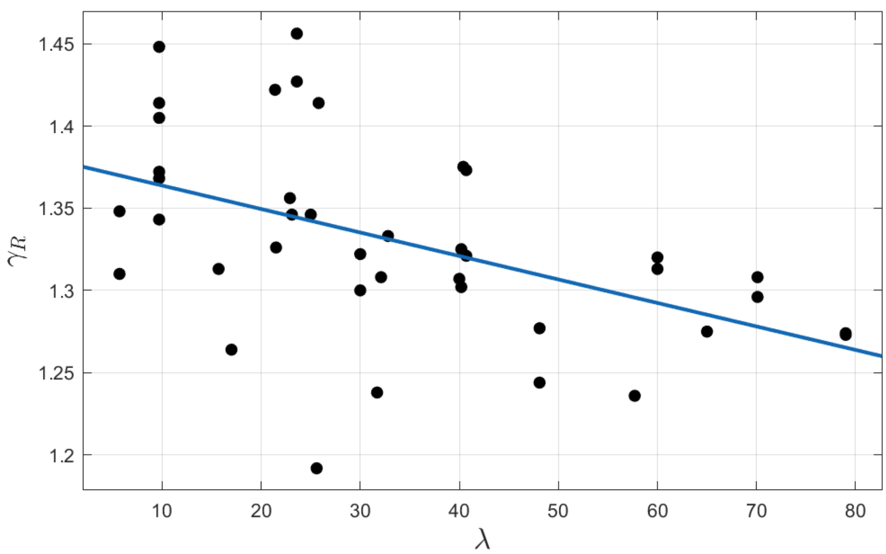

Figure 6.3: γ_R - λ

The blue line is the linear trend, which best fits the γ_R-λ points.
This trend shows that γ_R decreases when λ increase. This means that when the slenderness increase, the aleatoric uncertainty is less relevant in the failure problem. The instability failure is the dominant failure, which does not depends on the material uncertainties, but it depends on the geometric characteristics, which are assumed as deterministic parameters.

In conclusion, the results lead to define two different values of the aleatory uncertainty factor, which depends on the slenderness parameter. For slenderness from 3 to 40, the proposed value of α_R is equal to 1.35. For slenderness from 40 to 80, the proposed value of α_R is equal to 1.30.

Chapter 7

Assessment of the Model Uncertainties Factor for slender RC members

7.1 Introduction

Non-linear analysis are used to predict the actual structural response, but they are characterized by a certain level of uncertainty, mainly related to the definition of the resistance model. The essential structural characteristic behaviour is represented by a numerical model, which neglects some aspects. Hence, this is epistemic uncertainty, which is related to a lack of knowledge.

The aim of this Chapter is to evaluate the model uncertainties factor (γ_{Rd}), which takes into account all the resisting model uncertainties of 2D Non-Linear Analysis (NLA) performed on slender RC members. This factor is used in the global resistance method, to define the design structural resistance (R_d), as it is expressed in Eq. 3.19.

The resisting model uncertainty (θ_i) can be estimated as follows:

$$\theta_i = \frac{R_i(X,Y)}{R_{NLA,i}(X)} \tag{7.1}$$

where X is the vector of all the variables included into the resistance model, Y is the vector of all the variables that are neglected into the model, but affect the resisting mechanism. However, θ_i takes into account also of all the effects related to Y.

Then, a probabilistic model has to be defined in order to characterise the random variable θ, estimating its mean value (μ_θ) and its variance (σ_θ^2).
This process leads to the definition of the resistance model uncertainties factor (γ_{Rd}), using the following expression:

$$\gamma_{Rd} = \frac{1}{\mu_\theta \exp\left(-\alpha_R \beta V_\theta\right)} \tag{7.2}$$

where V_θ is the COV related to the resisting model uncertainties.

The following paragraphs describe all the steps of the process that leads to the definition of γ_R.

7.2 Description of the simulation

The selected experimental tests, reported in Chapter 6, are used to perform simulations, in order to estimate the resistance model uncertainties and calibrate γ_{Rd}, considering different plausible solution strategies and various types of software.

Three different software are used, in order to reproduce the structural response of the experimental tests:

- Diana [33];
- Adina [34];
- OpenSees [35].

A differentiation, with respect to the concrete tensile mechanical behaviour, in the definition of non-linear analysis models, is considered:

- elastic-brittle (Brittle);
- elastic with post peak Linear Tension Softening (LTS);
- elastic-perfectly plastic (Plastic).

The Brittle and the Plastic behaviour are considered as the upper and the lower approaches. The LTS is calibrated in each software, with the aim to best fit the experimental results. The calibration procedure is performed modifying the extension of the softening branch, and consequently the fracture energy.

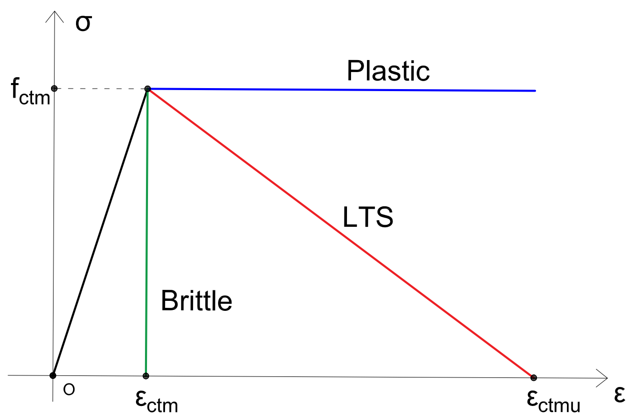

Figure 7.1: Concrete tensile mechanical behaviour

Hence, for each structural member, 9 different structural models are defined, combining the three different types of software with the three different concrete tensile behaviour.

As 40 columns have been selected, 360 non-linear structural models have been simulated, as it is showed in Fig. 7.2.

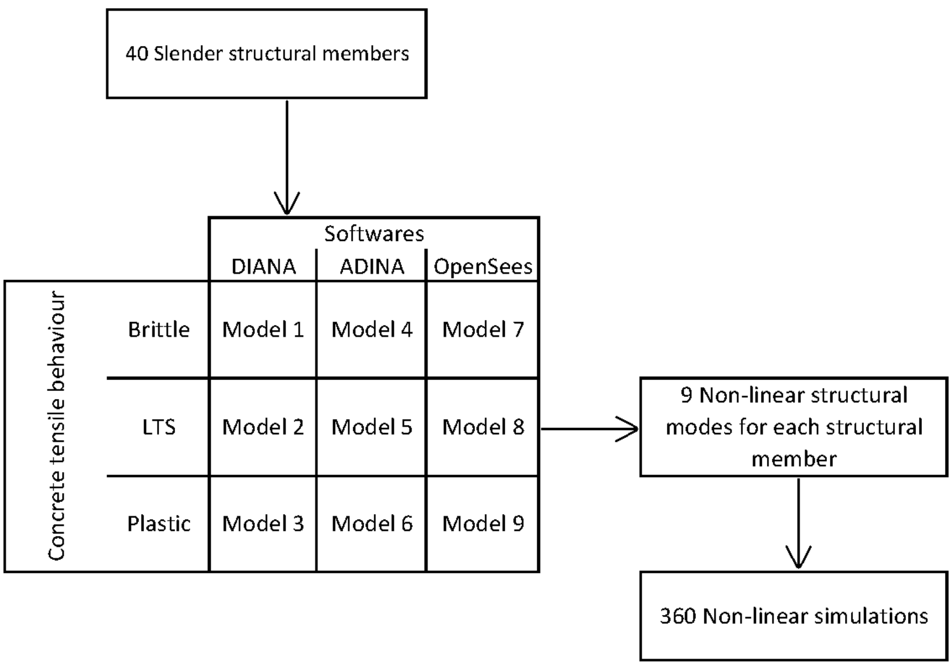

Figure 7.2: Distinction between the 9 models, for the 40 investigated columns

7.3 Assessment of the model uncertainty factor related to the resistance model

In this section, all the outcomes derived from the 360 simulations are treated to assess γ_R.

7.3.1 Estimation of model uncertainties

The model uncertainties (θ_i) are estimated as follows:

$$\theta_i = \frac{R_{exp,i}}{R_{NLA,i}} \tag{7.3}$$

where $R_{exp,i}$ is the i^{th} experimental ultimate resistance, and $R_{NLA,i}$ is the corresponding i^{th} outcome of the non-linear analysis.
The values of $R_{exp,i}$ and $R_{NLA,i}$ are reported in Tab. 7.1 and Tab. 7.2.

No.	**Ref.**	R_{exp} [kN]	$R_{NLA,1}$ [kN]	$R_{NLA,2}$ [kN]	$R_{NLA,3}$ [kN]	$R_{NLA,4}$ [kN]	$R_{NLA,5}$ [kN]	$R_{NLA,6}$ [kN]	$R_{NLA,7}$ [kN]	$R_{NLA,8}$ [kN]	$R_{NLA,9}$ [kN]
1	[24]	750.00	910.90	910.90	916.20	728.25	742.50	691.58	691.58	694.28	694.55
2	[24]	700.00	978.80	978.80	985.50	734.77	734.77	736.39	736.39	736.39	739.53
3	[27]	559.58	611.60	611.60	611.60	545.12	545.12	560.59	560.59	560.59	560.59
4	[24]	1092.00	1587.00	1587.00	1587.00	1087.32	1090.88	1152.72	1152.72	1152.72	1152.72
5	[27]	327.32	396.00	396.00	402.90	319.90	336.91	325.74	325.74	328.47	329.02
6	[24]	1100.00	1351.00	1351.00	1353.00	1110.90	1110.90	1032.90	1032.90	1032.90	1032.90
7	[24]	900.00	1037.00	1037.00	1046.00	787.50	787.50	826.10	826.10	830.68	830.68
8	[24]	1247.00	1608.00	1608.00	1608.00	1211.34	1211.34	1319.47	1319.47	1319.47	1319.47
9	[30]	343.23	341.80	341.80	341.80	332.43	332.43	347.26	347.26	347.26	347.26
10	[27]	271.46	298.60	298.60	308.60	219.20	227.24	257.02	257.02	263.74	263.74
11	[29]	280.00	11.64	11.90	11.90	23.50	23.50	16.18	16.18	16.61	17.60
12	[20]	782.57	827.30	827.30	835.90	787.46	787.46	856.35	856.35	856.35	866.52
13	[28]	1181.44	1273.00	1273.00	1307.00	1322.10	1322.10	1367.39	1367.39	1367.39	1393.92
14	[20]	735.50	745.60	745.60	793.50	725.35	725.35	810.84	810.84	810.84	853.75
15	[29]	412.00	13.90	13.90	13.90	17.10	17.10	17.88	17.88	17.88	20.52

Table 7.1: $R_{exp,i}$ values for each column and $R_{NLA,i}$ results for each model , part 1 (The Test No. is reported in Paragraph 6.2)

No.	Ref.	R_{exp} [kN]	$R_{NLA,1}$ [kN]	$R_{NLA,2}$ [kN]	$R_{NLA,3}$ [kN]	$R_{NLA,4}$ [kN]	$R_{NLA,5}$ [kN]	$R_{NLA,6}$ [kN]	$R_{NLA,7}$ [kN]	$R_{NLA,8}$ [kN]	$R_{NLA,9}$ [kN]
16	[30]	684.50	603.60	662.30	744.40	608.60	608.60	680.67	680.67	680.67	680.67
17	[30]	264.78	259.90	259.90	259.90	252.44	252.44	257.96	257.96	257.96	257.96
18	[23]	198.39	184.60	184.60	184.60	188.00	192.09	192.80	192.80	192.80	192.80
19	[28]	333.38	207.40	219.60	219.60	224.81	262.75	248.41	248.41	280.08	280.08
20	[27]	474.32	334.00	351.00	351.00	381.42	395.45	414.92	414.92	423.26	423.26
21	[30]	696.27	763.20	763.20	763.20	621.28	632.08	762.03	762.03	762.03	762.03
22	[20]	367.75	297.70	346.80	346.80	210.94	403.02	397.50	397.50	391.66	455.72
23	[30]	235.36	197.40	217.70	217.70	191.17	224.47	216.24	216.24	236.75	247.32
24	[30]	392.27	361.00	361.80	361.80	327.27	327.94	363.18	363.18	363.19	363.19
25	[23]	161.03	121.40	121.90	121.90	127.00	130.00	129.32	129.32	129.32	129.32
26	[26]	44.00	53.89	53.89	58.64	55.42	54.88	49.88	49.88	49.88	55.75
27	[30]	205.94	163.70	184.50	184.50	205.25	205.25	161.11	161.11	205.94	208.73
28	[26]	48.00	54.91	54.91	59.78	56.10	56.10	58.49	58.49	53.40	66.69
29	[30]	112.78	153.50	153.50	172.50	114.70	114.70	115.22	115.22	112.15	176.78
30	[30]	225.55	185.70	204.10	204.10	153.40	223.21	187.40	187.40	227.58	243.97
31	[30]	549.17	509.40	509.40	509.40	394.35	394.35	560.26	560.26	560.26	560.26
32	[30]	666.85	511.40	511.40	511.40	456.60	456.60	563.42	563.42	563.42	563.42
33	[26]	36.00	39.53	39.53	43.59	31.21	32.73	42.26	42.26	42.26	48.98
34	[25]	31.88	32.65	32.65	32.80	25.96	25.96	37.10	37.10	37.10	37.10
35	[25]	72.74	67.62	67.62	67.82	53.88	53.88	78.71	78.71	78.71	78.71
36	[25]	72.24	70.34	70.34	70.64	51.97	51.97	82.31	82.31	82.31	82.31
37	[25]	31.88	26.60	26.64	26.64	23.27	23.27	30.98	30.98	30.98	30.98
38	[25]	37.86	29.10	30.17	30.17	27.43	27.43	39.76	39.76	39.76	39.76
39	[25]	33.88	29.09	30.16	30.16	24.37	24.37	39.84	39.84	39.84	39.84
40	[25]	29.89	27.61	27.61	27.61	20.61	20.61	32.27	32.27	32.27	32.27

Table 7.2: $R_{exp,i}$ values for each column and $R_{NLA,i}$ results for each model , part 2 (The Test No. is reported in Paragraph 6.2)

In Tab. 7.3 and Tab. 7.4 all the θ_i values are reported.

No.	Ref.	Test No.	θ_1 [-]	θ_2 [-]	θ_3 [-]	θ_4 [-]	θ_5 [-]	θ_6 [-]	θ_7 [-]	θ_8 [-]	θ_9 [-]
1	[24]	2L20-30	0.82	0.82	0.82	1.03	1.01	1.01	1.08	1.08	1.08
2	[24]	2L20-60	0.72	0.72	0.71	0.95	0.95	0.94	0.95	0.95	0.95
3	[27]	C000	0.91	0.91	0.91	1.03	1.03	1.03	1.00	1.00	1.00
4	[24]	2L8-120R	0.69	0.69	0.69	1.00	1.00	1.00	0.95	0.95	0.95
5	[27]	C020	0.83	0.83	0.81	1.02	0.97	0.97	1.00	1.00	0.99
6	[24]	4L8-30	0.81	0.81	0.81	0.99	0.99	0.99	1.06	1.06	1.06
7	[24]	4L20-120	0.87	0.87	0.86	1.14	1.14	1.14	1.09	1.08	1.08
8	[24]	4L8-120R	0.78	0.78	0.78	1.03	1.03	1.03	0.95	0.95	0.95
9	[30]	III	1.00	1.00	1.00	1.03	1.03	1.03	0.99	0.99	0.99
10	[27]	B020	0.91	0.91	0.88	1.24	1.19	1.19	1.06	1.03	1.03
11	[29]	N30-10.5-C0-	1.42	1.39	1.39	0.71	0.71	0.67	1.02	1.00	0.94
12	[20]	3.3	0.95	0.95	0.94	0.99	0.99	0.97	0.91	0.91	0.90
13	[28]	A-17-0.25	0.93	0.93	0.90	0.89	0.89	0.88	0.86	0.86	0.85
14	[20]	5.1	0.99	0.99	0.93	1.01	1.01	0.97	0.91	0.91	0.86
15	[29]	H60-10.5-C0-	1.24	1.24	1.24	1.01	1.01	1.05	0.96	0.96	0.84
16	[30]	Va	1.13	1.03	0.92	1.12	1.12	1.12	1.01	1.01	1.01
17	[30]	I	1.02	1.02	1.02	1.05	1.05	1.05	1.03	1.03	1.03
18	[23]	24D-2	1.07	1.07	1.07	1.06	1.03	1.03	1.03	1.03	1.03
19	[28]	C-31.7-0.25	1.61	1.52	1.52	1.48	1.27	1.27	1.34	1.19	1.19
20	[27]	RL300	1.42	1.35	1.35	1.24	1.20	1.20	1.14	1.12	1.12
21	[30]	2	0.91	0.91	0.91	1.12	1.10	1.10	0.91	0.91	0.91
22	[20]	4.1	1.24	1.06	1.06	1.74	0.91	0.91	0.93	0.94	0.81
23	[30]	8	1.19	1.08	1.08	1.23	1.05	1.05	1.09	0.99	0.95
24	[30]	VI	1.09	1.08	1.08	1.20	1.20	1.20	1.08	1.08	1.08
25	[23]	15E -2	1.33	1.32	1.32	1.27	1.24	1.24	1.25	1.25	1.25
26	[26]	S28	0.82	0.82	0.75	0.79	0.80	0.80	0.88	0.88	0.79
27	[30]	9	1.26	1.12	1.12	1.00	1.00	1.00	1.28	1.00	0.99
28	[26]	S30	0.87	0.87	0.80	0.86	0.86	0.79	0.82	0.90	0.72
29	[30]	12	0.73	0.73	0.65	0.98	0.98	0.74	0.98	1.01	0.64
30	[30]	6	1.21	1.11	1.11	1.47	1.01	1.01	1.20	0.99	0.92

Table 7.3: The θ_i value for the different structural models, part 1

No.	Ref.	Test No.	θ_1	θ_2	θ_3	θ_4	θ_5	θ_6	θ_7	θ_8	θ_9
			[-]	[-]	[-]	[-]	[-]	[-]	[-]	[-]	[-]
31	[30]	15	1.08	1.08	1.08	1.39	1.39	1.39	0.98	0.98	0.98
32	[30]	3	1.30	1.30	1.30	1.46	1.46	1.69	1.18	1.18	1.18
33	[26]	S25	0.91	0.91	0.83	1.15	1.10	0.86	0.85	0.85	0.73
34	[25]	17A	0.98	0.98	0.97	1.23	1.23	1.32	0.86	0.86	0.86
35	[25]	5	1.08	1.08	1.07	1.35	1.35	1.35	0.92	0.92	0.92
36	[25]	6	1.03	1.03	1.02	1.39	1.39	1.39	0.88	0.88	0.88
37	[25]	8	1.20	1.20	1.20	1.37	1.37	1.37	1.03	1.03	1.03
38	[25]	20	1.30	1.25	1.25	1.38	1.38	1.38	0.95	0.95	0.95
39	[25]	18	1.16	1.12	1.12	1.39	1.39	1.39	0.85	0.85	0.85
40	[25]	7	1.08	1.08	1.08	1.45	1.45	1.45	0.93	0.93	0.93

Table 7.4: The θ_i value for the different structural models, part 2

7.3.2 Probabilistic analysis of the resisting model uncertainties

In this sections, the probabilistic analysis of θ_i is presented.

7.3.3 Bayesian updating

The Bayesian approach is used for the probabilistic treatment of the resisting model uncertainty for non-linear analysis.
The model uncertainty values, evaluated in the previous phase for a specific model, represent the prior information. The new information consists of the numerical outcomes related to the other models, and it is used to update the prior results. In other words, the prior information, related to each structural model, is updated considering the data obtained from the other models. Then, the posterior distributions are evaluated.
The Bayesian updating is described in the following steps:

- $F(M_j)$ $j = 1, ..., 9$ is the marginal distribution assessed considering the different models equiprobable;
- the prior distribution functions $F(\theta|M_j)$ for each resisting model M_j are assessed;

- for each structural model M_j, assessment of the statistical parameters, that are assumed determinism and summarized into the vector z, of the distribution function $F_{M_j}(\theta|M_j)$ averaging the statistical parameters of the models; in this way, nine $F_{M_j}(\theta|M_j)$, $j = 1, ..., 9$, are estimated and each one represents the new information, deriving from the results of the other eight models, for the structural model M_j;
- the posterior distribution functions $F(\theta|M_j, z)$ are assessed for each structural model M_j, and represent the posterior data;
- assessment of the posterior distribution function $F(\theta|Z)$ with the estimation of the distribution parameters, which are assumed deterministic and summarized into the vector z, averaging the statistical parameters of the posterior distribution of the different structural models.

The resisting model uncertainties for RC structures are modelled by unimodal log-normal distribution $F(\theta|M_j)$, according to [13].

Structural model	Prior distribution $F(\theta\|M_j)$			New distribution $F_{M_j}(\theta\|M_j)$			Posterior distribution $F(\theta\|M_j, z)$		
	μ_θ [-]	σ_θ [-]	V_θ [-]	μ_θ [-]	σ_θ [-]	V_θ [-]	μ_θ [-]	σ_θ [-]	V_θ [-]
1	1.05	0.21	0.20	1.03	0.17	0.17	1.10	0.21	0.19
2	1.02	0.19	0.19	1.03	0.18	0.17	1.08	0.20	0.19
3	1.01	0.20	0.20	1.03	0.17	0.17	1.08	0.21	0.19
4	1.16	0.22	0.19	1.01	0.17	0.17	1.17	0.21	0.18
5	1.11	0.18	0.17	1.03	0.17	0.17	1.13	0.19	0.17
6	1.10	0.22	0.20	1.03	0.17	0.17	1.13	0.21	0.18
7	1.00	0.12	0.12	1.03	0.18	0.18	1.04	0.17	0.17
8	0.99	0.09	0.09	1.03	0.19	0.18	1.02	0.18	0.17
9	0.96	0.13	0.13	1.04	0.18	0.17	1.03	0.19	0.19

Table 7.5: Statistical parameters and coefficients of variation of the prior, posterior and new information functions

In Tab. 7.5 are reported the values of statistical parameters (the mean value and variance) of the prior distributions ($F(\theta|M_j)$), of the new informations ($F_{M_j}(\theta|M_j)$),

and of the posterior density functions ($F(\theta|M_j, z)$). The statistical parameters of those functions are estimated by means of the maximum likehood technique and are reported in Tab. 7.5. It can be noticed that the mean values of the posterior distributions are higher than the corresponding prior distribution values, this is related to the updating by the new informations.
As an example, in Fig. 7.3(a) is reported the probability plot, while in Fig. 7.3(b) is reported probability density function and the histogram, both for the model uncertainties related to Model 5. The Anderson-Darling test has been performed, reporting a p-value=0.05.

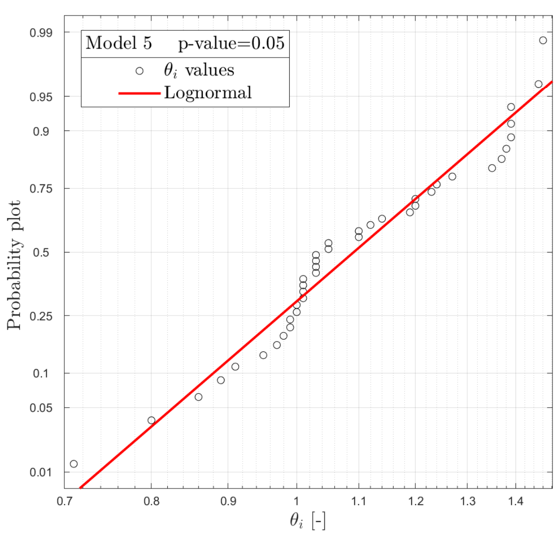

(a) Probability Plot

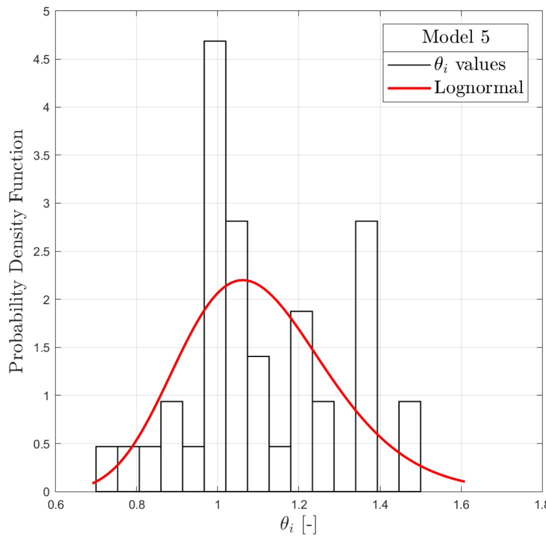

(b) Probability Density Function

Figure 7.3: Log-normal fit - Model 1

In Fig. 7.9(a) is reported the probability plot, while in Fig. 7.9(b) is reported probability density function and the histogram, both for the new information related to Model 5. The Anderson-Darling test has been performed, reporting a p-value=0.15. Similar results are achieved for the other models. The probability plot shows the uncertainty model distributions, and the corresponding new informations, are fitted by a log-normal distribution.

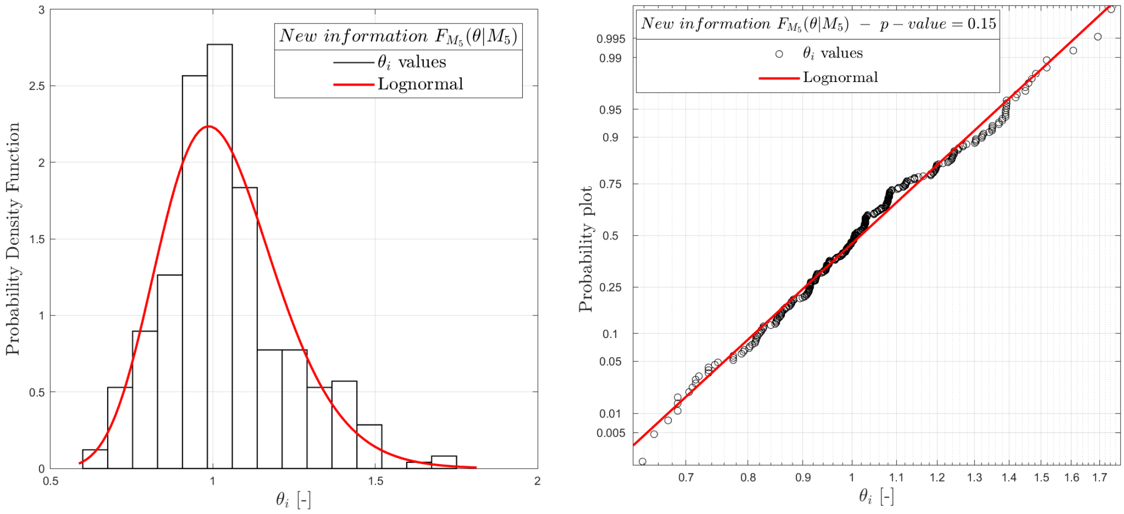

(a) Probability Plot (b) Probability Density Function

Figure 7.4: Log-normal fit - Model 1

In Tab. 7.6 the average statistical parameters of the posterior distribution are reported.

Posterior distribution $F(\theta\|Z)$		
μ_θ [-]	σ_θ [-]	V_θ [-]
1.09	0.20	0.18

Table 7.6: Average statistical parameters of the posterior distribution

The prior, the new, and the posterior probability density functions and the cumulative distribution functions are plotted in Fig. 7.5.

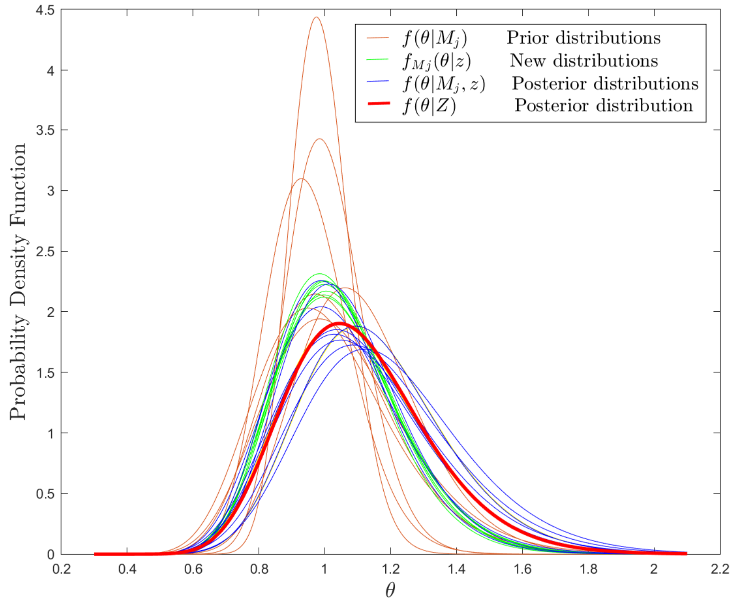

(a) Probability Density Function

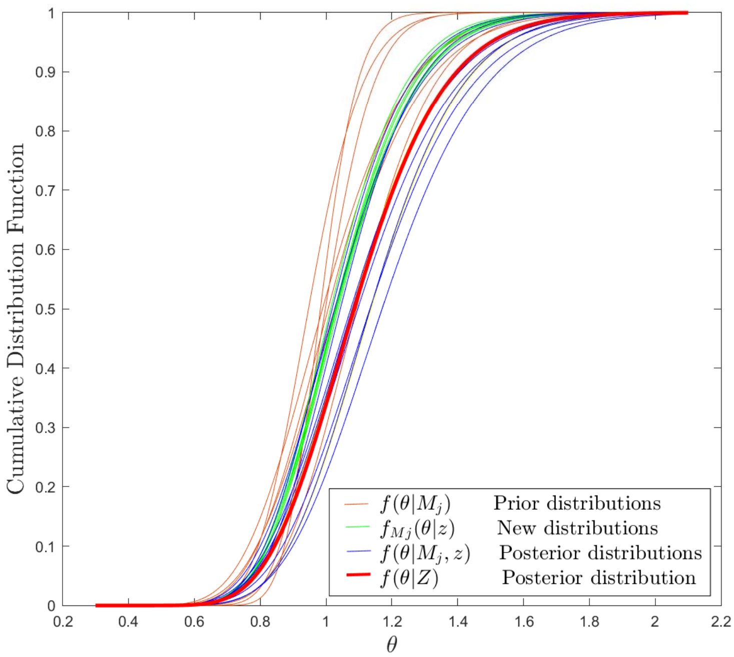

(b) Cumulative Distribution Function

Figure 7.5: Prior, new, and posterior information PDFs and CDFs

7.3.4 Partial safety factor evaluation

At this point, the partial safety factor γ_{Rd}, for the resisting model uncertainties of 2D non-linear slender RC members, can be evaluated by means of Eq. 7.2, for a required reliability level.

The parameters μ_θ and V_θ, used un the 7.2 are the average statistical parameters of

the posterior distribution, which are reported in Tab. 7.6.
Considering, in case of a new structures, a CC2, which means medium consequences of structural failure, and a design working life of 50 years ($\beta = 3.8$), the value of γ_{Rd} is equal to 1.14. Different class of consequences and different design working life can be also considered. For new structures, all the results are reported in Tab. 7.7. Whereas, the values for a existing structures are reported in Tab. 7.8. Those values of γ_{Rd} are evaluated considering the hypothesis of non-dominant resistance variable, hence, assuming the FORM sensitivity factor (α_R) equal to 0.32.

	Service life	**Consequences of failure**	**Reliability index β**	**FORM factor α_R**	**Partial safety γ_{Rd}**
New structures	[Years]	[-]	[-]	[-]	[-]
	50	Low	3.1		**1.10**
	50	Moderate	3.8	0.32	**1.15**
	50	High	4.3		**1.17**

Table 7.7: Partial safety factor values for model uncertainties in non-linear analysis of reinforced concrete slender members - New structures

	Residual service life	**Reliability index β**	**FORM factor α_R**	**Partial safety γ_{Rd}**
Existing structures	[Years]	[-]	[-]	[-]
	50	3.1 - 3.8		**1.10 - 1.15**
	15	3.4 - 4.1	0.32	**1.11 - 1.16**
	1	4.1 - 4.7		**1.16 - 1.20**

Table 7.8: Partial safety factor values for model uncertainties in non-linear analysis of reinforced concrete slender members - Existing structures

The range γ_{Rd} values for existing structures is suitable to be chosen owing to the residual service life and to the costs for an upgrading of the structure.

7.3.5 γ_{Rd} dependence on other factors

To demonstrate that the uncertainty distributions do not depend on other factors involved in the analysis, the following graphs, related to the Model 1 are plotted.

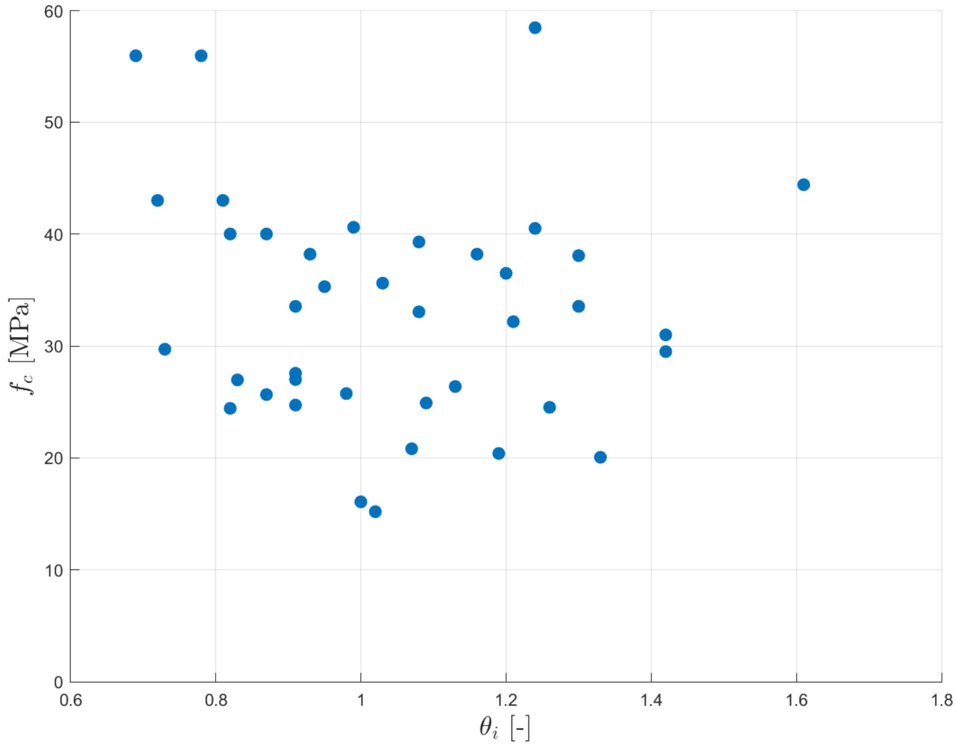

Figure 7.6: f_c - γ_{Rd}

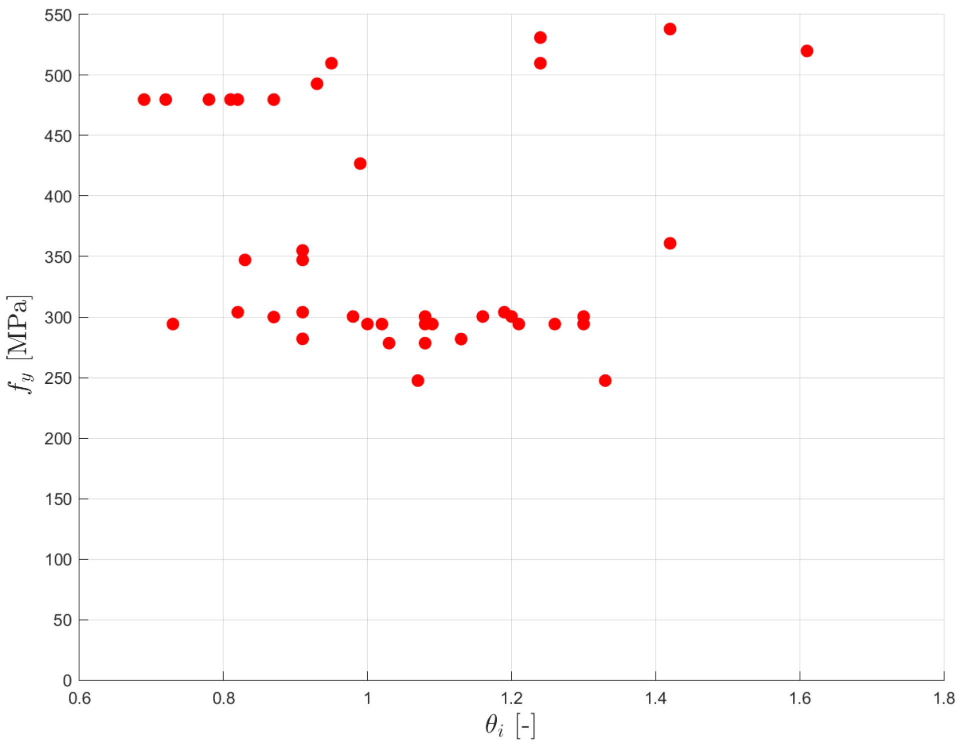

Figure 7.7: f_y - γ_{Rd}

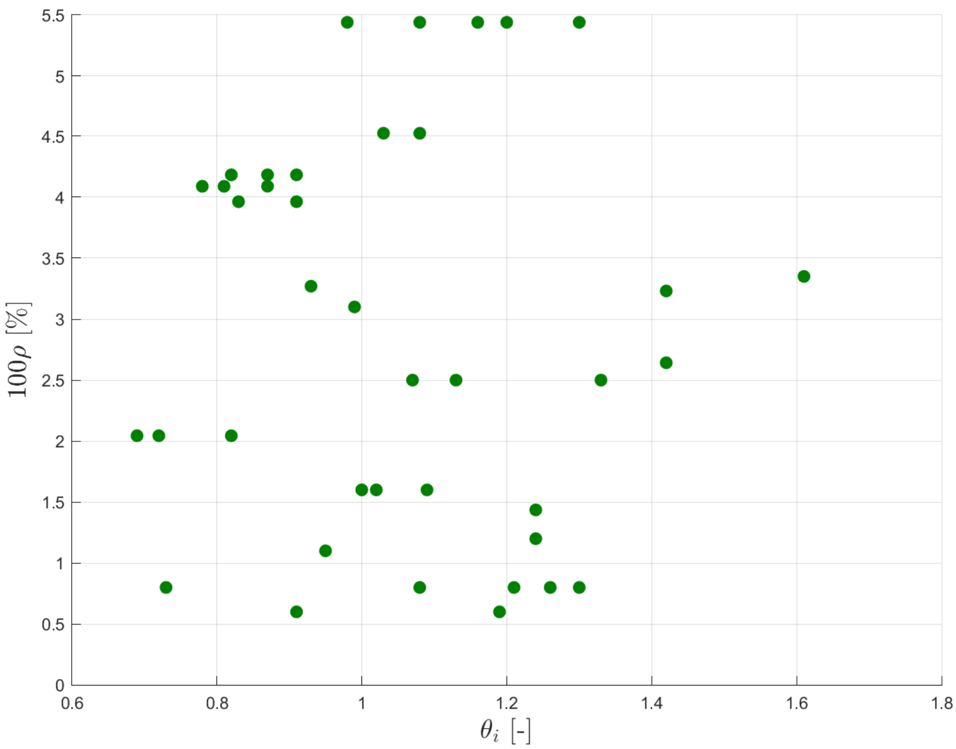

Figure 7.8: 100ρ - γ_{Rd}

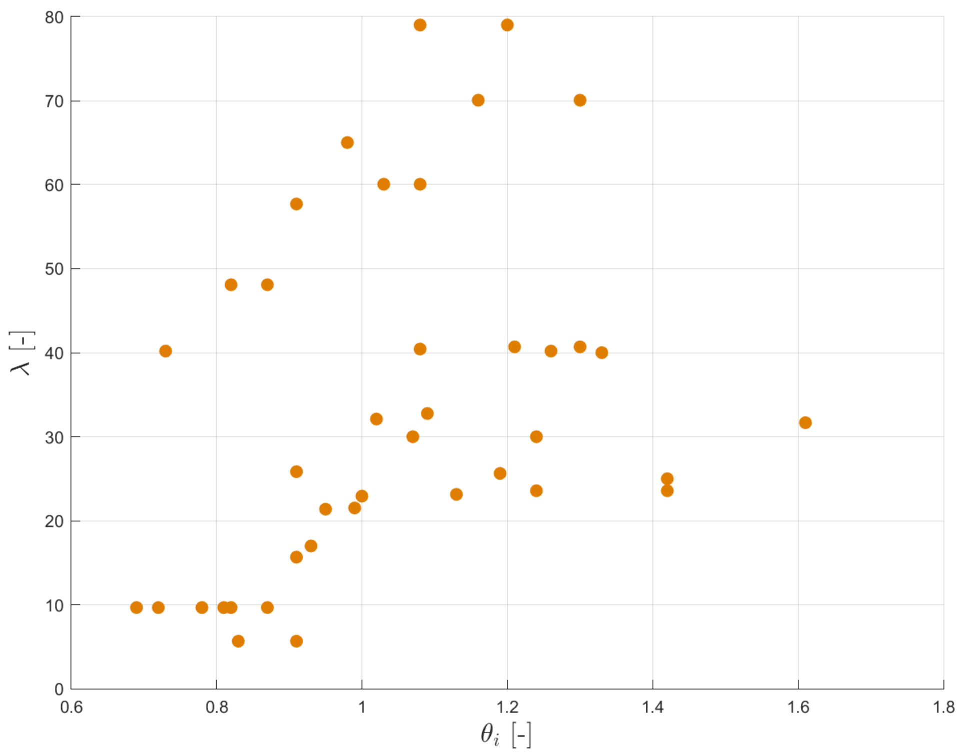

Figure 7.9: λ - γ_{Rd}

The graphs show that the relation between the model 1 uncertainty distribution and f_c, f_y, 100ρ, and λ do not follow any trend, hence, those parameters are not involved in the model uncertainty factor assessment. Same results can be proved for the other 8 model uncertainty distributions.

Chapter 8

Conclusions

This Master's Thesis work proposes and evaluates the partial safety factors related to the aleatoric and the model uncertainties, regarding the overall structural resistance for non-linear analysis of slender reinforced concrete members.
Several experimental tests have been found in literature, considering different types of column subjected to an axial load or an eccentric load.

For each experimental test, one structural model have been defined, in order to evaluate the aleatoric uncertainty on the non-linear analysis of reinforced concrete structures.
The aleatory uncertainty are related to the material uncertainty, which aleatory behaviour can be described by a log-normal distribution.
The Latin Hypercube Sample method has been performed for each columns, taking into account of the material log-normality, in order to obtain a set of material parameters, which takes into account of their intrinsic aleatory characteristic. Those sets have been used as input into the non-linear models, in order to evaluate the resulting resistance distribution of each column model. This leads to a total number of 1200 non-linear analysis. Those distributions lead to define a aleatory uncertainty factor for each columns. The analysis results show that α_R decreases when the slenderness increase. This means that when the slenderness increase, the aleatoric uncertainty is less relevant in the failure problem. When the slenderness increase, the instability failure becomes the dominant failure, which does not depends on the material uncertainties, but it depends on the geometric characteristics, which are assumed as deterministic parameters. Hence, the results lead to define two different values of the aleatory uncertainty factor, which depends on the slenderness parameter. For slenderness from 3 to 40, the proposed value of α_R is equal to 1.35. For slenderness

from 40 to 80, the proposed value of α_R is equal to 1.30.

Several structural models have been defined for each experimental test, in order to investigate the model uncertainty influence, on the non-linear analysis on reinforced concrete slender members. Then, three different software codes and three different constitutive laws for the behaviour of concrete in tension have been adopted, which lead to a total number of 360 non-linear analysis. The resistance model uncertainties have been evaluated and characterized by appropriate log-normal distributions. Then, the Bayesian approach has been used in the probabilistic analysis, in order to assess a posterior uncertainty distribution, which has mean value and coefficient of variation equal to 1.09 and 0.18 respectively.
Finally, the value of the partial safety factor related to the resisting model uncertainties, in agreement with the safety format for non-linear analysis, have been assessed for each reliability level corresponding to new or existing structures, of the failure consequences and of the hypothesis of non-dominant resistance variables.
Then, the partial safety factor related to the resisting model uncertainties presents a range of variation for new structures between 1.10 and 1.17, and for existing structures between 1.10 and 1.20.
In conclusion, for both new and existing ordinary structures, in the hypotheses of non-dominant resistance variable, of moderate consequences of structural failure and for service life of 50 years, a partial safety factor for the resisting model uncertainties for non-linear analysis of reinforced concrete slender members equal to 1.15 is suggested.

Appendix A

Experimental data

A.1 Kim, J. K., and Yang, J. K. 1993

Test No.	ltot [mm]	l [mm]	l/h [-]	b [mm]	h [mm]	d'b [mm]	d'h [mm]	100p [%]	As [mm$_2$]	ϕs [mm]	n° tot [-]	n° b [-]	n° h [-]	Asw [mm$_2$]	ϕst [mm]	s [mm]	fc [Mpa]	fy [Mpa]	fu [Mpa]	ei,h,t/h [-]	ei,h,b/h [-]	Type	Nexp [kN]
10L4-1	240	220	3	80	80	15.0	15.0	3.94	252.2	6.4	8	3	3	7.1	3.0	60	25.50	387.00	-	0.300	0.300	B	109.50
10L4-2	240	220	3	80	80	15.0	15.0	3.94	252.2	6.4	8	3	3	7.1	3.0	60	25.50	387.00	-	0.300	0.300	B	109.30
60L2-1	1440	1420	18	80	80	15.0	15.0	1.98	126.7	6.4	4	2	2	7.1	3.0	60	25.50	387.00	-	0.300	0.300	B	63.70
60L2-2	1440	1420	18	80	80	15.0	15.0	1.98	126.7	6.4	4	2	2	7.1	3.0	60	25.50	387.00	-	0.300	0.300	B	65.70
100L2-1	2400	2380	30	80	80	15.0	15.0	1.98	126.7	6.4	4	2	2	7.1	3.0	60	25.50	387.00	-	0.300	0.300	B	38.20
100L2-2	2400	2380	30	80	80	15.0	15.0	1.98	126.7	6.4	4	2	2	7.1	3.0	60	25.50	387.00	-	0.300	0.300	B	35.00
100L4-1	2400	2380	30	80	80	15.0	15.0	3.94	252.2	6.4	8	3	3	7.1	3.0	60	25.50	387.00	-	0.300	0.300	B	49.00
100L4-2	2400	2380	30	80	80	15.0	15.0	3.94	252.2	6.4	8	3	3	7.1	3.0	60	25.50	387.00	-	0.300	0.300	B	47.00

Figure A.1: Data taken from [19]

A.2 Mehmel, A., Schwarz, H.,Kasparek, K. H. and Makovi, J. 1969

Test No.	ltot [mm]	l [mm]	l/h [-]	b [mm]	h [mm]	d'b [mm]	d'h [mm]	100ρ [%]	As [mm$_2$]	φs [mm]	n°tot [-]	n°b [-]	n°h [-]	Asw [mm$_2$]	φst [mm]	s [mm]	fc [Mpa]	fy [Mpa]	fu [Mpa]	ei,h,t/h [-]	ei,h,b/h [-]	Type	Nexp [kN]
0.1	1400	800	9	253	159	22.0	22.0	1.10	452.4	12.0	4	2	2	28.3	6.0	120	37.36	509.90	-	0.082	0.082	B	942.42
0.2	1400	800	8.97	254	156	22.0	22.0	1.10	452.4	12.0	4	2	2	28.3	6.0	120	40.50	509.90	-	1.000	1.000	B	137.29
1.1	3400	2700	16.7	253	203	32.0	32.0	1.20	615.8	14.0	4	2	2	28.3	6.0	160	39.23	483.40	-	0.177	0.170	B	857.10
1.2	3400	2700	16.8	253	202	32.0	32.0	1.20	615.8	14.0	4	2	2	28.3	6.0	160	37.76	483.40	-	0.475	0.475	B	319.70
2.1	4500	3800	22.3	252	202	30.0	30.0	1.20	615.8	14.0	4	2	2	28.3	6.0	160	37.27	483.40	-	0.178	0.178	B	588.40
2.2	4500	3800	22.2	252	203	32.0	32.0	1.20	615.8	14.0	4	2	2	28.3	6.0	160	40.70	483.40	-	0.478	0.478	B	258.90
3.1	3400	2700	22.4	252	152	26.0	26.0	1.20	452.4	12.0	4	2	2	28.3	6.0	140	38.25	509.90	-	0.164	0.164	B	470.72
3.2	3400	2700	22.5	252	151	26.0	26.0	1.20	452.4	12.0	4	2	2	28.3	6.0	140	41.09	509.90	-	0.503	0.497	B	176.52
3.3	3400	2700	21.4	254	159	25.0	25.0	1.10	452.4	12.0	4	2	2	28.3	6.0	120	35.30	509.90	-	0.082	0.082	B	782.57
3.4	3400	2700	21.5	253	158	25.0	25.0	1.10	452.4	12.0	4	2	2	28.3	6.0	120	42.76	509.90	-	1.000	1.000	B	101.99
4.1	4500	3800	30	253	150	25.0	25.0	1.20	452.4	12.0	4	2	2	28.3	6.0	140	40.50	509.90	-	0.163	0.163	B	367.75
4.2	4500	3800	30.4	253	148	25.0	25.0	1.20	452.4	12.0	4	2	2	28.3	6.0	140	41.48	509.90	-	0.493	0.493	B	145.14
5.1	3400	2700	21.5	253	158	30.0	30.0	3.10	1256.6	20.0	4	2	2	28.3	6.0	160	40.60	426.80	-	0.165	0.165	B	735.50
5.2	3400	2700	21.4	252	159	25.0	25.0	3.10	1256.6	20.0	4	2	2	28.3	6.0	160	36.97	426.80	-	0.503	0.503	B	369.71

Figure A.2: Data taken from [20]

A.3 Drysdale, R. G. and Huggins, M. W. 1971

Test No.	ltot	l	l/h	b	h	d'b	d'h	100ρ	As	φs	n° tot	n° b	n° h	Asw	φst	s	fc	fy	fu	ei,h,t/h	ei,h,b/h	Type	Nexp
	[mm]	[mm]	[-]	[mm]	[mm]	[mm]	[mm]	[%]	[mm$_2$]	[mm]	[-]	[-]	[-]	[mm$_2$]	[mm]	[mm]	[Mpa]	[Mpa]	[Mpa]	[-]	[-]		[kN]
D-1-A	3962	3283	31.2	127	127	19.1	19.1	3.142	506.7	12.7	4	2	2	11.4	3.8	101.6	30.34	386.66	-	0.200	0.200	B	173.04
D-1-B	3962	3283	31.2	127	127	19.1	19.1	3.14	506.7	12.7	4	2	2	11.4	3.8	101.6	30.34	386.66	-	0.200	0.200	B	171.70
D-2-C	3962	3283	31.2	127	127	19.1	19.1	3.14	506.7	12.7	4	2	2	11.4	3.8	101.6	29.16	386.66	-	0.200	0.200	B	176.59
D-2-D	3962	3283	31.2	127	127	19.1	19.1	3.14	506.7	12.7	4	2	2	11.4	3.8	101.6	29.16	386.66	-	0.200	0.200	B	180.15

Figure A.3: Data taken from [21]

A.4 Khalil, N., Cusens, A. R. and Parker M. D. 2001

Test No.	ltot [mm]	l [mm]	l/h [-]	b [mm]	h [mm]	d'b [mm]	d'h [mm]	100ρ [%]	As [mm$_2$]	ϕs [mm]	n° tot [-]	n° b [-]	n° h [-]	Asw [mm$_2$]	ϕst [mm]	s [mm]	fc [Mpa]	fy [Mpa]	fu [Mpa]	ei,h,t/h [-]	ei,h,b/h [-]	Type	Nexp [kN]
C1	2300	2250	18.4	125	125	21.3	21.3	2.90	453.1	12.01	4	2	2	7.1	3.0	125.00	52.20	530.00	-	0.08	0.08	B	450.00
C2	2300	2250	18.4	125	125	21.3	21.3	2.90	453.1	12	4	2	2	7.1	3.0	125.00	53.20	530.00	-	0.08	0.08	B	400.00
C3	2300	2250	27.1	125	85	19.6	19.6	2.96	314.5	10	4	2	2	4.9	2.5	85.00	57.30	530.00	-	0.12	0.12	B	210.00
C4	2300	2250	27.1	125	85	19.6	19.6	2.96	314.5	10	4	2	2	4.9	2.5	85.00	48.70	530.00	-	0.12	0.12	B	180.00
C5	3650	3600	29.2	152	125	27.5	27.5	4.23	803.7	16	4	2	2	12.6	4.0	125.00	56.40	530.00	-	0.08	0.08	B	360.00
C7	4250	4200	34	152	125	27.5	27.5	4.23	803.7	16	4	2	2	12.6	4.0	125.00	51.80	530.00	-	0.08	0.08	B	250.00
C9	4850	4800	38.8	152	125	27.5	27.5	4.23	803.7	16	4	2	2	12.6	4.0	125.00	52.00	530.00	-	0.08	0.08	B	205.00
C11	4550	4500	45.5	152	100	21.0	21.0	2.97	451.4	12	4	2	2	7.1	3.0	100.00	47.40	530.00	-	0.10	0.10	B	102.00
C14	5050	5000	50.5	152	100	21.0	21.0	2.97	451.4	12	4	2	2	7.1	3.0	100.00	52.80	530.00	-	0.10	0.10	B	85.00
C17	5050	5000	56.1	152	90	21.6	21.6	3.30	451.4	12	4	2	2	7.1	3.0	90.00	54.80	530.00	-	0.11	0.11	B	65.00
C19	5050	5000	63.1	152	80	17.6	17.6	2.58	313.7	10	4	2	2	4.9	2.5	80.00	50.10	530.00	-	0.13	0.13	B	45.00

Figure A.4: Data taken from [22]

A.5 Saenz, L. P. and Martin, I. 1963

Test No.	ltot [mm]	l [mm]	l/h [-]	b [mm]	h [mm]	d'b [mm]	d'h [mm]	100ρ [%]	As [mm$_2$]	ϕs [mm]	n° tot [-]	n° b [-]	n° h [-]	Asw [mm$_2$]	ϕst [mm]	s [mm]	fc [Mpa]	fy [Mpa]	fu [Mpa]	ei,h,t/h [-]	ei,h,b/h [-]	Type	Nexp [kN]
26D-1	2248	2248	25	127	89.92	14.3	14.3	1.10	125.6	6.3	4	2	2	7.3	3.1	91	23.10	263.38	-	-	-	D	216.18
26D-2	2248	2248	25	127	89.9	14.3	14.3	1.10	125.6	6.3	4	2	2	7.3	3.1	91	23.10	263.38	-	-	-	D	271.79
26D-3	2248	2248	25	127	89.9	14.3	14.3	1.10	125.6	6.3	4	2	2	7.3	3.1	91	23.10	263.38	-	-	-	D	236.20
23D-1	2248	2248	25	127	89.9	15.9	15.9	2.50	285.5	9.5	4	2	2	7.3	3.1	91	19.58	247.52	-	-	-	D	276.68
23D-2	2248	2248	25	127	89.9	15.9	15.9	2.50	285.5	9.5	4	2	2	7.3	3.1	91	19.58	247.52	-	-	-	D	233.53
23D-3	2248	2248	25	127	89.9	15.9	15.9	2.50	285.5	9.5	4	2	2	7.3	3.1	91	19.58	247.52	-	-	-	D	250.88
3E -1	2248	2248	25	127	89.9	14.3	14.3	1.10	125.6	6.3	4	2	2	7.3	3.1	91	31.44	263.38	-	-	-	D	333.62
3E -2	2248	2248	25	127	89.9	14.3	14.3	1.10	125.6	6.3	4	2	2	7.3	3.1	91	31.44	263.38	-	-	-	D	235.76
31D-1	2248	2248	25	127	89.9	15.9	15.9	2.50	285.5	9.5	4	2	2	7.3	3.1	91	34.82	247.52	-	-	-	D	395.00
31D-2	2248	2248	25	127	89.9	15.9	15.9	2.50	285.5	9.5	4	2	2	7.3	3.1	91	34.82	247.52	-	-	-	D	374.99
31D-3	2248	2248	25	127	89.9	15.9	15.9	2.50	285.5	9.5	4	2	2	7.3	3.1	91	34.82	247.52	-	-	-	D	343.40
27D-1	2697	2697	30	127	89.9	14.3	14.3	1.10	125.6	6.3	4	2	2	7.3	3.1	91	24.55	263.38	-	-	-	D	214.85
27D-2	2697	2697	30	127	89.9	14.3	14.3	1.10	125.6	6.3	4	2	2	7.3	3.1	91	24.55	263.38	-	-	-	D	215.74
27D-3	2697	2697	30	127	89.9	14.3	14.3	1.10	125.6	6.3	4	2	2	7.3	3.1	91	24.55	263.38	-	-	-	D	191.72
24D-1	2697	2697	30	127	89.9	15.9	15.9	2.50	285.5	9.5	4	2	2	7.3	3.1	91	20.82	247.52	-	-	-	D	211.29
24D-2	2697	2697	30	127	89.9	15.9	15.9	2.50	285.5	9.5	4	2	2	7.3	3.1	91	20.82	247.52	-	-	-	D	198.39
24D-3	2697	2697	30	127	89.9	15.9	15.9	2.50	285.5	9.5	4	2	2	7.3	3.1	91	20.82	247.52	-	-	-	D	215.29
1E -1	2697	2697	30	127	89.9	14.3	14.3	1.10	125.6	6.3	4	2	2	7.3	3.1	91	33.99	263.38	-	-	-	D	297.14
1E -2	2697	2697	30	127	89.9	14.3	14.3	1.10	125.6	6.3	4	2	2	7.3	3.1	91	33.99	263.38	-	-	-	D	342.96
10E -2	2697	2697	30	127	89.9	15.9	15.9	2.50	285.5	9.5	4	2	2	7.3	3.1	91	31.92	247.52	-	-	-	D	364.75
10E -3	2697	2697	30	127	89.9	15.9	15.9	2.50	285.5	9.5	4	2	2	7.3	3.1	91	31.92	247.52	-	-	-	D	370.09
29D-1	3147	3147	35	127	89.9	14.3	14.3	1.10	125.6	6.3	4	2	2	7.3	3.1	91	21.99	263.38	-	-	-	D	177.48
29D-2	3147	3147	35	127	89.9	14.3	14.3	1.10	125.6	6.3	4	2	2	7.3	3.1	91	21.99	263.38	-	-	-	D	158.80
29D-3	3147	3147	35	127	89.9	14.3	14.3	1.10	125.6	6.3	4	2	2	7.3	3.1	91	21.99	263.38	-	-	-	D	189.49
30D-1	3147	3147	35	127	89.9	15.9	15.9	2.50	285.5	9.5	4	2	2	7.3	3.1	91	21.03	247.52	-	-	-	D	171.26

Figure A.5: Data taken from [23], part 1

Test No.	ltot	l	l/h	b	h	d'b	d'h	100ρ	As	ϕs	n° tot	n° b	n° h	Asw	ϕst	s	fc	fy	fu	ei,h,t/h	ei,h,b/h	Type	Nexp
	[mm]	[mm]	[-]	[mm]	[mm]	[mm]	[mm]	[%]	[mm_2]	[mm]	[-]	[-]	[-]	[mm_2]	[mm]	[mm]	[Mpa]	[Mpa]	[Mpa]	[-]	[-]		[kN]
30D-2	3147	3147	35	127	89.9	15.9	15.9	2.50	285.5	9.5	4	2	2	7.3	3.1	91	21.03	247.52	-	-	-	D	194.83
30D-3	3147	3147	35	127	89.9	15.9	15.9	2.50	285.5	9.5	4	2	2	7.3	3.1	91	21.03	247.52	-	-	-	D	192.16
2E -1	3147	3147	35	127	89.9	14.3	14.3	1.10	125.6	6.3	4	2	2	7.3	3.1	91	36.96	263.38	-	-	-	D	247.77
2E -2	3147	3147	35	127	89.9	14.3	14.3	1.10	125.6	6.3	4	2	2	7.3	3.1	91	36.96	263.38	-	-	-	D	246.43
2E -3	3147	3147	35	127	89.9	14.3	14.3	1.10	125.6	6.3	4	2	2	7.3	3.1	91	36.96	263.38	-	-	-	D	250.43
20D-1	3147	3147	35	127	89.9	15.9	15.9	2.50	285.5	9.5	4	2	2	7.3	3.1	91	28.68	247.52	-	-	-	D	229.97
20D-2	3147	3147	35	127	89.9	15.9	15.9	2.50	285.5	9.5	4	2	2	7.3	3.1	91	28.68	247.52	-	-	-	D	229.08
20D-3	3147	3147	35	127	89.9	15.9	15.9	2.50	285.5	9.5	4	2	2	7.3	3.1	91	28.68	247.52	-	-	-	D	242.43
6E -1	3597	3597	40	127	89.9	14.3	14.3	1.10	125.6	6.3	4	2	2	7.3	3.1	91	19.17	263.38	-	-	-	D	148.57
6E -2	3597	3597	40	127	89.9	14.3	14.3	1.10	125.6	6.3	4	2	2	7.3	3.1	91	19.17	263.38	-	-	-	D	151.24
6E -3	3597	3597	40	127	89.9	14.3	14.3	1.10	125.6	6.3	4	2	2	7.3	3.1	91	19.17	263.38	-	-	-	D	141.01
15E -1	3597	3597	40	127	89.9	15.9	15.9	2.50	285.5	9.5	4	2	2	7.3	3.1	91	20.06	247.52	-	-	-	D	190.38
15E -2	3597	3597	40	127	89.9	15.9	15.9	2.50	285.5	9.5	4	2	2	7.3	3.1	91	20.06	247.52	-	-	-	D	161.03
15E -3	3597	3597	40	127	89.9	15.9	15.9	2.50	285.5	9.5	4	2	2	7.3	3.1	91	20.06	247.52	-	-	-	D	167.70
5E -1	3597	3597	40	127	89.9	14.3	14.3	1.10	125.6	6.3	4	2	2	7.3	3.1	91	38.54	263.38	-	-	-	D	238.42
5E -2	3597	3597	40	127	89.9	14.3	14.3	1.10	125.6	6.3	4	2	2	7.3	3.1	91	38.54	263.38	-	-	-	D	243.76
14E -1	3597	3597	40	127	89.9	15.9	15.9	2.50	285.5	9.5	4	2	2	7.3	3.1	91	29.30	247.52	-	-	-	D	226.86
14E -2	3597	3597	40	127	89.9	15.9	15.9	2.50	285.5	9.5	4	2	2	7.3	3.1	91	29.30	247.52	-	-	-	D	242.87
14E -3	3597	3597	40	127	89.9	15.9	15.9	2.50	285.5	9.5	4	2	2	7.3	3.1	91	29.30	247.52	-	-	-	D	223.30
21F-1	3866	3866	43	127	89.9	15.9	15.9	2.50	285.5	9.5	4	2	2	7.3	3.1	91	18.20	247.52	-	-	-	D	169.03
21F-2	3866	3866	43	127	89.9	15.9	15.9	2.50	285.5	9.5	4	2	2	7.3	3.1	91	18.20	247.52	-	-	-	D	151.68
21F-3	3866	3866	43	127	89.9	15.9	15.9	2.50	285.5	9.5	4	2	2	7.3	3.1	91	18.20	247.52	-	-	-	D	137.45
28F-1	3866	3866	43	127	89.9	15.9	15.9	2.50	285.5	9.5	4	2	2	7.3	3.1	91	30.20	247.52	-	-	-	D	196.17
28F-2	3866	3866	43	127	89.9	15.9	15.9	2.50	285.5	9.5	4	2	2	7.3	3.1	91	30.20	247.52	-	-	-	D	225.08
28F-3	3866	3866	43	127	89.9	15.9	15.9	2.50	285.5	9.5	4	2	2	7.3	3.1	91	30.20	247.52	-	-	-	D	225.52
1E -3	1942	1942	21.6	127	89.9	14.3	14.3	1.10	125.6	6.3	4	2	2	7.3	3.1	91	33.99	263.38	-	-	-	D	395.89
10E -1	1942	1942	21.6	127	89.9	15.9	15.9	2.50	285.5	9.5	4	2	2	7.3	3.1	91	31.92	247.52	-	-	-	D	381.21

Figure A.6: Data taken from [23], part 2

A.6 Foster, S. J. and Attard, M. M. 1997

Test No.	ltot [mm]	l [mm]	l/h [-]	b [mm]	h [mm]	d'b [mm]	d'h [mm]	100ρ [%]	As [mm2]	φs [mm]	n° tot [-]	n° b [-]	n° h [-]	Asw [mm2]	φst [mm]	s [mm]	fc [Mpa]	fy [Mpa]	fu [Mpa]	ei,h,t/h [-]	ei,h,b/h [-]	Type	Nexp [kN]
2L8-30	1450	650	9.67	150	150	21.4	21.4	2.04	460.0	12.1	4	2	2	31.2	6.3	30	43.00	480.00	-	0.053	0.053	B	960.00
2L8-60	1450	650	9.67	150	150	24.4	24.4	2.04	460.0	12.1	4	2	2	31.2	6.3	60	43.00	480.00	-	0.053	0.053	B	857.00
2L8-120	1450	650	9.67	150	150	27.4	27.4	2.04	460.0	12.1	4	2	2	31.2	6.3	120	43.00	480.00	-	0.053	0.053	B	912.00
2L20-30	1450	650	9.67	150	150	22.4	22.4	2.04	460.0	12.1	4	2	2	31.2	6.3	30	40.00	480.00	-	0.133	0.133	B	750.00
2L20-60	1450	650	9.67	150	150	24.4	24.4	2.04	460.0	12.1	4	2	2	31.2	6.3	60	43.00	480.00	-	0.133	0.133	B	700.00
2L20-120	1450	650	9.67	150	150	26.4	26.4	2.04	460.0	12.1	4	2	2	31.2	6.3	120	43.00	480.00	-	0.133	0.133	B	782.00
2L50-30	1450	650	9.67	150	150	24.4	24.4	2.04	460.0	12.1	4	2	2	31.2	6.3	30	40.00	480.00	-	0.333	0.333	B	440.00
2L50-60	1450	650	9.67	150	150	22.4	22.4	2.04	460.0	12.1	4	2	2	31.2	6.3	60	43.00	480.00	-	0.333	0.333	B	472.00
2L50-120	1450	650	9.67	150	150	26.4	26.4	2.04	460.0	12.1	4	2	2	31.2	6.3	120	40.00	480.00	-	0.333	0.333	B	440.00
4L8-30	1450	650	9.67	150	150	27.4	27.4	4.09	919.9	12.1	8	3	3	31.2	6.3	30	43.00	480.00	-	0.053	0.053	B	1100.00
4L8-60	1450	650	9.67	150	150	21.4	21.4	4.09	919.9	12.1	8	3	3	31.2	6.3	60	43.00	480.00	-	0.053	0.053	B	1150.00
4L8-120	1450	650	9.67	150	150	25.4	25.4	4.09	919.9	12.1	8	3	3	31.2	6.3	120	43.00	480.00	-	0.053	0.053	B	975.00
4L20-30	1450	650	9.67	150	150	23.4	23.4	4.09	919.9	12.1	8	3	3	31.2	6.3	30	40.00	480.00	-	0.133	0.133	B	1020.00
4L20-60	1450	650	9.67	150	150	27.4	27.4	4.09	919.9	12.1	8	3	3	31.2	6.3	60	40.00	480.00	-	0.133	0.133	B	968.00
4L20-120	1450	650	9.67	150	150	25.4	25.4	4.09	919.9	12.1	8	3	3	31.2	6.3	120	40.00	480.00	-	0.133	0.133	B	900.00
4L50-30	1450	650	9.67	150	150	29.4	29.4	4.09	919.9	12.1	8	3	3	31.2	6.3	30	40.00	480.00	-	0.333	0.333	B	517.00
4L50-60	1450	650	9.67	150	150	21.4	21.4	4.09	919.9	12.1	8	3	3	31.2	6.3	60	40.00	480.00	-	0.333	0.333	B	550.00
4L50-120	1450	650	9.67	150	150	25.4	25.4	4.09	919.9	12.1	8	3	3	31.2	6.3	120	40.00	480.00	-	0.333	0.333	B	525.00
2L8-120R	1450	650	9.67	150	150	27.4	27.4	2.04	460.0	12.1	4	2	2	31.2	6.3	120	56.00	480.00	-	0.053	0.053	B	1092.00
2L20-120R	1450	650	9.67	150	150	25.4	25.4	2.04	460.0	12.1	4	2	2	31.2	6.3	120	56.00	480.00	-	0.133	0.133	B	897.00
4L8-120R	1450	650	9.67	150	150	22.4	22.4	4.09	919.9	12.1	8	3	3	31.2	6.3	120	56.00	480.00	-	0.053	0.053	B	1247.00
4L20-120R	1450	650	9.67	150	150	25.4	25.4	4.09	919.9	12.1	8	3	3	31.2	6.3	120	53.00	480.00	-	0.133	0.133	B	945.00
4L50-30R	1450	650	9.67	150	150	26.4	26.4	4.09	919.9	12.1	8	3	3	31.2	6.3	30	40.00	480.00	-	0.333	0.333	B	546.00

Figure A.7: Data taken from [24]

A.7 Pancholi, V. R. 1977

Test No.	ltot	l	l/h	b	h	d'b	d'h	100ρ	As	ϕs	n° tot	n° b	n° h	Asw	ϕst	s	fc	fy	fu	ei,h,t/h	ei,h,b/h	Type	Nexp
	[mm]	[mm]	[-]	[mm]	[mm]	[mm]	[mm]	[%]	[mm$_2$]	[mm]	[-]	[-]	[-]	[mm$_2$]	[mm]	[mm]	[Mpa]	[Mpa]	[Mpa]	[-]	[-]		[kN]
5	6004	6004	60	100	100	26.0	26.0	4.52	452.4	12.0	4	2	2	8.3	3.3	100	33.05	278.45	-	-	-	A	72.74
6	6004	6004	60	100	100	26.0	26.0	4.52	452.4	12.0	4	2	2	8.3	3.3	100	35.61	278.45	-	-	-	A	72.24
7	6004	6004	79	76	76	17.5	17.5	5.44	314.2	10.0	4	2	2	8.3	3.3	76	39.29	300.42	-	-	-	A	29.89
8	6004	6004	79	76	76	17.5	17.5	5.44	314.2	10.0	4	2	2	8.3	3.3	76	36.49	300.42	-	-	-	A	31.88
10	6004	6004	79	76	76	17.5	17.5	5.44	314.2	10.0	4	2	2	8.3	3.3	76	42.50	300.42	-	-	-	A	21.92
11	4570	4570	60.1	76	76	17.5	17.5	5.44	314.2	10.0	4	2	2	8.3	3.3	76	45.66	300.42	-	-	-	A	35.87
13	4570	4570	60.1	76	76	17.5	17.5	5.44	314.2	10.0	4	2	2	8.3	3.3	76	41.29	300.42	-	-	-	A	39.86
14	4570	4570	60.1	76	76	17.5	17.5	5.44	314.2	10.0	4	2	2	8.3	3.3	76	43.88	300.42	-	-	-	A	39.86
15	4940	4940	65	76	76	17.5	17.5	5.44	314.2	10.0	4	2	2	8.3	3.3	76	45.66	300.42	-	-	-	A	31.88
16	4940	4940	65	76	76	17.5	17.5	5.44	314.2	10.0	4	2	2	8.3	3.3	76	48.43	300.42	-	-	-	A	37.86
17A	4940	4940	65	76	76	17.5	17.5	5.44	314.2	10.0	4	2	2	8.3	3.3	76	25.75	300.42	-	-	-	A	31.88
18	5327	5327	70.1	76	76	17.5	17.5	5.44	314.2	10.0	4	2	2	8.3	3.3	76	38.20	300.42	-	-	-	A	33.88
19	5327	5327	70.1	76	76	17.5	17.5	5.44	314.2	10.0	4	2	2	8.3	3.3	76	40.89	300.42	-	-	-	A	25.91
20	5327	5327	70.1	76	76	17.5	17.5	5.44	314.2	10.0	4	2	2	8.3	3.3	76	38.07	300.42	-	-	-	A	37.86
21	5700	5700	75	76	76	17.5	17.5	5.44	314.2	10.0	4	2	2	8.3	3.3	76	41.11	300.42	-	-	-	A	19.93
23	5700	5700	75	76	76	17.5	17.5	5.44	314.2	10.0	4	2	2	8.3	3.3	76	37.84	300.42	-	-	-	A	21.92
24	5700	5700	75	76	76	17.5	17.5	5.44	314.2	10.0	4	2	2	8.3	3.3	76	36.60	300.42	-	-	-	A	21.92
25	3810	3810	50.1	76	76	17.5	17.5	5.44	314.2	10.0	4	2	2	8.3	3.3	76	37.98	300.42	-	-	-	A	53.81
26	3810	3810	50.1	76	76	17.5	17.5	5.44	314.2	10.0	4	2	2	8.3	3.3	76	35.69	300.42	-	-	-	A	51.81
27	3810	3810	50.1	76	76	17.5	17.5	5.44	314.2	10.0	4	2	2	8.3	3.3	76	40.40	300.42	-	-	-	A	59.78
28	5000	5000	50	100	100	26.0	26.0	4.52	452.4	12.0	4	2	2	8.3	3.3	100	39.04	278.45	-	-	-	A	89.68
29	5000	5000	50	100	100	26.0	26.0	4.52	452.4	12.0	4	2	2	8.3	3.3	100	32.30	278.45	-	-	-	A	71.74
30	5000	5000	50	100	100	26.0	26.0	4.52	452.4	12.0	4	2	2	8.3	3.3	100	39.40	278.45	-	-	-	A	85.69
31	4000	4000	40	100	100	26.0	26.0	4.52	452.4	12.0	4	2	2	8.3	3.3	100	39.33	278.45	-	-	-	A	114.59
32	4000	4000	40	100	100	26.0	26.0	4.52	452.4	12.0	4	2	2	8.3	3.3	100	46.12	278.45	-	-	-	A	119.57
33	4000	4000	40	100	100	26.0	26.0	4.52	452.4	12.0	4	2	2	8.3	3.3	100	39.91	278.45	-	-	-	A	119.57
36	3000	3000	30	100	100	26.0	26.0	4.52	452.4	12.0	4	2	2	8.3	3.3	100	38.56	278.45	-	-	-	A	189.32
37	3000	3000	30	100	100	26.0	26.0	4.52	452.4	12.0	4	2	2	8.3	3.3	100	40.89	278.45	-	-	-	A	219.21
38	3000	3000	30	100	100	26.0	26.0	4.52	452.4	12.0	4	2	2	8.3	3.3	100	36.27	278.45	-	-	-	A	219.21

Figure A.8: Data taken from [25]

A.8 Dracos, A. 1982

Test No.	ltot [mm]	l [mm]	l/h [-]	b [mm]	h [mm]	d'b [mm]	d'h [mm]	100p [%]	As [mm$_2$]	φs [mm]	n° tot [-]	n° b [-]	n° h [-]	Asw [mm$_2$]	φst [mm]	s [mm]	fc [Mpa]	fy [Mpa]	fu [Mpa]	ei,h,t/h [-]	ei,h,b/h [-]	Type	Nexp [kN]
S1	3000	3000	28.9	104	104	28.0	22.0	4.18	452.4	12.0	4	2	2	8.3	3.3	100	37.85	313.00	-	0.096	0.096	A	160.00
S2	3000	3000	28.9	104	104	28.0	22.0	4.18	452.4	12.0	4	2	2	8.3	3.3	100	39.93	315.00	-	0.144	0.144	A	128.00
S3	3000	3000	28.9	104	104	28.0	22.0	4.18	452.4	12.0	4	2	2	8.3	3.3	100	32.68	277.00	-	0.096	0.096	B	155.00
S4	3000	3000	28.9	104	104	28.0	22.0	4.18	452.4	12.0	4	2	2	8.3	3.3	100	35.81	282.00	-	0.144	0.144	B	128.00
S5	3000	3000	28.9	104	104	28.0	22.0	4.18	452.4	12.0	4	2	2	8.3	3.3	100	36.87	278.00	-	0.096	0.096	B	174.00
S6	3000	3000	28.9	104	104	28.0	22.0	4.18	452.4	12.0	4	2	2	8.3	3.3	100	37.85	280.00	-	0.144	0.144	B	118.00
S7	4000	4000	38.5	104	104	28.0	22.0	4.18	452.4	12.0	4	2	2	8.3	3.3	100	32.40	280.00	-	0.144	0.144	B	68.00
S8	4000	4000	38.5	104	104	28.0	22.0	4.18	452.4	12.0	4	2	2	8.3	3.3	100	36.79	280.00	-	0.096	0.096	B	98.00
S9	4000	4000	38.5	104	104	28.0	22.0	4.18	452.4	12.0	4	2	2	8.3	3.3	100	39.16	280.00	-	0.144	0.144	B	78.00
S10	4000	4000	38.5	104	104	28.0	22.0	4.18	452.4	12.0	4	2	2	8.3	3.3	100	40.25	293.00	-	0.096	0.096	B	84.00
S11	4000	4000	38.5	104	104	28.0	22.0	4.18	452.4	12.0	4	2	2	8.3	3.3	100	37.16	293.00	-	0.144	0.144	B	82.00
S12	4000	4000	38.5	104	104	28.0	22.0	4.18	452.4	12.0	4	2	2	8.3	3.3	100	37.89	292.00	-	0.096	0.096	B	107.00
S13	5000	5000	48.1	104	104	28.0	22.0	4.18	452.4	12.0	4	2	2	8.3	3.3	100	33.11	283.00	-	0.144	0.144	B	45.00
S14	5000	5000	48.1	104	104	28.0	22.0	4.18	452.4	12.0	4	2	2	8.3	3.3	100	32.49	315.00	-	0.096	0.096	B	54.00
S15	5000	5000	48.1	104	104	28.0	22.0	4.18	452.4	12.0	4	2	2	8.3	3.3	100	34.37	300.00	-	0.096	0.096	B	66.00
S16	5000	5000	48.1	104	104	28.0	22.0	4.18	452.4	12.0	4	2	2	8.3	3.3	100	33.40	293.00	-	0.144	0.144	B	52.00
S17	5000	5000	48.1	104	104	28.0	22.0	4.18	452.4	12.0	4	2	2	8.3	3.3	100	38.18	300.00	-	0.096	0.096	B	56.00
S18	5000	5000	48.1	104	104	28.0	22.0	4.18	452.4	12.0	4	2	2	8.3	3.3	100	35.12	300.00	-	0.144	0.144	B	52.00
S19	6000	6000	57.7	104	104	28.0	22.0	4.18	452.4	12.0	4	2	2	8.3	3.3	100	33.22	280.00	-	0.096	0.096	B	44.00
S20	6000	6000	57.7	104	104	28.0	22.0	4.18	452.4	12.0	4	2	2	8.3	3.3	100	36.28	282.00	-	0.144	0.144	B	36.00
S21	6000	6000	57.7	104	104	28.0	22.0	4.18	452.4	12.0	4	2	2	8.3	3.3	100	33.68	275.00	-	0.096	0.096	B	42.00
S22	6000	6000	57.7	104	104	28.0	22.0	4.18	452.4	12.0	4	2	2	8.3	3.3	100	34.68	275.00	-	0.144	0.144	B	30.00
S23	6000	6000	57.7	104	104	28.0	22.0	4.18	452.4	12.0	4	2	2	8.3	3.3	100	37.45	278.00	-	0.096	0.096	B	39.00
S24	6000	6000	57.7	104	104	28.0	22.0	4.18	452.4	12.0	4	2	2	8.3	3.3	100	36.94	280.00	-	0.144	0.144	B	34.00
S25	6000	6000	57.7	104	104	28.0	22.0	4.18	452.4	12.0	4	2	2	8.3	3.3	100	24.72	282.00	-	0.144	0.144	B	36.00
S26	6000	6000	57.7	104	104	28.0	22.0	4.18	452.4	12.0	4	2	2	8.3	3.3	100	24.51	273.00	-	0.144	0.144	B	30.00
S27	6000	6000	57.7	104	104	28.0	22.0	4.18	452.4	12.0	4	2	2	8.3	3.3	100	20.51	297.00	-	0.144	0.144	B	30.00
S28	5000	5000	48.1	104	104	28.0	22.0	4.18	452.4	12.0	4	2	2	8.3	3.3	100	24.43	304.00	-	0.144	0.144	B	44.00
S29	5000	5000	48.1	104	104	28.0	22.0	4.18	452.4	12.0	4	2	2	8.3	3.3	100	22.35	290.00	-	0.144	0.144	B	40.00
S30	5000	5000	48.1	104	104	28.0	22.0	4.18	452.4	12.0	4	2	2	8.3	3.3	100	25.66	300.00	-	0.144	0.144	B	48.00
S31	4000	4000	39.2	102	102	27.0	21.0	4.35	452.4	12.0	4	2	2	8.3	3.3	100	23.59	405.00	-	0.147	0.147	B	67.00
S32	4000	4000	39.2	102	102	27.0	21.0	4.35	452.4	12.0	4	2	2	8.3	3.3	100	21.76	410.00	-	0.147	0.147	B	60.00
S33	4000	4000	39.2	102	102	27.0	21.0	4.35	452.4	12.0	4	2	2	8.3	3.3	100	24.32	410.00	-	0.147	0.147	B	60.00
S34	3000	3000	29.4	102	102	27.0	21.0	4.35	452.4	12.0	4	2	2	8.3	3.3	100	27.70	410.00	-	0.147	0.147	B	115.00
S35	3000	3000	29.4	102	102	27.0	21.0	4.35	452.4	12.0	4	2	2	8.3	3.3	100	27.59	395.00	-	0.147	0.147	B	106.00
S36	3000	3000	29.4	102	102	27.0	21.0	4.35	452.4	12.0	4	2	2	8.3	3.3	100	22.27	410.00	-	0.147	0.147	B	108.00

Figure A.9: Data taken from [26]

A.9 Iwai, S., Minami, K. and Wakabayashi, M. 1986

Test No.	ltot [mm]	l [mm]	l/h [-]	b [mm]	h [mm]	d'b [mm]	d'h [mm]	100p [%]	As [mm$_2$]	φs [mm]	n° tot [-]	n° b [-]	n° h [-]	Asw [mm$_2$]	φst [mm]	s [mm]	fc [Mpa]	fy [Mpa]	fu [Mpa]	ei,h,t/h [-]	ei,h,b/h [-]	Type	Nexp [kN]
C000	680	600	5.7	120	120	20.0	20.0	3.96	570.6	9.5	8	3	3	15.9	4.5	60	26.97	347.16	516.81	-	-	A	559.58
B000	1880	1800	15.7	120	120	20.0	20.0	3.96	570.6	9.5	8	3	3	15.9	4.5	60	27.56	355.00	507.00	-	-	A	469.42
A000a	3080	3000	25.7	120	120	20.0	20.0	3.96	570.6	9.5	8	3	3	15.9	4.5	60	30.50	342.25	539.37	-	-	A	542.92
A000b	3080	3000	25.7	120	120	20.0	20.0	3.96	570.6	9.5	8	3	3	15.9	4.5	60	30.50	342.25	539.37	-	-	A	538.02
C020	680	600	5.7	120	120	20.0	20.0	3.96	570.6	9.5	8	3	3	15.9	4.5	60	26.97	347.16	516.81	0.200	0.200	B	327.32
B020	1880	1800	15.7	120	120	20.0	20.0	3.96	570.6	9.5	8	3	3	15.9	4.5	60	27.56	355.00	507.00	0.200	0.200	B	271.46
A020	3080	3000	25.7	120	120	20.0	20.0	3.96	570.6	9.5	8	3	3	15.9	4.5	60	30.50	342.25	539.37	0.200	0.200	B	184.24
RS300	1200	1120	10.0	120	180	20.0	20.0	2.64	570.6	9.5	8	3	3	15.9	4.5	60	30.99	360.88	507.98	0.167	0.167	B	601.72
RS390	1200	1120	10.0	180	120	20.0	20.0	2.64	570.6	9.5	8	3	3	15.9	4.5	60	30.99	360.88	507.98	0.250	0.250	B	419.44
RL300	3000	2920	25.0	120	180	20.0	20.0	2.64	570.6	9.5	8	3	3	15.9	4.5	60	30.99	360.88	507.98	0.167	0.167	B	474.32
RL390	3000	2920	25.0	180	120	20.0	20.0	2.64	570.6	9.5	8	3	3	15.9	4.5	60	30.99	360.88	507.98	0.250	0.250	B	230.30

Figure A.10: Data taken from [27]

A.10 Chuang, P. H. and Kong, F. K. 1997

Test No.	ltot [mm]	l [mm]	l/h [-]	b [mm]	h [mm]	d'b [mm]	d'h [mm]	100ρ [%]	As [mm$_2$]	φs [mm]	n° tot [-]	n° b [-]	n° h [-]	Asw [mm$_2$]	φst [mm]	s [mm]	fc [Mpa]	fy [Mpa]	fu [Mpa]	ei,h,t/h [-]	ei,h,b/h [-]	Type	Nexp [kN]
A-15-0.25	3000	2400	15	300	200	20.0	20.0	3.27	1962.0	25.0	4	2	2	78.5	10.0	150	31.10	493.00	-	0.250	0.250	B	1290.96
A-17-0.25	3400	2800	17	300	200	20.0	20.0	3.27	1962.0	25.0	4	2	2	78.5	10.0	150	38.20	493.00	-	0.250	0.250	B	1181.44
A-18-0.25	3600	3000	18	300	200	20.0	20.0	3.27	1962.0	25.0	4	2	2	78.5	10.0	150	32.80	493.00	-	0.250	0.250	B	1087.20
A-19-0.25	3800	3200	19	300	200	20.0	20.0	3.27	1962.0	25.0	4	2	2	78.5	10.0	150	32.30	493.00	-	0.250	0.250	B	1195.56
A-15-0.50	3000	1900	15	300	200	20.0	20.0	3.27	1962.0	25.0	4	2	2	78.5	10.0	150	33.00	493.00	-	0.500	0.500	B	889.35
A-17-0.50	3400	2300	17	300	200	20.0	20.0	3.27	1962.0	25.0	4	2	2	78.5	10.0	150	40.30	493.00	-	0.500	0.500	B	903.12
A-18-0.50	3600	2500	18	300	200	20.0	20.0	3.27	1962.0	25.0	4	2	2	78.5	10.0	150	32.70	493.00	-	0.500	0.500	B	851.76
A-19-0.50	3800	2700	19	300	200	20.0	20.0	3.27	1962.0	25.0	4	2	2	78.5	10.0	150	30.30	493.00	-	0.500	0.500	B	812.89
B-17-0.25	3400	2800	17	300	200	20.0	20.0	1.34	804.0	16.0	4	2	2	50.3	8.0	150	37.20	519.00	-	0.250	0.250	B	1087.44
B-18-0.25	3600	3000	18	300	200	20.0	20.0	1.34	804.0	16.0	4	2	2	50.3	8.0	150	42.10	519.00	-	0.250	0.250	B	989.82
B-19-0.25	3800	3200	19	300	200	20.0	20.0	1.34	804.0	16.0	4	2	2	50.3	8.0	150	39.70	519.00	-	0.250	0.250	B	1043.28
B-17-0.50	3400	2300	17	300	200	20.0	20.0	1.34	804.0	16.0	4	2	2	50.3	8.0	150	38.60	519.00	-	0.500	0.500	B	477.36
B-18-0.50	3600	2500	18	300	200	20.0	20.0	1.34	804.0	16.0	4	2	2	50.3	8.0	150	42.50	519.00	-	0.500	0.500	B	478.13
B-19-0.50	3800	2700	19	300	200	20.0	20.0	1.34	804.0	16.0	4	2	2	50.3	8.0	150	45.00	519.00	-	0.500	0.500	B	460.35
C-27.5-0.25	3300	2760	27.5	200	120	20.0	20.0	3.35	804.0	16.0	4	2	2	28.3	6.0	150	42.10	520.00	-	0.250	0.250	B	531.96
C-30.0-0.25	3600	3060	30	200	120	20.0	20.0	3.35	804.0	16.0	4	2	2	28.3	6.0	150	42.60	520.00	-	0.250	0.250	B	484.30
C-31.7-0.25	3800	3260	31.7	200	120	20.0	20.0	3.35	804.0	16.0	4	2	2	28.3	6.0	150	44.40	520.00	-	0.250	0.250	B	333.38
C-27.5-0.50	3300	2520	27.5	200	120	20.0	20.0	3.35	804.0	16.0	4	2	2	28.3	6.0	150	42.60	520.00	-	0.500	0.500	B	205.11
C-30.0-0.50	3600	2820	30	200	120	20.0	20.0	3.35	804.0	16.0	4	2	2	28.3	6.0	150	41.50	520.00	-	0.500	0.500	B	319.78
C-31.7-0.50	3800	3020	31.7	200	120	20.0	20.0	3.35	804.0	16.0	4	2	2	28.3	6.0	150	43.70	520.00	-	0.500	0.500	B	255.36

Figure A.11: Data taken from [28]

A.11 Barrera, A. C., Bonet, J. L., Romero, M. L. and Miguel, P. F. 2011

Test No.	ltot [mm]	l [mm]	l/h [-]	b [mm]	h [mm]	d'b [mm]	d'h [mm]	100ρ [%]	As [mm₂]	ϕs [mm]	n° tot [-]	n° b [-]	n° h [-]	Asw [mm₂]	ϕst [mm]	s [mm]	fc [Mpa]	fy [Mpa]	fu [Mpa]	V [kN]	Type	Nexp [kN]
N30-10.5-C0-2-00	3300	2940	24	140	150	20.0	20.0	2.24	471.2	10.0	6	2	3	28.3	6.0	100	32.20	537.00	631.00	17.07	C	0.00
N30-10.5-C0-2-15	3300	2940	23.6	140	150	20.0	20.0	2.24	471.2	10.0	6	2	3	28.3	6.0	100	31.80	537.00	631.00	18.63	C	123.00
N30-10.5-C0-2-30	3300	2940	23.6	140	150	20.0	20.0	2.24	471.2	10.0	6	2	3	28.3	6.0	100	31.60	537.00	631.00	16.14	C	255.00
N30-10.5-C0-2-45	3300	2940	23.6	140	150	20.0	20.0	2.24	471.2	10.0	6	2	3	28.3	6.0	100	34.50	537.00	631.00	16.25	C	381.00
N30-7.5-C0-2-30	3300	2940	22	200	150	20.0	20.0	2.26	678.6	12.0	6	2	3	28.3	6.0	100	30.10	538.00	645.00	55.19	C	350.00
N30-7.5-C0-2-45	3300	2940	22	200	150	20.0	20.0	2.26	678.6	12.0	6	2	3	28.3	6.0	100	33.00	538.00	645.00	47.40	C	533.00
N30-15-C0-2-30	3300	2940	33	100	150	20.0	20.0	2.01	301.6	8.0	6	2	3	28.3	6.0	100	32.70	531.00	668.00	4.60	C	180.00
N30-15-C0-2-45	3300	2940	33	100	150	20.0	20.0	2.01	301.6	8.0	6	2	3	28.3	6.0	100	32.90	531.00	668.00	4.17	C	265.00
N30-10.5-C0-1-30	3300	2940	23.6	140	150	20.0	20.0	1.44	301.6	8.0	6	2	3	28.3	6.0	100	42.20	531.00	668.00	15.55	C	228.00
N30-10.5-C0-1-45	3300	2940	23.6	140	150	20.0	20.0	1.44	301.6	8.0	6	2	3	28.3	6.0	100	35.20	531.00	668.00	14.74	C	440.00
N30-10.5-C0-3-15	3300	2940	23.6	140	150	20.0	20.0	3.23	678.6	12.0	6	2	3	28.3	6.0	100	33.50	538.00	645.00	21.57	C	142.00
N30-10.5-C0-3-30	3300	2940	23.6	140	150	20.0	20.0	3.23	678.6	12.0	6	2	3	28.3	6.0	100	29.50	538.00	645.00	16.57	C	280.00
H60-10.5-C0-2-00	3300	2940	23.6	140	150	20.0	20.0	2.24	471.2	10.0	6	2	3	28.3	6.0	100	55.80	537.00	631.00	18.06	C	0.00
H60-10.5-C0-2-15	3300	2940	23.6	140	150	20.0	20.0	2.24	471.2	10.0	6	2	3	28.3	6.0	100	54.10	537.00	631.00	21.39	C	208.00
H60-15-C0-2-30	3300	2940	33	100	150	20.0	20.0	2.01	301.6	8.0	6	2	3	28.3	6.0	100	58.20	531.00	668.00	4.39	C	300.00
H60-15-C0-2-45	3300	2940	33	100	150	20.0	20.0	2.01	301.6	8.0	6	2	3	28.3	6.0	100	58.70	531.00	668.00	2.92	C	465.00
H60-10.5-C0-1-15	3300	2940	23.6	140	150	20.0	20.0	1.44	301.6	8.0	6	2	3	28.3	6.0	100	57.80	531.00	668.00	16.86	C	220.00
H60-10.5-C0-1-30	3300	2940	23.6	140	150	20.0	20.0	1.44	301.6	8.0	6	2	3	28.3	6.0	100	58.50	531.00	668.00	17.23	C	412.00
H60-10.5-C0-3-15	3300	2940	23.6	140	150	20.0	20.0	3.23	678.6	12.0	6	2	3	28.3	6.0	100	58.30	538.00	645.00	24.20	C	238.00
N30-10.5-C3-2-30	3300	2940	23.6	140	150	20.0	20.0	2.24	471.2	10.0	6	2	3	50.3	8.0	60	41.00	537.00	631.00	13.91	C	258.00
N30-10.5-C3-2-45	3300	2940	23.6	140	150	20.0	20.0	2.24	471.2	10.0	6	2	3	50.3	8.0	60	34.20	537.00	631.00	13.34	C	387.00
N30-7.5-C3-2-30	3300	2940	22	200	150	20.0	20.0	2.26	678.6	12.0	6	2	3	50.3	8.0	50	35.80	538.00	645.00	47.93	C	364.00
N30-7.5-C3-2-45	3300	2940	22	200	150	20.0	20.0	2.26	678.6	12.0	6	2	3	50.3	8.0	50	35.00	538.00	645.00	44.59	C	546.00

Figure A.12: Data taken from [29]

A.12 Baumann, O. 1935

Test No.	ltot [mm]	l [mm]	l/h [-]	b [mm]	h [mm]	d'b [mm]	d'h [mm]	100p [%]	As [mm2]	φs [mm]	n° tot [-]	n° b [-]	n° h [-]	Asw [mm2]	φst [mm]	s [mm]	fc [Mpa]	fy [Mpa]	fu [Mpa]	ei,h,t/h [-]	ei,h,b/h [-]	Type	Nexp [kN]
I	3210	3000	32	200	100	10.0	10.0	1.60	314.0	10.0	4	2	2	*	*	*	15.20	294.20	-	-	-	A	264.78
III	3210	3000	22.9	140	140	14.0	14.0	1.60	314.0	10.0	4	2	2	*	*	*	16.08	294.20	-	-	-	A	343.23
V	3240	3000	23.3	177	139	13.9	13.9	2.50	615.0	14.0	4	2	2	*	*	*	26.38	281.84	-	-	-	A	647.24
Va	3240	3000	23.1	178	140	14.0	14.0	2.50	615.0	14.0	4	2	2	*	*	*	26.38	281.84	-	-	-	A	684.50
VI	3210	3000	32.8	198	98	9.8	9.8	1.60	314.0	10.0	4	2	2	*	*	*	24.91	294.20	-	-	-	A	392.27
VIa	3210	3000	32.1	200	100	10.0	10.0	1.60	314.0	10.0	4	2	2	*	*	*	24.91	294.20	-	-	-	A	402.07
VII	3210	3000	18	182	178	17.8	17.8	1.90	615.0	14.0	4	2	2	*	*	*	28.24	281.84	-	-	-	A	686.47
VIIa	3210	3000	17.8	180	180	18.0	18.0	1.90	615.0	14.0	4	2	2	*	*	*	28.24	281.84	-	-	-	A	823.76
VIII	3110	2680	17.5	182	178	17.8	17.8	1.90	615.0	14.0	4	2	2	*	*	*	28.83	281.84	-	-	-	A	1068.92
VIIIa	2800	2370	15.6	180	180	18.0	18.0	1.90	615.0	14.0	4	2	2	*	*	*	28.83	281.84	-	-	-	A	1216.02
1	2970	2710	11.9	250	250	25.0	25.0	1.30	803.0	16.0	4	2	2	*	*	*	33.54	271.64	-	-	-	A	2039.78
2	3230	3010	25.8	250	125	12.5	12.5	0.60	201.0	8.0	4	2	2	*	*	*	33.54	304.01	-	-	-	A	696.27
3	6510	6310	40.7	250	160	16.0	16.0	0.80	314.0	10.0	4	2	2	*	*	*	33.54	294.20	-	-	-	A	666.85
15	6510	6310	40.4	247	161	16.1	16.1	0.80	314.0	10.0	4	2	2	*	*	*	33.05	294.20	-	-	-	A	549.17
Ia	3210	3000	32.1	200	100	10.0	10.0	1.60	314.0	10.0	4	2	2	*	*	*	15.79	294.20	-	0.100	0.100	B	152.00
IIIa	3210	3000	22.9	140	140	14.0	14.0	1.60	314.0	10.0	4	2	2	*	*	*	16.28	294.20	-	0.100	0.100	B	235.36
4	3000	2710	12	250	250	25.0	25.0	1.30	803.0	16.0	4	2	2	*	*	*	32.17	272.04	-	0.200	0.200	B	961.05
5	3230	3010	25.8	250	125	12.5	12.5	0.60	201.0	8.0	4	2	2	*	*	*	31.97	304.01	-	0.200	0.200	B	343.23
6	6510	6310	40.7	250	160	16.0	16.0	0.80	314.0	10.0	4	2	2	*	*	*	32.17	294.20	-	0.200	0.200	B	225.55
7	2930	2710	11.7	250	250	25.0	25.0	1.30	803.0	16.0	4	2	2	*	*	*	20.40	271.64	-	0.200	0.200	B	843.37
8	3230	3010	25.6	250	126	12.6	12.6	0.60	201.0	8.0	4	2	2	*	*	*	20.40	304.01	-	0.200	0.200	B	235.36
9	6510	6310	40.2	250	162	16.2	16.2	0.80	314.0	10.0	4	2	2	*	*	*	24.52	294.20	-	0.200	0.200	B	205.94
10	2930	2710	11.7	253	251	25.1	25.1	1.30	803.0	16.0	4	2	2	*	*	*	29.91	271.64	-	0.300	0.300	B	691.37
11	3230	3010	25.6	252	126	12.6	12.6	0.60	201.0	8.0	4	2	2	*	*	*	29.91	304.01	-	0.300	0.300	B	196.13
12	6510	6310	40.2	250	162	16.2	16.2	0.80	314.0	10.0	4	2	2	*	*	*	29.71	294.20	-	0.300	0.300	B	112.78
13	2970	2710	12	251	247	24.7	24.7	1.30	803.0	16.0	4	2	2	*	*	*	32.85	271.64	-	0.300	0.300	B	700.19
14	3230	3010	25.6	248	126	12.6	12.6	0.60	201.0	8.0	4	2	2	*	*	*	32.85	304.01	-	0.300	0.300	B	162.79

Figure A.13: Data taken from [30]

Appendix B

Probability density functions, probability papares and p-values related to the 40 columns

B.1 2L20-60

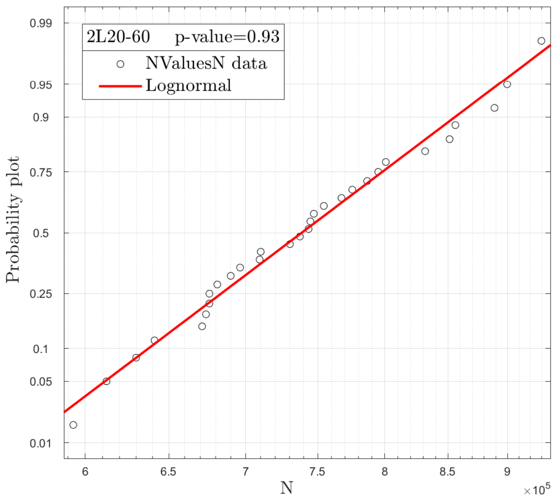

(a) Probability Plot

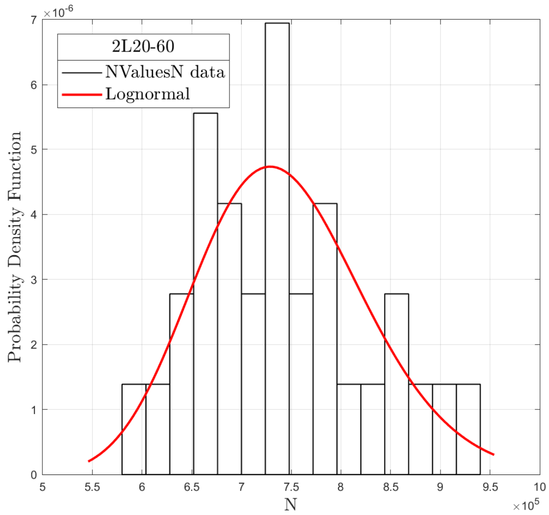

(b) Probability Density Function

Figure B.1: Log-normal fit - 2L20-60

B.2 4L20-120

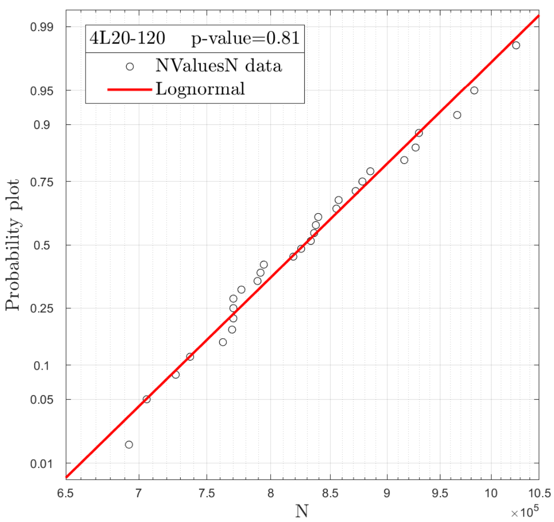

(a) Probability Plot

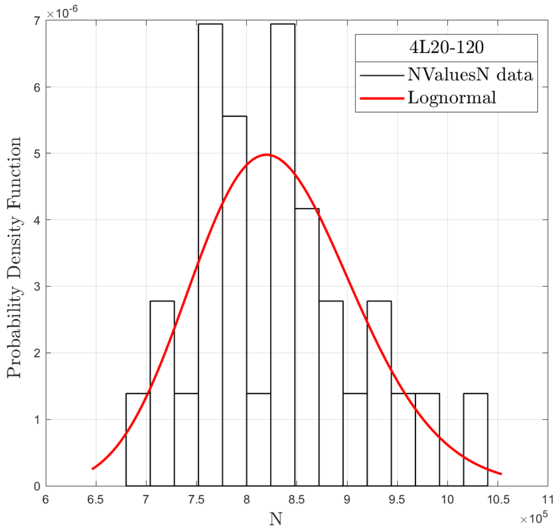

(b) Probability Density Function

Figure B.2: Log-normal fit - 4L20-120

B.3 B020

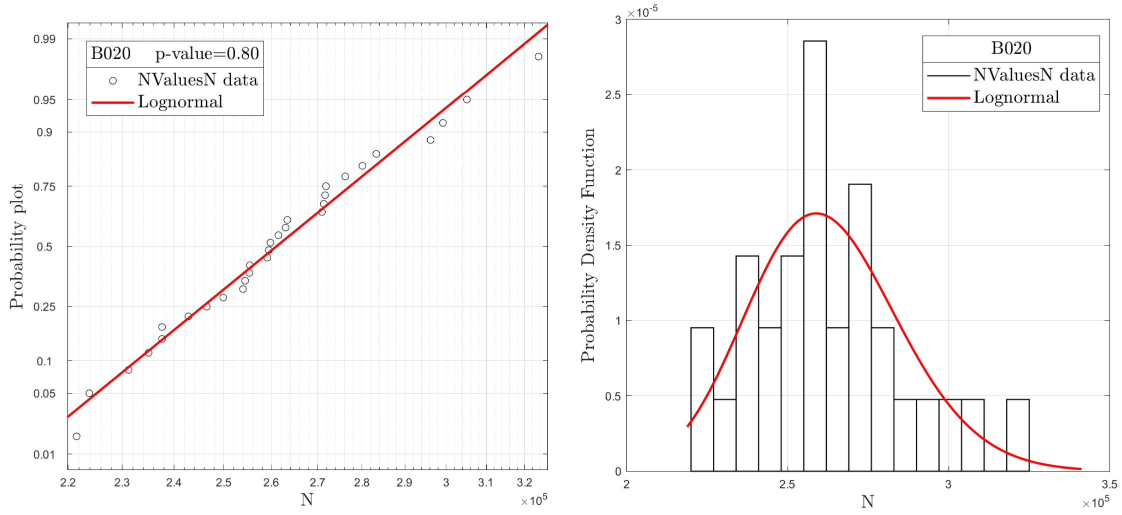

(a) Probability Plot (b) Probability Density Function

Figure B.3: Log-normal fit - B020

B.4 5.1

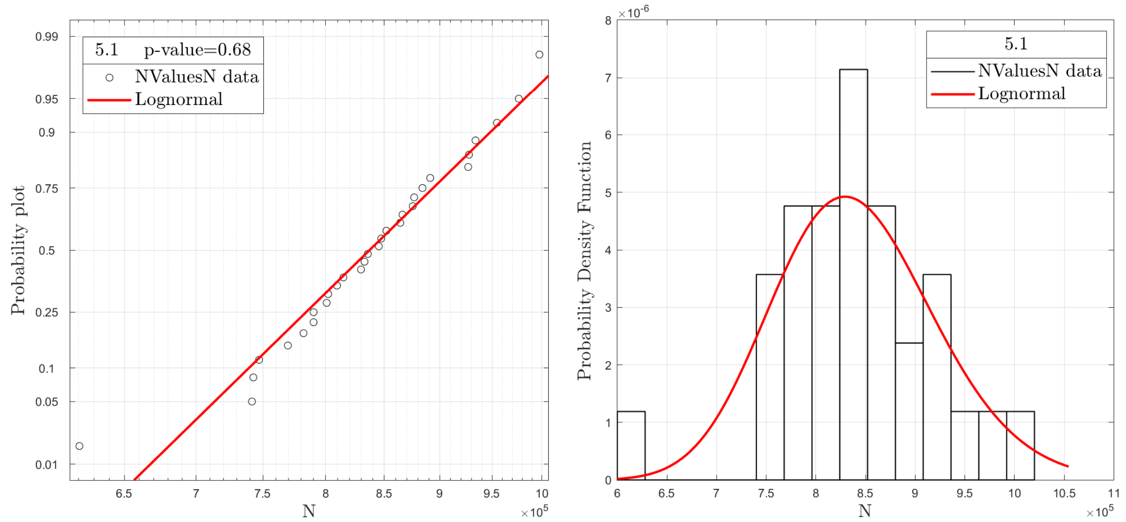

(a) Probability Plot (b) Probability Density Function

Figure B.4: Log-normal fit - 5.1

B.5 24D-2

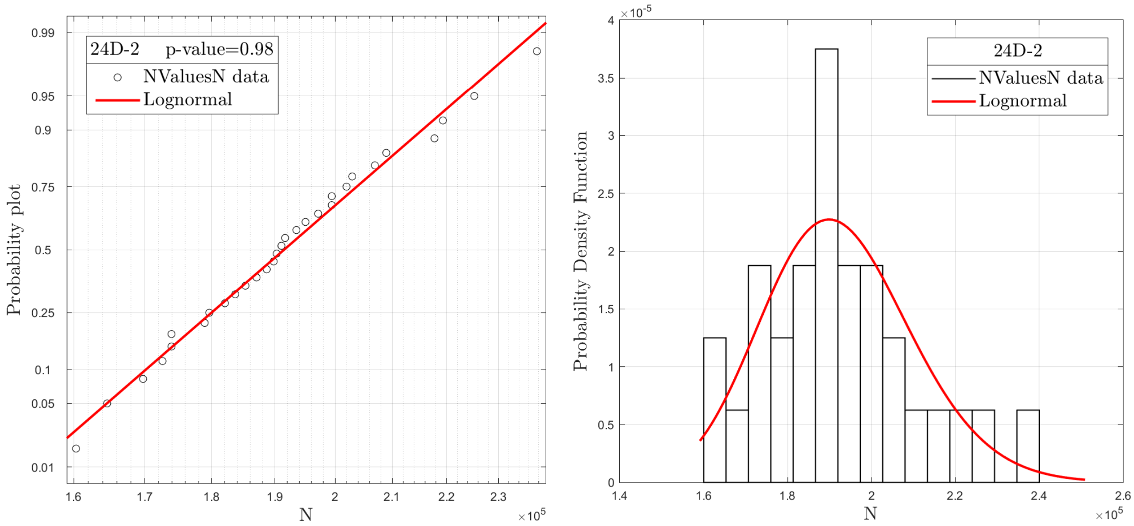

(a) Probability Plot (b) Probability Density Function

Figure B.5: Log-normal fit - 24D-2

B.6 4.1

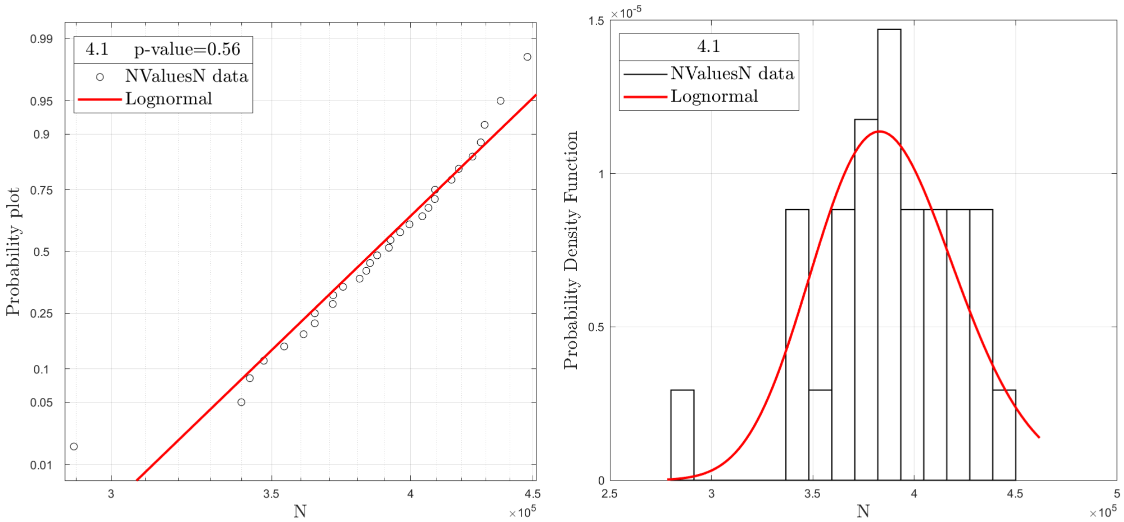

(a) Probability Plot (b) Probability Density Function

Figure B.6: Log-normal fit - 4.1

B.7 S28

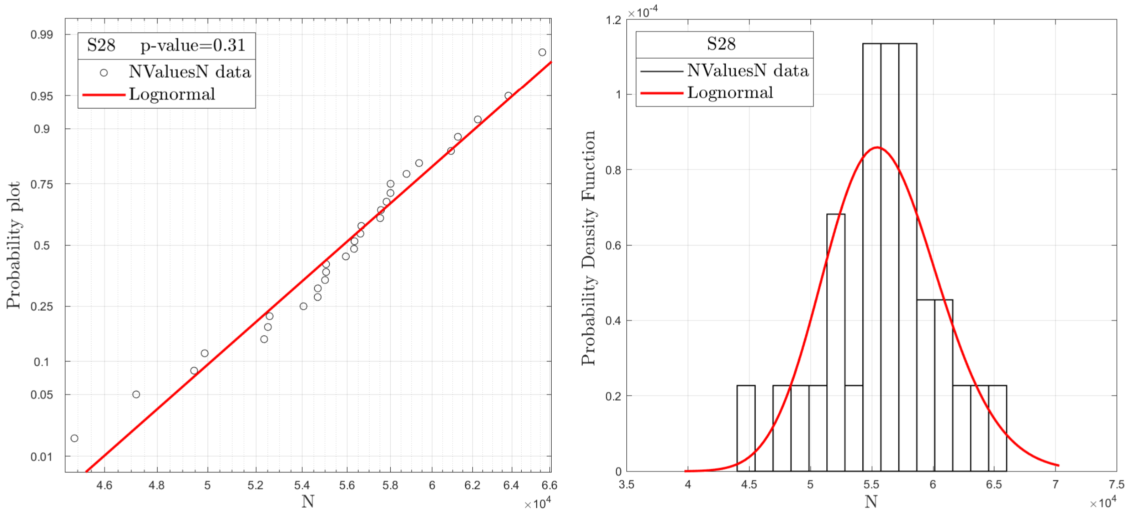

(a) Probability Plot (b) Probability Density Function

Figure B.7: Log-normal fit - S28

B.8 6

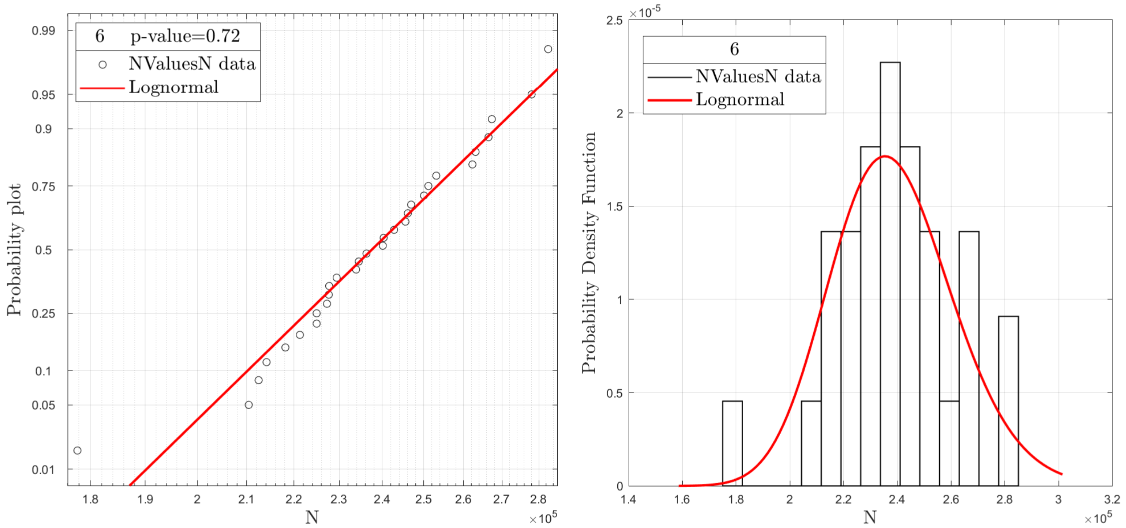

(a) Probability Plot (b) Probability Density Function

Figure B.8: Log-normal fit - 6

B.9 17A

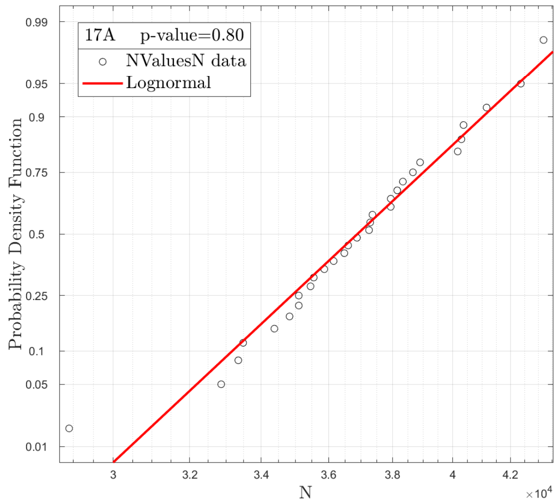

(a) Probability Plot

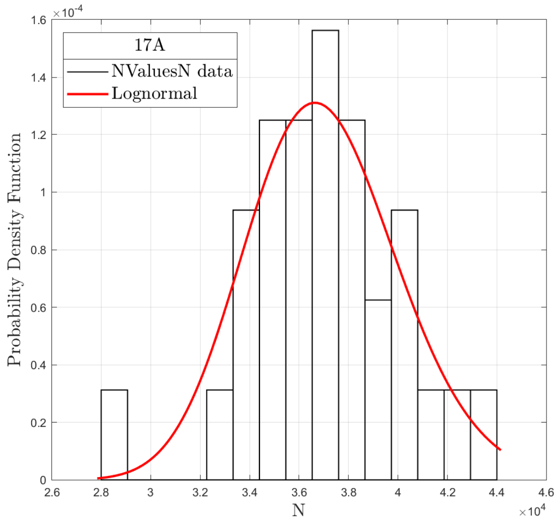

(b) Probability Density Function

Figure B.9: Log-normal fit - 17A

B.10 20

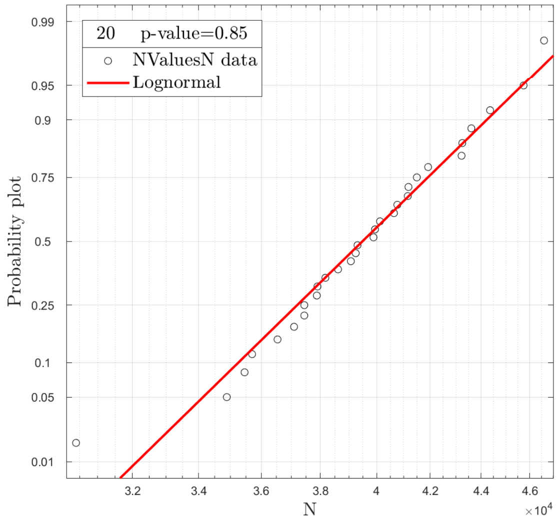

(a) Probability Plot

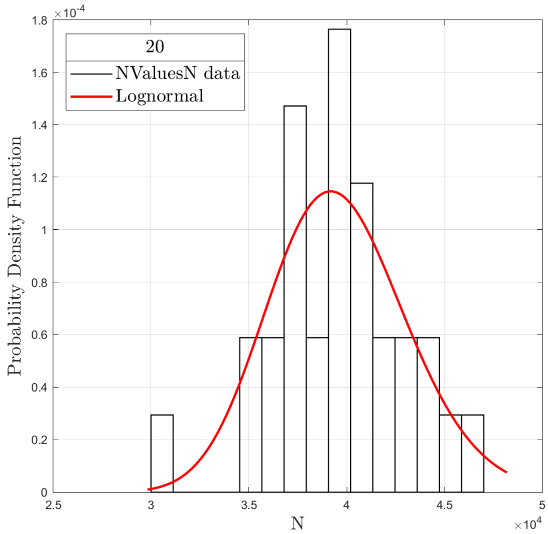

(b) Probability Density Function

Figure B.10: Log-normal fit - 20

Bibliography

[1] *CEN. EN 1990: Eurocode – Basis of structural design, CEN, Brussels, 2013.*

[2] Achintya Haldar and Sankaran Mahadevan. *Probability, reliability, and statistical methods in engineering design*, volume 1. Wiley New York, 2000.

[3] Grazia Vicario and Raffaello Levi. *Metodi statistici per la sperimentazione.* Società Editrice Esculapio, 2009.

[4] Robin L Plackett. Karl pearson and the chi-squared test. *International Statistical Review/Revue Internationale de Statistique*, pages 59–72, 1983.

[5] Theodore W Anderson and Donald A Darling. A test of goodness of fit. *Journal of the American statistical association*, 49(268):765–769, 1954.

[6] MATLAB User's Guide. The mathworks. *Inc., Natick, MA*, 5:333, 1998.

[7] Mario Como and Antonio Grimaldi. *Theory of stability of continuous elastic structures*, volume 1. CRC Press, 1995.

[8] Tim Gudmand-Høyer and Lars Zenke Hansen. *Stability of concrete columns.* BYG. DTU, 2005.

[9] CEB FIB. *Manual of buckling and Instability.* The costruction Press, Lancaster, London, New York, 1978.

[10] *CEN. EN 1992-1-1: Eurocode 2 – Design of concrete structures. Part 1-1: general rules and rules for buildings, CEN, Brussels, 2014.*

[11] Hendrik Schlune, Mario Plos, and Kent Gylltoft. Safety formats for non-linear analysis of concrete structures. *Magazine of Concrete Research*, 64(7):563–574, 2012.

[12] Armen Der Kiureghian and Ove Ditlevsen. Aleatory or epistemic? does it matter? *Structural Safety*, 31(2):105–112, 2009.

[13] JCSS Probabilistic Model Code. Joint committee on structural safety. *URL: www. jcss. ethz. ch*, 2001.

[14] Milan Holickỳ, Johan V Retief, and Miroslav Sỳkora. Assessment of model uncertainties for structural resistance. *Probabilistic Engineering Mechanics*, 45:188–197, 2016.

[15] G König, D Pommerening, and N TUE. Safety concept for the application of non linear analysis in the design of concrete structures, general considerations. *CEB Bulletin No*, 229:13–31, 1995.

[16] Milan Holicky and Miroslav Sykora. Global resistance factors for reinforced concrete members. *Acta Polytechnica, CTU in Prague*, 2006.

[17] CEB FIB. Model code 2010. Technical report, 2010.

[18] Diego Lorenzo Allaix, Vincenzo Ilario Carbone, and Giuseppe Mancini. Global safety format for non-linear analysis of reinforced concrete structures. *Structural Concrete*, 14(1):29–42, 2013.

[19] Jin-Keun Kim and Joo-Kyoung Yang. Buckling behaviour of slender high-strength concrete columns. *Engineering Structures*, 17(1):39–51, 1995.

[20] A Mehmel, H Schwarz, KH Karperek, and J Makovi. Tragverhalten ausmittig beanspruchter stahlbetondruckglieder. institut für baustatik, eht, deutscher ausschuss für stahlbeton, heft 204, 1969.

[21] Robert G Drysdale and Mark William Huggins. Sustained biaxial load on slender concrete columns. *Journal of the Structural Division*, 1971.

[22] N Khalil, AR Cusens, and MD Parker. Tests on slender reinforced concrete columns. *Structural Engineer*, 79(18):21–3, 2001.

[23] Luis P Saenz and Ignacio Martin. Test of reinforced concrete columns with high slenderness ratios. In *Journal Proceedings*, volume 60, pages 589–616, 1963.

[24] Stephen J Foster and Mario M Attard. Experimental tests on eccentrically loaded high strength concrete columns. *Structural Journal*, 94(3):295–303, 1997.

[25] VR Pancholi. *The Instability of Slender Reinforced Concrete Columns*. PhD thesis, University of Bradford, 1977.

[26] Adriana Dracos. *Long slender reinforced concrete columns.* PhD thesis, University of Bradford, 1982.

[27] Satoshi IWAI, Koichi MINAMI, and Minoru WAKABAYASHI. Stability of slender reinforced concrete columns subjected to biaxially eccentric loads. 1986.

[28] PH Chuang and FK Kong. Large-scale tests on slender, reinforced concrete columns. *Structural Engineer*, 75(23):410–16, 1997.

[29] AC Barrera, JL Bonet, Manuel L Romero, and PF Miguel. Experimental tests of slender reinforced concrete columns under combined axial load and lateral force. *Engineering Structures*, 33(12):3676–3689, 2011.

[30] Oskar Baumann. *Die Knickung der Eisenbeton-Säulen.* PhD thesis, ETH Zurich, 1935.

[31] Murat Saatcioglu and Salim R Razvi. Strength and ductility of confined concrete. *Journal of Structural engineering*, 118(6):1590–1607, 1992.

[32] Gabriele Bertagnoli and VI Carbone. A finite element formulation for concrete structures in plane stress. *Structural Concrete*, 9(2):87–99, 2008.

[33] *DIANA FEA BV, Delftechpark 19a 2628 XJ Delft, The Netherlands, 2017.*

[34] *ADINA R D, Inc., 71 Elton Avenue Watertown, MA 02472, USA, 2014.*

[35] *F. McKenna, G.L. Fenves, M.H. Scott, Open system for earthquake engineering simulation, University of California, Berkeley, CA, 2000.*